AD
A065491

MICROCOPY RESOLUTION TEST CHART
NATIONAL BUREAU OF STANDARDS-1963-A

1.0

4.5
50
56
63

2.8
3.2
3.6
40

2.5
2.2
2.0

1.1

1.8

1.25

1.4

1.6

AN ANALYSIS OF THE DATA COLLECTION MODES OF A
DIGITAL WEATHER RADAR SYSTEM WITH RESPECT TO
SIGNIFICANT SEVERE WEATHER FEATURES

A Thesis

by

MICHAEL ARTHUR NEYLAND

THIS DOCUMENT IS BEST QUALITY PRACTICABLE.
THE COPY FURNISHED TO DDC CONTAINED A
SIGNIFICANT NUMBER OF PAGES WHICH DO NOT
REPRODUCE LEGIBLY.

Approved as to style and content by:

(Chairman of Committee)

(Head of Department)

(Member)

(Member)

August 1978

DDC
RECEIVED
MAR 9 1979
E

79 02 26 177

REPORT DOCUMENTATION PAGE		READ INSTRUCTIONS BEFORE COMPLETING FORM
1. REPORT NUMBER CI 79-111T	2. GOVT ACCESSION NO.	3. RECIPIENT'S CATALOG NUMBER
4. TITLE *(and Subtitle)* An analysis of the data collection modes of a digital weather radar system with respect to significant severe weather features		5. TYPE OF REPORT & PERIOD COVERED Thesis
		6. PERFORMING ORG. REPORT NUMBER
7. AUTHOR(s) Michael Arthur Neyland		8. CONTRACT OR GRANT NUMBER(s) Master's thesis
9. PERFORMING ORGANIZATION NAME AND ADDRESS AFIT student at the University of Utah		10. PROGRAM ELEMENT, PROJECT, TASK AREA & WORK UNIT NUMBERS
11. CONTROLLING OFFICE NAME AND ADDRESS AFIT/CI WPAFB OH 45433		12. REPORT DATE August 1978
	155p.	13. NUMBER OF PAGES 143
14. MONITORING AGENCY NAME & ADDRESS*(if different from Controlling Office)* AFIT-CI-79-111T		15. SECURITY CLASS. *(of this report)* UNCLASSIFIED
		15a. DECLASSIFICATION/DOWNGRADING SCHEDULE
16. DISTRIBUTION STATEMENT *(of this Report)* Approved for Public Release, Distribution Unlimited		
17. DISTRIBUTION STATEMENT *(of the abstract entered in Block 20, if different from Report)*		
18. SUPPLEMENTARY NOTES FEB 8 1979 JOSEPH P. HIPPS, Major, USAF Director of Information, AFIT		
19. KEY WORDS *(Continue on reverse side if necessary and identify by block number)*		
20. ABSTRACT *(Continue on reverse side if necessary and identify by block number)*		

DD $\frac{\text{FORM}}{\text{1 JAN 73}}$ 1473   EDITION OF 1 NOV 65 IS OBSOLETE

012 200

UNCLASSIFIED

REPORT DOCUMENTATION PAGE

1. REPORT NUMBER
CI 79-147T

5. TYPE OF REPORT & PERIOD COVERED
Thesis

4. TITLE (and Subtitle)
An analysis of the data collection modes of a digital weather radar system with respect to significant weather radar features

7. AUTHOR
Michael Arthur Neyland

9. PERFORMING ORGANIZATION NAME AND ADDRESS
AFIT student at the University of Utah

11. CONTROLLING OFFICE NAME AND ADDRESS
AFIT/CI
WPAFB OH 45433

12. REPORT DATE
November 1979

13. NUMBER OF PAGES
142

15. SECURITY CLASS (of this report)
UNCLASSIFIED

16. DISTRIBUTION STATEMENT (of this Report)
Approved for Public Release; Distribution Unlimited

JOSEPH P. HIPPS, Major, USAF
Director of Information, AFIT

DD FORM 1473 EDITION OF 1 NOV 65 IS OBSOLETE   UNCLASSIFIED

ABSTRACT

An Analysis of the Data Collection Modes of a

Digital Weather Radar System with Respect to

Significant Severe Weather Features.   (August 1978)

Michael Arthur Neyland, B.S., United States Military Academy;

B.S., University of Utah

Chairman of Advisory Committee: Dr. George Huebner

Dual wavelength digital weather radar data were collected at zero
deg elevation angle in all four modes of collection possible with the
Texas A&M University weather radar system (1 and 2 deg and 1 and 2 km
modes). These data were processed and displayed as contoured maps of
reflectivity. These maps were then analyzed, both qualitatively and
quantitatively, in an (effort to determine) an optimum mode of collection
with respect to retention of meteorological features and data processing
resources required to produce the maps.

The results indicated that significant differences exist between
the reflectivity displays obtained from the different collection modes.
Results from two of the modes are good, while the other two modes suf-
fer from enough loss of detail and accuracy to make their usefulness
questionable.

Additionally, the Texas A&M University digital weather radar system
and the two computer programs used to process the data were explained.

79 02 26 177

ACKNOWLEDGMENTS

DEDICATION

To my wonderful wife, Joy, whose understanding and assistance have made this thesis possible.

TABLE OF CONTENTS

TABLE OF CONTENTS (Continued)

LIST OF TABLES

LIST OF FIGURES

LIST OF FIGURES (Continued)

LIST OF FIGURES (Continued)

LIST OF ACRONYMS

BWER   — bounded weak echo region

CAPPI   — constant altitude plan position indicator

CAZM   — constant altitude reflectivity map

DVIP   — digital video integrator and processor

PPI   — plan position indicator

MDS   — minimum detectable signal

PRF   — pulse repetition frequency

PVIL   — partial vertical integration of liquid water

PVSZ   — partial vertically-summed reflectivity maps

R   — rainfall rate

STC   — sensitivity time control

TAMU   — Texas A&M University

VIL   — vertical integration of liquid water content

WER   — weak echo region

Z   — reflectivity

This list does not include the names of computer programs, sub-routines, and arrays, or their assorted variables and parameters.

CHAPTER I

INTRODUCTION

Within only a short time of the initial development of radar, it was recognized that the device could locate and track areas of severe weather and precipitation. Since that time, radar has come to be considered one of the most important tools available to the meteorologist for the detection of severe local weather phenomena, such as tornadoes, hailstorms, and severe thunderstorms. Until recently, however, the usefulness of radar data was limited by the qualitative, rather than quantitative, nature of the interpretation to which it lent itself. This interpretation was subject to many variables, especially the experience level of the observer and his ability to recognize correctly the type and severity of a storm by a series of variable radar signatures. The development of digital radar systems represents a significant and important technological advance. When this advance is coupled with an efficient and responsive means of data reduction and display, it will afford the meteorologist the opportunity quantitatively to observe and analyze severe weather phenomena in near real time.

The Need for This Investigation

A great amount of research has been done recently using digitized radar data, and the National Weather Service (NWS) has a plan to in-

---

The citations on the following pages follow the style of the *Journal of Geophysical Research*.

stall digitizers on many of their weather radar systems in the United
States to provide input to the new Automation of Field Operations and
Services (AFOS) system. However, the operational implementation of
digital weather radar systems still faces some problems. One of these
is the problem of how to assimilate, reduce, and display in a usable
form, the massive amount of data generated by a digital radar system,
and be able to utilize the data display in near real time. Until now,
one of the most widely accepted real time uses of these data has been
in the computation of vertical integration of liquid water content
(VIL), a technique developed by Greene (1971). While it is agreed by
Vogel (1973), Canipe (1973), and Pittman (1976) that VIL may indeed be
an indicator of the potential for development of severe storms, it is
also agreed that the technique does not adequately represent the im-
portant three-dimensional aspects of a severe storm. Both Canipe's
partial vertical integration of liquid water (PVIL) and Pittman's
partial vertically-summed reflectivity (Z) maps (PVSZ) better accomp-
lish this task. However, both of these techniques are more difficult
to accomplish in real time. Sieland (1977) developed a computer pro-
gram that makes it possible to process digital radar data and produce
PVIL and PVSZ displays in near real time. The operational usefulness
of this program could possibly be greatly enhanced by several additional
refinements. One such refinement is the determination of an optimum
mode of data collection.

Objectives of This Investigation

The objectives of this investigation were two-fold. The primary objective was to examine and compare dual wavelength digital radar data collected near-simultaneously in the four modes of collection possible by the Texas A&M University weather radar system, for the purpose of determining an optimum mode of data collection for operational use of the radar system. This determination was based on such considerations as the range of the storm from the radar, wavelength of the radar, and data processing requirements, both hardware and software. These considerations have been weighed against those of resolution of data, retention of detail, and smoothing of fine scale meteorological features. Digital data collected from the 3 and 10 cm radars of the Department of Meteorology at TAMU have been processed by Sieland's (1977) computer program, modified to produce only the zero-tilt reflectivity maps. These displays have provided the basis for the comparisons and evaluations of the different data collection modes.

A secondary objective of this investigation was to provide a detailed description of the composition of the TAMU digital weather radar system itself.

Present Status of the Question

The importance of weather radar as a means of detecting, observing and forecasting severe weather, and in providing timely warning of the approach of that severe weather to concerned parties, is historically well established. Until fairly recently, this use of the radar was restricted to radar scope pattern-recognition techniques, many of which

were summarized by Whiton (1971). These patterns included: the hook-shaped echo, which is normally shaped like the figure "6"; the V-shaped notch; pendants or protrusions, normally from the right rear portion of a storm; and fingers, or scalloped edges of the echoes, protruding from the rear portion of the storm. Later investigations focused attention on the vertical, as well as the horizontal, structure of severe storms. Such features as the height of the echo tops in relation to the tropopause (Pautz, 1963), echo-free vaults or the weak echo region (WER) (Bigler, 1955), and high reflectivity spikes protruding from the tops of severe storms (Yates, 1963). All of these techniques, however, rely entirely upon the ability of the radar operator to observe adequately these features, and this ability varies greatly with experience and exposure to severe storms. Additionally, the value of qualitative severe weather indicators depends on the operator's ability to assimilate mentally information pertaining to both the vertical and horizontal structure and extent of the storm, an exceedingly difficult task. The recent introduction of electronic digitizing systems for weather radar has eased, somewhat, the burden on radar operators, while it has created a requirement for a method of reducing and analyzing the data in near real time.

Digital Radar Data

Digitizing systems quantize the reflected power returned to the radar receiver over a prescribed number of pulses, and store the data in a spherical coordinate system of range (r), azimuth (α), and antenna elevation angle (ϵ). A typical data set for each scan sequence

of a particular storm system may consist of as many as 100 radials (each with 200 range gates) per elevation angle, and up to 10 elevation angles. Since it is necessary to sample a storm continuously (one scan every 5 to 10 minutes), the amount of data collected quickly becomes unmanageable; consequently, reduction and display of the data requires the use of computer methods.

One of the earliest efforts to display digital data was developed by Marshall (1957), who processed manually digitized photographic data and displayed it in a constant altitude plan-position-indicator (CAPPI) format. Greene (1971) developed a computer technique to produce·constant altitude reflectivity (Z) maps (CAZM). With this technique, digital data were linearly interpolated from a spherical coordinate system (r, α, ε) to a cylindrical coordinate system (s, α, h), where s is the distance along a flat earth surface and h is the height above ground. Then the data were interpolated in the vertical plane of α, and transformed to a rectangular coordinate system (x, y, h) through a quadratic interpolation scheme. The result was a plan view of interpolated radar reflectivity factors in constant height planes with the data points aligned vertically above the range gates in the zero-tilt, or 0-deg elevation, level. These CAZMs were constructed in intervals of 5 kft from 0-deg tilt up to 50 kft and proved to be a valuable tool for analyzing severe storm data. Greene also originated the concept of integrating the liquid water content of a storm through its depth, and labeled the technique "vertical integration of liquid water content" (VIL). This technique was an attempt to compress the three dimensional aspects of a storm into two dimensions (x, y).

Greene noted that the VIL maxima of tornado producing storms would increase to high values approximately one hour prior to the occurrence of a tornado, and then increase to even higher values at the time of a confirmed tornado. Greene realized moderate success with this technique, and his early efforts led to additional research using VIL and variations of VIL.

Morgan and Mueller (1972) studied the VIL and total water mass of a large Illinois hailstorm, using photographically derived digital data from a 3 cm radar. They discovered that hail-producing storms were characterized by very large values of VIL and rapid increases in the total water mass of the storm. Clark and Canipe (1972) studied the applicability of VIL as an indicator of rainfall rate (R), for hydrological purposes, and concluded that VIL was a better indicator of R than simple Z-R relationships. Vogel (1973) used VIL and CAZM analyses to study several severe storms, and he concluded that: 1) CAZMs are the best method with which to analyze severe storms; 2) analyses of single-tilt data may severely limit the detection of severe storms; and 3) VIL is an important indicator of the potential for severe storms to develop, but it masks some of the three-dimensional features, such as the tilt of the maximum reflectivity core and the weak echo region (WER). Canipe (1973) and Canipe and Das (1975) developed a technique for partial vertical integration of liquid water content (PVIL) to combine the simplicity and speed of the VIL analysis with the detail of the CAZM. In this technique, the liquid water content is integrated over three layers of the storm: 0-deg to 15 kft (the source region of the storm-no freezing); 15 kft to 35 kft (the active region-freezing);

and 35 kft to 50 kft (the ice region-above the -40 deg isotherm).
Canipe found that small bounded weak echo regions (BWER)[1] were present
through the lower CAZM analyses of tornadic storms. In addition, he
concluded that PVIL was superior to VIL because it depicted both the
tilt of the storm system and the loss of mass in the upper levels of
the storm, features which have proven to be valuable indicators of
tornadic activity.

Elvander (1975) investigated some severe storm data from the
spring of 1972 provided by NSSL, and studied the relationship between
severe storm events and both zero-tilt indicators (two-dimensional) and
VIL. His results yielded a correlation coefficient for the zero-tilt
indicators of only 0.22, while that for the VIL was 0.45. Elvander
attributed the low correlation of the zero-tilt indicators to the fact
that they do not indicate the intensity of a storm throughout its
depth. Correspondingly, he felt that the correlation of VIL was much
higher due to the fact that VIL is a three-dimensional measurement.

Pittman (1976) extended Canipe's work, including additional data
from tornadic storms. Instead of computing PVIL, however, Pittman
summed the reflectivity at each grid point in the layer and converted
the resultant reflectivity to a dBZ value. This produced partial
vertically-summed reflectivity (PVSZ) maps. He found that the BWERs
associated with tornadoes were evident in the lower layer PVSZ maps and

---

[1]The BWER is an intense updraft within which the entrained water
vapor is carried aloft so rapidly that it does not have time to con-
dense. Therefore, the updraft has very few water droplets to back-
scatter radar energy and appears as a weak echo region bounded by
higher reflectivity values (Canipe, 1973; Sieland, 1977).

that the reflectivity contours around the BWERs exhibited hook-shaped patterns. This feature, together with the tilt of the storm becoming either more nearly vertical, or inclined towards the BWER, and a decrease of the upper level reflectivity maximum, correlated well with the occurrence of tornadoes.

Sieland (1977) developed an improved computer method by which digital radar data are reduced into an optimum number of PVSZ layers. This new method resulted in significant savings of computer processing time and memory, as compared to the more cumbersome methods of Canipe or Pittman, while at the same time it retained all of the significant features of the storm complex revealed by the other methods. By improving the interpolation techniques employed, Sieland's analyses showed greater resolution between the BWERs and the reflectivity contours surrounding them. His technique also improved the detection of marginal BWERs, where Pittman's technique had a tendency to smooth over the data.

Radlein (1977) further refined Sieland's computer program to the extent that it would process data from the TAMU digital weather radar system in the 1 deg by 1 km mode. She then examined simultaneous, dual wavelength data from a Texas thunderstorm, in an effort to determine whether any of the radar signatures associated with tornado-producing thunderstorms elsewhere were present in this central Texas storm.

The Basis for the Investigation

With the initiation of the Digitized Radar Experiment (D/RADEX), the need for an operational technique to process digital radar data

became evident. Since the NWS, and possibly the U.S. Air Force Air
Weather Service (AWS), will have many of their radar systems digitized
in the near future, data reduction schemes that can be used in real
time are a necessity. Any such system must allow for easy analysis of
the three-dimensional aspects of a storm, since zero-tilt reflectivity
patterns alone have proved to be inadequate as indicators of severe
storms. It is also imperative that any data reduction, interpolation,
and presentation schemes preserve the significant details of the indi-
vidual CAZM analyses and the three-dimensional characteristics of
the storm. It is very possible that the retention of significant
details and characteristic features of a storm is highly dependent
upon the resolution of the data and, correspondingly, upon the mode of
data collection.

Techniques of the Investigation

The data for this investigation were obtained from the dual
wavelength digital weather radar system in the Department of
Meteorology at Texas A&M University. The reduction, interpolation,
and display of the data were accomplished by the Amdahl 470V/6 com-
puter at TAMU using the technique developed by Sieland.

Zero-tilt data were collected simultaneously at both 3 and 10 cm
wavelengths, and near simultaneously in all four modes of data col-
lection (1 deg by 1 km, 1 deg by 2 km, 2 deg by 1 km, and 2 deg by
2 km), for targets at both near range (approximately 50 km) and far
range (greater than 100 km). The data were processed and contoured
reflectivity maps generated for the zero-tilt display. These maps

were analyzed with respect to one another for such characteristics as resolution, retention of significant echo features, smoothing of fine scale detail, and differences due to range of the storm and radar wavelength. Additionally, these factors were weighed against the amount of computer resources, both hardware and software, required to process the data. The ultimate objective was to determine an operationally optimum mode of data collection based on all of these considerations.

CHAPTER II

THE TEXAS A&M UNIVERSITY WEATHER RADAR SYSTEM

Basic Radar Theory

The form of the radar equation used in this investigation follows the derivation of Probert-Jones (1962), who assumed a more realistic beam shape in order to reduce the error in a derivation by Battan (1959). In the Probert-Jones derivation, we assume that there is no significant attenuation of microwave energy between the radar antenna and the target, and that the target completely fills the spatial volume illuminated by the radar beam. Under these conditions, the average backscattered power, $\overline{P}_r$ (watts), received from the target at range r(km), is given by

$$\overline{P}_r = \frac{C|k|^2}{r^2} Z_e \tag{1}$$

where C (w $km^2 m^3 mm^{-6}$) is the radar constant, which is unique for each individual radar, $|k|^2$ (dimensionless) is the dielectric constant used in scattering theory, and Z_e ($mm^6 m^{-3}$) is the equivalent radar reflectivity factor. The equation for C is

$$C = \frac{\pi^3 P_t G^2 h\theta\phi}{512 \lambda^2 2 \ln 2} \tag{2}$$

where P_t is the transmitted power during a radar pulse (w), G is the antenna gain (dimensionless), h is the pulse length in space of the transmitted pulse (cm), θ is the horizontal beamwidth (radians), ϕ is

the vertical beamwidth (radians), and λ is the wavelength of the transmitted microwave energy (cm). The factor 2 ln 2 is the Probert-Jones correction factor, which results from the fact that the beam power density nearly approximates a Gaussian distribution; consequently, the transmitting and receiving gains are not equal. The value of C for each of the TAMU radars is found below, and the value of $|k|^2$ is chosen as 0.93 (Battan, 1973).

The final output of the radar system, which is digitized values of the returned power, $\overline{P}_r$, must be converted to values of reflectivity before any further data reduction techniques can be applied. The usual practice is to measure the returned power in terms of decibels with respect to a standard reference power level, normally 1 mw. Power levels are then expressed in units of dBm, either above (+) or below (−) 1 mw. The equation is

$$P(dBm) = 10 \log_{10} \frac{P(watts)}{10^{-3} \ watts} \tag{3}$$

For example, a returned power (P_r) of 10^{-11} watts would yield a value of −80 dBm for P.[2]

To determine values of Z_e, we solve Eq (1) for Z_e and have

$$Z_e = \frac{r^2}{C|k|^2} \ \overline{P}_r \tag{4}$$

---

[2]See Battan (1973) for a more complete discussion of radar reflectivity factor, Z, equivalent radar reflectivity factor, Z_e, and dBm. Also, in this investigation, ln refers to base e logarithms, and log to base 10 logarithms.

The logarithm of Eq (4) is

$$\log Z_e = 2 \log r + \log \overline{P}_r - \log C|k|^2 \qquad (5)$$

Using the values of C for the TAMU radars given below and that of $|k|^2$ given earlier, we have

$$C_3 = 1.0089 \times 10^{-9} \qquad \log C_3|k|^2 = 9.0 \qquad (6a)$$

$$C_{10} = 8.609 \times 10^{-11} \qquad \log C_{10}|k|^2 = 10.1 \qquad (6b)$$

By substituting Eq (6) into Eq (5) we get

$$\log Z_{e3} = 2 \log r + \log \overline{P}_r + 9.0 \qquad (7a)$$

$$\log Z_{e10} = 2 \log r + \log \overline{P}_r + 10.1 \qquad (7b)$$

The digital value of $\overline{P}_r$ is converted to its dBm equivalent (always negative) through the use of calibration data for each of the two radars.[3] The received power in watts is then related to the received power in dBm by

$$\log \overline{P}_r \text{ (watts)} = 0.1 \overline{P}_r \text{ (dBm)} - 3.0 \qquad (8)$$

Substitution of Eq (8) into Eq (7) yields

$$\log Z_{e3} = 0.1 \overline{P}_r + 2 \log r + 6.0 \qquad (9a)$$

$$\log Z_{e10} = 0.1 \overline{P}_r + 2 \log r + 7.1 \qquad (9b)$$

Finally, the value of Z_e is given by

---

[3] The digital system produces $\overline{\log P_r}$ rather than $\log \overline{P}_r$. Wilk and Kessler (1970) developed an equation which corrects Eq (7), but the correction is usually less than 1 dB.

$$Z_e = 10^{(0.1 \bar{P}_r + 2 \log r + w_c)} \tag{10}$$

where, by convention, Z_e is in units of $mm^6 m^{-3}$, and w_c is 6.0 for the 3 cm radar and 7.1 for the 10 cm radar.

Assumptions Made in the Theoretical Development

There are several assumptions that are inherent in the development of Eq (10). These include:

1. The transmitted microwave energy is not significantly attenuated between the radar antenna and the target. This has been shown to be valid for radars with wavelengths near 10 cm, but is not strictly true for wavelengths in the vicinity of 3 cm (Greene, 1964). The returned power of a 3 cm radar will suffer some reduction due to attenuation by atmospheric gases, cloud droplets, and precipitation. The attenuation due to atmospheric gases will be on the order of 10^{-2} dB km^{-1}, while that due to cloud droplets, depending on their physical state and temperature, will vary between 10^{-4} and 10^{-1} dB km^{-1}. Attenuation due to precipitation is generally proportional to rainfall rate and temperature, and from derived Z-R relationships, can be approximately expressed as $2.9 \times 10^{-4} Z^{0.72}$ dB km^{-1} (Battan, 1973).

2. The spatial volume illuminated by the radar beam is completely filled by the target. This condition is not always met, particularly on the periphery of a storm. The result will be a loss of resolution of fine scale detail in these areas (Greene, 1971), but it will not significantly affect the major features present in the digital data.

3. The Rayleigh approximation is used to describe the scattering properties of spherical liquid water drops having diameters on the

order of 0.04 λ, where λ is the radar wavelength in centimeters. In the case of severe storms, large, non-spherical water drops and hail-stones may be present that do not meet the Rayleigh criteria; however, the enhanced reflectivity that is characteristic of these particles may be useful in identifying severe storms.

Two additional assumptions that are made concerning the digital data in this investigation are:

1. Each digital datum value represents a point in the center of the radar volume.

2. The equivalent radar reflectivity factors, Z_e, obtained from the digital data, are representative of a continuous scalar field.

The Earth Curvature Correction

Microwave radiation propagating in free space will follow a straightline path. However, the microwave radiation of a radar beam propagating through the atmosphere will follow a curved path, due to refraction. The amount of curvature of the path depends upon the vertical gradient of the index of refraction (n). Under normal at-mospheric conditions, where temperature and humidity decrease with height, the path of the radar beam will curve slightly downwards to-wards the surface of the earth. Appleton (1946) studied the curvature of a radio wave traveling through an atmosphere in which the index of refraction varies with height. Figure 1 shows the case in which the transmitter is located at a height, h_o, above the earth's surface and sends out a beam at an elevation angle ε from the horizontal plane.
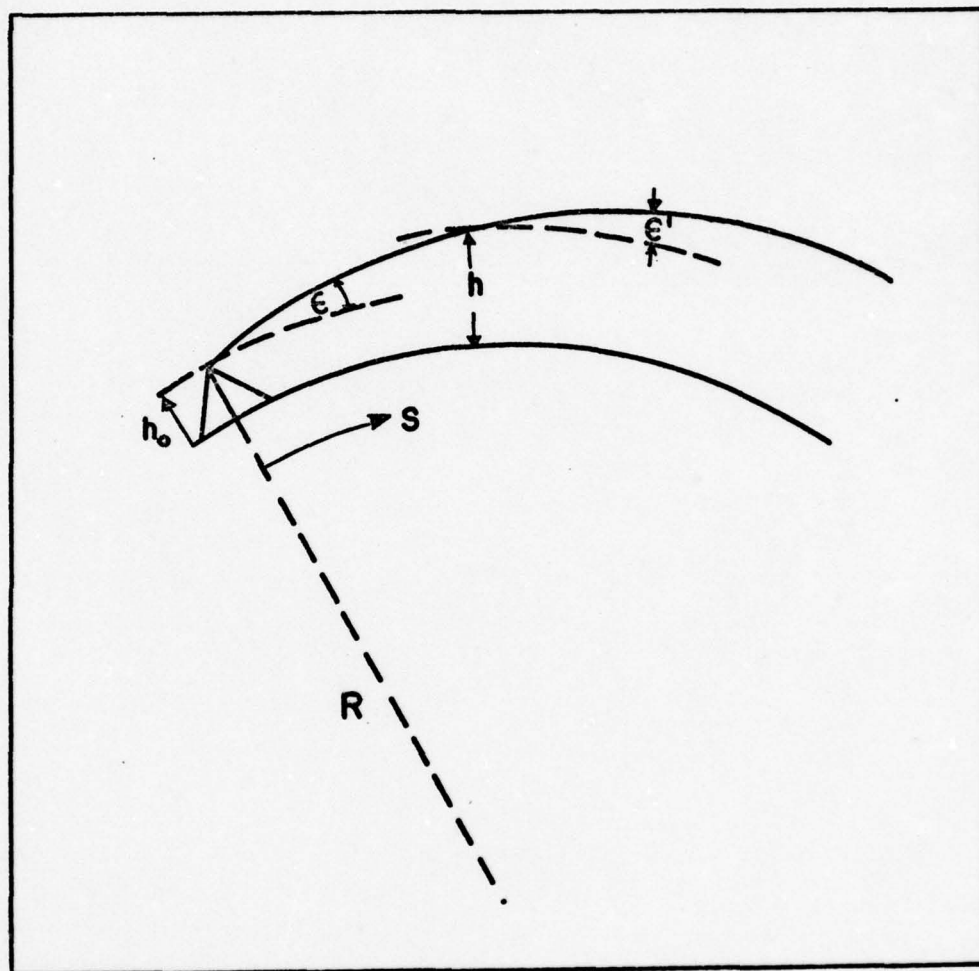
Fig. 1. Schematic of a ray path. [After Greene, 1971]

Ray theory may be applied to the problem if the change with height of the index of refraction, $\frac{dn}{dh}$, is small. In that case, the exact differential equation for a ray in a spherically stratified atmosphere is

$$\frac{d^2h}{ds^2} = \left(\frac{2}{R+h} + \frac{1}{n}\frac{dn}{dh}\right)\left(\frac{dh}{ds}\right)^2 + \left(\frac{R+h}{R}\right)^2 \left(\frac{1}{R+h} + \frac{1}{n}\frac{dn}{dh}\right) \tag{11}$$

where h is the height of the beam above the earth's surface at a distance s from the transmitter, R is the earth's radius, and n is the index of refraction. Since ε is usually very small, $\left(\frac{dh}{ds}\right)^2 = \tan^2 \varepsilon \ll 1$. Additionally, $n \simeq 1$, and $h \ll R$, so for all practical purposes, Eq (11) can be reduced to

$$\frac{d^2h}{ds^2} = \frac{1}{R} + \frac{dn}{dh} \tag{12}$$

In this investigation it is necessary to consider the radar beam axis as a straight line, so we will assume a fictitious earth having a radius given by (Battan, 1959)

$$R' = \frac{R}{1 + R\frac{dn}{dh}} \tag{13}$$

It has been shown that $\frac{dn}{dh}$ is small and nearly linear with a value of $-4 \times 10^{-8} m^{-1}$. Therefore, an earth curvature correction of $R' = \frac{4}{3} R$ will be used, and the resultant radar beam may be considered a straight line, as shown in Figure 2.
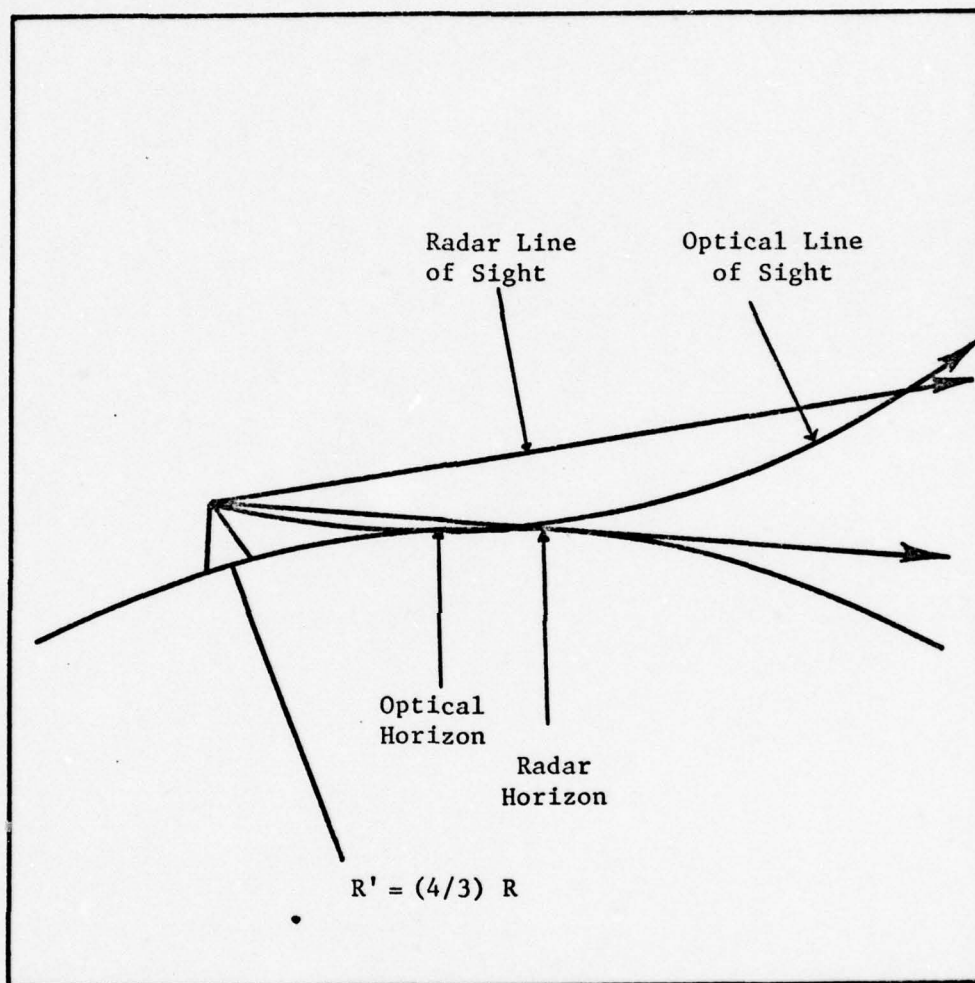
Fig. 2. Radar and optical lines of sight over an earth having an effective radius, R' = (4/3)R. [After Battan, 1959].

The TAMU Weather Radar System

Physical Description

The TAMU Weather Radar System consists of two complete weather
radar systems operating in parallel. The makeup of the two systems is
nearly identical, and each consists of the following major sub-systems:
antenna, conventional analog weather radar set, digital video
integrator and processor (DVIP) with PPI display, and a nine-track
tape unit to record the buffered digital output of the DVIP. Each of
these subsystems will be addressed separately. The technical charac-
teristics of both radar sets and the antenna system are contained in
Table 1.

<u>Antennas</u>. The antenna system consists of an array of three solid
parabolic dish antennas that are mounted on a single pedestal and
permanently aligned in relation to one another. (The purpose of the
third antenna is to allow the possible installation of a K band radar
at some future date.) The large S band antenna (10 cm radar) is
mounted in the center, with the two smaller X (3 cm) and K band anten-
nas mounted on either side.

<u>Radar sets</u>. The 3-cm radar is basically a modified CPS-9 radar,
while the 10-cm radar was constructed at TAMU using components taken
from a variety of different radar sets. Both units do have new re-
ceivers, however, and both are mounted in CPS-9 consoles. The system
has only a single synchronizing pulse generator that is used to trigger
both radars. This, combined with the single antenna pedestal, insures
that both radars scan the same illuminated volume simultaneously. The

TABLE 1. WSR/TAM-2 Weather Radar Technical Characteristics.

PEDESTAL & ANTENNA

ANTENNA LOCATION ----- Lat. 30° 37' 04" N.
Long. 96° 20' 10" W.
ANTENNA HEIGHT ----- 559 ft above MSL
224 ft above ground
NUMBER & SIZES OF ANTENNAS - K BAND 4.8 ft.
X BAND 4.8 ft.
S BAND 16.0 ft.

ANTENNA CONTROL CHARACTERISTICS
PEDESTAL TYPE
Scientific of Atlanta Series 3200
Model K-446

ELEVATION
Travel Limits -- -2° to + 95°
Maximum Velocity 30° per sec.
MODES OF OPERATION
---- Manual rate (variable)
---- Slave to drive input

AZIMUTH
Travel Limits -----None
Max. Velocity -----30°/Sec.
MODES OF OPERATION -----(CW & CCW) Manual & Slave
(CW & CCW) Manual and slave modes
(Programmed Elevation Being Added)

POSITION ACCURACY
S.A. Position Indicator Read-Out
Manual rate (1:1 & 36:1) -- 0.65°
Slave Positioning----------- 0.10°
PPI Scope Readouts
Azimuth & Elevation ---- 1.00°

SYNCHRONIZING SYSTEM
Pulse Generator 0-81/CPS-9 Modified
(Used for both 3 cm and 10 cm systems)
Output Triggers
For both 3cm & 10 cm Modulators
931 P.P.S. (Short Pulse)
186 P.P.S. (Long Pulse)
System Triggers -----100 Statute Mile
Range Standard (Short Pulse)
---- 500 Statute Mile
Range Standard (Long Pulse)
Range Marks ---- 1, 5, 25, and 100 S. Miles
(Supplied by Crystal Oscillator)

3 cm RADAR

ANTENNA REFLECTOR --Parabolic 4.8 ft. dia (Solid Dish)
Feed Type -------- Horn
Polarization -------- Vertical-Linear
ANTENNA BEAM-WIDTH (Mid.-Freq.)
Vertical & Horizontal 1.54°
FREQUENCY----------- 9317 ± 87 MHz
WAVELENGTH---------- 3.2 cm
ANTENNA GAIN-------- 40.50 dB
ATTENUATION OF BACK & SIDE LOBES - Greater than 20 dB

I. GENERAL CHARACTERISTICS
RANGE -------- Nominal Max. 250 S. Miles
Minimum ---- 1/2 S. Mile
Accuracy @ Max. Range ---- 0.2%
RESOLUTION-----123 ft. S.P. & 1230 ft. L.P.

BEARING (AZIMUTH)
Accuracy --------- 1.54° Beam Width
Resolving -------- Approx. 1.54°
Elevation -------- Same as Above

II.TRANSMITTING SYSTEM
Peak Power (fixed) Max. 250 KW (S.P.)
(Determined by magnetron) Nominal - 200 KW
Average Power -------115 Watts (S.P.)
230 Watts (L.P.)
Pulse Repetition Rate ----- 931 PPS (S.P.)
186 PPS (L.P.)
Pulse Length --------- 0.5 u Sec. S.P.
5.0 u Sec. L.P.
Magnetron Type ----- Raytheon 6002
TR Tube------------- 5863
ATR Tube------------ 5864

III. RECEIVING SYSTEM
A. LINEAR RECEIVER
Operating Freq. ----------9317 ± 87 MHz
(Fixed by Magnetron)
Nominal IF Gain ----------93 dB (Wide Band)
103 dB (Narrow Band)
Klystron-------- Type 2K25 With AFC @ 30 MHz
Above Mag. Freq.
Mixer --Balanced Signal & AFC (1N23B Crystals)
I.F. Frequency
Signal & AFC --- 30 MHz
Band Width ------- Approx. 5 MHz on S.P.
0.5 MHz on L.P.
Auxiliary Output --Source Follower 30 MHz pre-
amplifier for Log. Receiver

B. LOGARITHMIC I.F. AMPLIFIER
Same as 10 cm Unit

10 cm RADAR

ANTENNA REFLECTOR ----Parabolic 16 ft.Solid Dish
Feed Type -------------------Horn
Polarization ----------------Vertical-Linear
Beam Width   (2880 MHz) 1.54°
(2840 MHz) 1.52°
OPERATING FREQUENCY
2840 MHz (10.55 cm)

ANTENNA GAIN
40.3 dB With Side Lobes Less Than 20 dB

I. GENERAL CHARACTERISTICS
(Same as 3 cm Radar)

II. TRANSMITTING SYSTEM
Peak Power (Operating) -----200 KW as is
Determined by 3 cm Magnetron (For Match)
Average Power
Pulse Rep. Rate
Pulse Length ------Same as 3 cm Radar

MAGNETRON TYPE --- 5586 (Tuneable-2720 To 2900)
TR TUBE----------- 1B58
ATR TUBE---------- 1B56

III. RECEIVING SYSTEM
A. Linear Receiver
Nominal I.F. Gain --93 dB (Wide Band, S.P.)
103 dB (Narrow Band,L.P.)
Klystron ----------- 720C With AFC 30 MHz
Above Mag. Freq.
Mixer ------------ Balanced Signal & AFC
1N21 Crystals
I.F. Frequency --Signal & AFC - 30 MHz
Auxiliary Output--Source-Follower
for Log. Receiver

B. Logarithmic I.F. Amplifier
Type --RHG LST 3002 RF1
Center Frequency -- 30 MHz
3 dB Bandwidth---- 2 MHz
Input Impedance---- 50 Ohms
Input VSWR----- 1.5:1
Dynamic Range------ Less than 1 dB Over
60 dB Range
Rise Time---------- 0.3 u Sec
Output Voltage Range 0 - 2.6 Volts

synchronizing trigger signal and the radar receiver logarithmic video output comprise the input into the next major subsystem, the DVIP.

The Digital Video Integrator and Processor (DVIP)

The DVIP is a high speed data acquisition, digitizing, and processing system, which continuously averages radar logarithmic video output in range (range averaging) and in direction of antenna scan (time averaging), using exponentially weighted digital integrator techniques and synchronized by the radar system trigger.[4] The results are quantitative estimates of mean detected precipitation returns and an improvement in the accuracy (standard deviation) of the mean intensity estimates, over that of a logarithmic radar receiver, to 1.0 dB or less, based on range increments of 1 or 2 km. The DVIP installation provides for real time contoured PPI displays and digital recording of the digitized, integrated data. Both radars are coupled to identical DVIP systems, except that the 3 cm system also has a tape playback facility incorporated into it.

DVIP accuracy. The DVIP can improve the accuracy, measured in terms of standard deviation, of precipitation intensity estimates to 1.0 dB or less, at range increments of 1 or 2 kilometers. This improvement is accomplished by a combination of range averaging (an average over several sample volumes in range) and an average over several pulses returned from the same volume (continuous pulse-to-pulse integration or time averaging).

---

[4]The discussion of the DVIP and DVIP accuracy is derived from a DVIP technical manual, which contains considerably more detail than this summary (Enterprise Electronic Corp., 1975).

The accuracy, or standard deviation (σ), of the estimate of the mean intensity values of radar returns from a precipitation volume is a function of two things, the effective sample size, and the fluctuation of the output of a logarithmic receiver. The latter, fluctuating characteristics of precipitation returns from a log receiver, are defined by a standard deviation of 5.57 dB. Accordingly then, if a number of statistically independent samples (N) from a particular precipitation volume (the output of the log receiver) are averaged by the DVIP, the standard deviation of the intensity estimates is reduced by $\frac{1}{\sqrt{N}}$, or

$$\sigma = \frac{5.57 \text{ dB}}{\sqrt{N}} \tag{14}$$

To determine the number of independent samples to be integrated by the DVIP, we assume that the radar return signal from a sample precipitation volume, V_s, varies randomly with time and has a Gaussian distribution. The total number of samples, N_s, obtained from the volume, V_s, is dependent upon the mechanics of the radar set itself, specifically antenna beamwidth, PRF, and antenna scan rate. Because there may be some sample-to-sample correlation, the number of independent samples, N, in the total sample, N_s, must be determined. The degree of correlation between the samples is dependent upon both radar and meteorological parameters, the latter being the standard deviation of the velocity distribution of the scatterers, σ_v, in the sample volume. The number of independent samples, N, is related to the total number of samples, N_s, by

$$N = \frac{4\sqrt{\pi} \; \sigma_v \; T_s \; N_s}{\lambda} \tag{15}$$

where T_s is the sampling time (1/PRF), and λ is the transmitted wavelength. If we set $N = N_s$, assume $\sigma_v = 2$ m/s, and solve for T_s, we find that the PRF required for independent sampling with a 3 cm (X band) radar is

$$T_s = \frac{\lambda}{4\sqrt{\pi} \; \sigma_v} = \frac{.032}{4\sqrt{\pi} \; 2} = .002257 \; sec \tag{16}$$

$$PRF = \frac{1}{T_s} = 443 \; pps \tag{17}$$

Therefore, if the radar PRF is 443 pps or less, all pulse-to-pulse samples, or time samples, of the volume, V_s, will be independent.

The number of statistically independent samples, N, that the DVIP must average to meet the standard deviation requirement of 1.0 dB or less is

$$N = \frac{(5.57 \; dB)^2}{\sigma^2} \tag{18}$$

so for $\sigma = 1.0$, the DVIP must process 31 independent samples.

The pulse length of the TAMU radars is 5 microseconds, while the specified 1 km range increment is 6.67 microseconds long, so each range increment contains 1.34 independent range samples. If at least 31 independent samples must be processed by the DVIP, then the number of time samples, or pulses, that must be processed in the digital integrator is 23.13 (31/1.34 = 23.13). For the case where PRF = 186 with an antenna scan rate of 1.3 rpm, we get 23.85 pulses per degree of

azimuth for a 1 km range increment. The 2 km range increment contains 2.67 independent range samples, so by solving Eq (18) for σ, and substituting these numbers (23.85 and 2.67) into N, we find that, for the 2 km range increment, σ = 0.698 dB. On the other hand, the maximum allowable antenna scan rate that will insure an accuracy of 1.0 dB is increased to 2.67 rpm.

Integration technique. The only inputs to the DVIP are 115 VAC power, the radar logarithmic video, and the radar system trigger. The range increment integration, over either 1 or 2 km, and the number of time samples (pulses) to be integrated, either 15 or 31, are controlled by switches on the front panel of the unit. The azimuth increment to be integrated, either 1 or 2 deg, is controlled by the tape unit and will be covered separately later.

The incoming log video signal from the radar set is first amplified by a video scaling amplifier, and then the analog signal is sampled once every 1.66 microseconds (about every 250 meters in range) and the samples fed into an analog-to-digital converter. The A/D conversion takes about one microsecond and converts the analog video signal to digital bits. From the A/D converter, the digital data samples are sent to a range bin circulator. Here the samples are added to one another, either four or eight of them, depending on the range increment selected, and then the sum is divided by either four or eight, resulting in an average value for that range increment. The next step is through a multiplexer and into range bin storage. It is during this step that the time sample integration occurs, controlled by the time sample switch on the front panel. This switch provides a choice of 15 or 31

steps in the integration curve between the 10 and 90 percent amplitude points, where each step covers one sample time. The integrator equation forms a mathematical progression where one-eighth of a number added to seven-eighths of one-eighth of that number will arrive at 90 percent of the original number in 15 steps. Where one-sixteenth is chosen instead of one-eighth, the number of steps between the 10 and 90 percent amplitude points is 31. The maximum antenna scan rates that will allow 15 and 31 pulses per degree of azimuth are 2.07 rpm and 1.00 rpm, respectively.

It should be noted that this time sample integration step, which requires 15 or 31 separate radar pulses, is not to be confused with the range increment integration, which requires 31 statistically independent samples, which can be obtained from 23.13 time samples (pulses). Likewise, neither of these processes should be confused with the 250 m (1.66 μ sec) sampling and averaging used to produce mean values for the 1 and 2 km range increment received power values, or the azimuth increment integration, which is controlled by the tape unit.

DVIP output. The DVIP output signal is split into two channels, the digital channel and the display channel. The display channel provides either log video or contoured log video to the system PPI scope. The DVIP can be calibrated to detect and display six discrete levels of precipitation intensity. The presentation of these six intensity levels as three alternating shades of grey is called video contouring. These threshold levels can be set digitally in 0.5 dB steps. A radar return that falls within level 1 is displayed as grey (half brightness), level 2 is displayed as white (full brightness), and level 3 is

black (zero brightness). The cycle then repeats itself; level 4 is grey, level 5 is white, and level 6, the highest intensity return, is black.

The digital output consists of the 1 or 2 km range increment integrated video samples, provided in a buffered 8 bit parallel binary configuration compatible with standard TTL logic levels. Each digital output word represents a digital value of the integrated video intensity on a linear scale over the input dynamic range of 80 dB. At the digital output there are 215 2-km or 430 1-km digital samples representing the range increments from 21 through 450 km of range, depending upon the range increment selected.

Range normalization (STC). The range normalization function (sensitivity time control-STC) compensates the integrated video signal for attenuation due to range. It provides a $1/R^2$ correction (R = radar range) in the range interval from 20 to 230 km, with 0 dB correction at 20 km and +21 dB correction at 230 km, applied in increments of 0.5 dB. Range normalization is applied only to video signals of precipitation intensity level 2 or higher. Range normalization is not applied to the digital output channel at all, and can be disabled for the display channel as well, by means of a front panel switch.

Range blanking. Two range blanking options are available, a fixed 0-20 km interval, and a variable range blanking interval adjustable from 0-199 km. Within these intervals, all contoured log video to the radar displays is inhibited. The type of range blanking interval employed is selected by a front panel switch, the operation of which does not affect the digital output data, since these data are blanked in the 0-20 km interval only.

Precipitation level selection. Six front panel mounted switches are provided to select any one or more of the six precipitation intensity levels for display. Selection of one or more of the levels disables normal contouring, and only those levels selected are displayed. All selected levels are displayed as white (full brightness). For example, if level 3 is selected, all precipitation areas with intensity between the level 3 threshold and the level 4 threshold are displayed as white, and no other precipitation areas or intensities are displayed.

Digital Output Recording System

The digital output channel of the DVIP is fed into a 9-track magnetic tape recording unit. This tape drive unit serves two functions; it records the digital data in a format that makes it readily accessible by computer, and it controls the azimuth increment integration of the data. The first function will be addressed further in the section on data reduction.

Control of the azimuth integration increment (data integrated over either 1 deg or 2 deg of azimuth) is accomplished through the use of a switch on the front panel of the tape unit. At the end of each azimuth increment, the tape unit generates a signal and calls for a digital value from the DVIP that is based upon the most recent time samples from a particular range bin. The number of samples called for is determined by the time sample switch on the DVIP, which selects either 15 or 31 samples. The digital value derived from those samples represents the mean received power from that entire azimuth increment.

Consequently, it becomes very important to match the antenna scan rate with the azimuth increment selected. For example, if the time sample selected is 31 and the azimuth increment selected is 1 deg, the value recorded for that range bin is derived from the last 31 time samples over that 1 deg of azimuth. At 1.0 rpm there will just be 31 samples in the 1 deg of azimuth. If the azimuth increment selected is 2 deg, the digital value recorded is still derived from the last 31 samples. However, if the antenna scan rate is still 1.0 rpm, those 31 samples will all have come from the second half of the 2 deg azimuth increment, and consequently may not represent that range bin accurately. Therefore, with an azimuth increment of 2 deg it is necessary to increase the antenna scan rate to 2.0 rpm. Conversely, it is also important that the antenna scan rate not be too fast, since, in that case, the recorded values are derived from an integration scheme which requires a fixed number of samples, but does not get them. Once again, the recorded value may not be representative of the actual value.

Data collection modes. There are four possible modes of data collection with this system. They are:

1. 1 deg by 1 km. The data are integrated over 1 km range increments by the DVIP and the integrated time sample data called for by the tape unit represent 1 deg of azimuth.

2. 1 deg by 2 km. The data are integrated over 2 km range increments by the DVIP and the integrated time sample data called for by the tape unit represent 1 deg of azimuth.

3. 2 deg by 1 km. The data are integrated over 1 km range increments by the DVIP and the integrated time sample data called for

by the tape unit represent 2 deg of azimuth.

4. 2 deg by 2 km. The data are integrated over 2 km range increments by the DVIP and the integrated time sample data called for by the tape unit represent 2 deg of azimuth.

In all cases the data are recorded one azimuth increment at a time, beginning with the range bin nearest the radar, and proceeding sequentially outwards along the radial.

Table 2 presents the antenna scan rates required to maintain an accuracy of 1.0 dB in all four collection modes, for both 15 and 31 time samples.

TABLE 2. Antenna Scan Rates (rpm) Required for 1.0 dB Accuracy.

Collection Mode	15 Time Samples	31 Time Samples
1 deg x 1 km	2.07	1.00
1 deg x 2 km	2.07	1.00
2 deg x 1 km	4.13	2.00
2 deg x 2 km	4.13	2.00

Data shift. Both output channels, the coded PPI display channel and the digital channel, suffer from a slight shifting of the displayed location of the data points, both in range and in azimuth. This is due to the nature of the integration processes employed by the DVIP, and the magnitude of the effect is a function of the range and azimuth increments selected. In both cases, the shift occurs because the incoming reflectivity values are integrated across the entire range or

azimuth increment, from its leading edge to its trailing edge. Then the integrated value is displayed at the end of the increment, rather than at the mid-point of the increment over which the data were integrated. In the contoured PPI display, this data shift manifests itself in several ways. First, the leading edges of all targets at all threshold levels are shifted outward and clockwise by one range interval and one azimuth interval, respectively. The magnitude of the shifts depends upon whether the 1 deg, 2 deg, 1 km, or 2 km modes are being utilized. Additionally, the trailing edges of all targets are shifted outwards 1 to 2 range increments, depending upon the amplitude of the target's reflectivity at the range increment boundary.

The data shift in the digital output channel is partially overcome by the use of the assumption that the data represent points in the center of the illuminated radar volume. This negates the range shift, but only partially counteracts the azimuth shift. This is because the data points are assumed to lie on the radial at the end of the azimuth increment, rather than at the angular mid-point of that increment. Even so, this reduces the shift to only one half of one azimuth increment.

The reduction and display of the digital data output of the DVIP are addressed in the next chapter.

CHAPTER III

DATA REDUCTION AND DISPLAY

The digital output channel of the DVIP is recorded on 9-track tape, and this tape then becomes the input into the TAMU Amdahl 470V/6 computer. Through the use of the program developed by Sieland (1977) and a library subroutine called CONREC, the computer processes the digital radar data, and presents it to the user in a functional format. Both of these computer programs are described and explained in the following sections.

Sieland's RADAR Program

The computer program developed by Sieland, called RADAR, begins with the digital radar data, which is recorded in a spherical coordinate system (r, α, ε) and first transforms it into a cylindrical coordinate system (r, α, h) with three separate height divisions, or PVSZ layers. Finally, the data are transformed into a two-dimensional rectangular coordinate system (x, y) and five maps are produced, a zero level reflectivity map, the three PVSZ layer maps, and a VIL map. The conversion of coordinate systems requires the use of two interpolation schemes, a Lagrangian linear or cubic interpolation scheme along each radial of data (in the $r-\varepsilon$ plane) and a quadratic scheme for the conversion to rectangular coordinates. An extensive explanation of the development and functioning of these interpolation schemes is contained in Sieland (1977), the main points of which are presented here.

PVSZ Layers

This program creates three PVSZ layers, where the reflectivity factors are summed in a vertical column above a given (x,y) point at the surface into the lower layer (0-deg to 15 kft), the middle layer (15 to 35 kft), and the upper layer (35 to 50 kft) of a storm complex. The first step in this procedure is to convert the data from a spherical coordinate system (r,α,ε) to a cylindrical one (r,α,h). Figure 3 shows the relationship between these two coordinate systems, and the interpolation points used to convert from one to another. (Each dot at the intersection of a column and a radial is an interpolation point.) Note that the number of interpolation points in each layer varies with the range, r, so it becomes necessary to determine the number of interpolation points (and hence, elevation angles of data) contained in each layer above each range bin. This is accomplished by a subroutine called DIVIDE, which calculates the number of tilt angles contained in each of the three layers at each range and stores them in the arrays IDIV1, IDIV2, and IDIV3, for the lower, middle, and upper layers.

Conversion to Cylindrical Coordinate System

The Lagrangian linear or cubic interpolation scheme incorporated by Sieland to convert the data from a spherical to a cylindrical coordinate system is applied to the data along each radial of information at each separate elevation angle. The steps involved in this interpolation follow (See Figure 4):
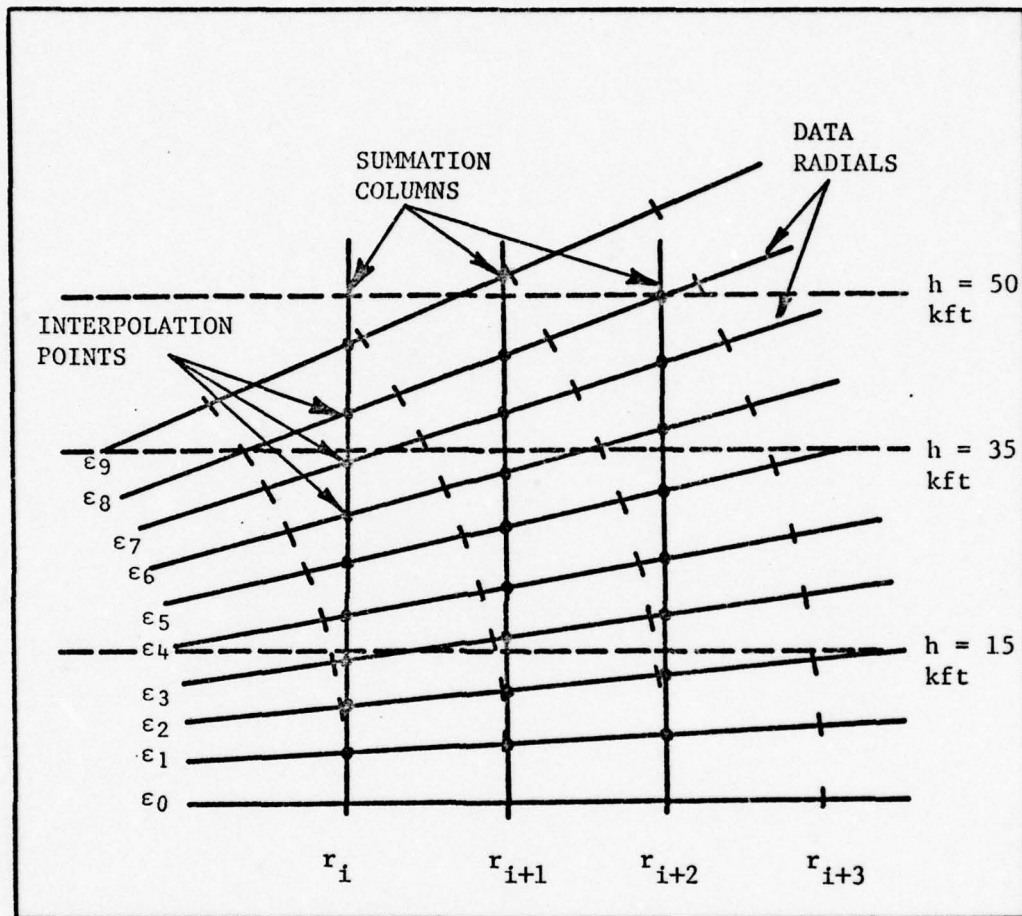
Fig. 3. Interpolation points in the plane of α used in constructing PVSZ layers.
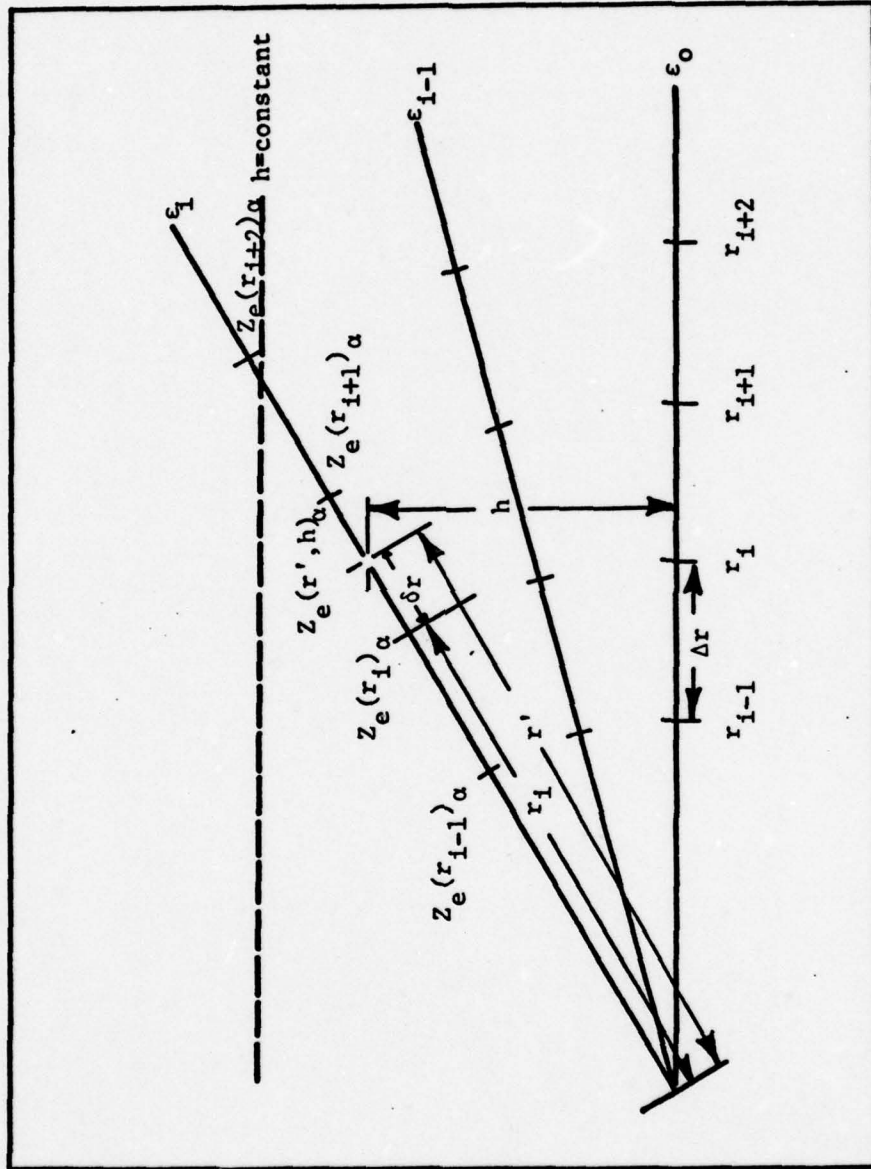
Fig. 4. The interpolation of $Z_e(r', h)_\alpha$ along a radial (ϵ_i) in the plane of α.

1. Proceed sequentially in range along a given radial (α_i) until the first non-zero reflectivity factor is found.

2. If the reflectivity factors at the given range, r_i, and at r_{i+1} are equal, no interpolation is required.

3. If the reflectivity factors are unequal, then calculate the radial distance, r', to the point on the data radial that intersects the vertical column extending above the applicable range gate, r_i, at the surface. Here h is given by

$$h = r_i \tan\varepsilon_i + \frac{r_i^2}{2R'}, \tag{19}$$

where $R' = \frac{4}{3}R$ and r' is given by

$$r' = \sqrt{r_i^2 + h^2} \tag{20}$$

Equation (19) includes corrections for both Earth's curvature and refraction of the radar beam under standard atmospheric conditions.

4. Compute the distance from r_i to r'

$$\delta r = r' - r_i \tag{21}$$

If $\delta r < 1$, the four data points used in the Lagrangian cubic interpolation formula are r_{i-1}, r_i, r_{i+1}, and r_{i+2}. If $\delta r \geq 1$, i is increased by 1 and δr is decreased by 1; if $\delta r \geq 2$, i is increased by 2 and δr is decreased by 2; etc.

5. Interpolate the value of the reflectivity factor at the point (r',h) by using the Lagrangian cubic form of the interpolating polynomial given, in general terms, by

$$Z_e (r') = \sum_{k=0}^{3} Z_e (r_{i-1+k}) L_k (r') \tag{22}$$

where

$$L_k (r') = \prod_{\substack{j=0 \\ j \neq k}}^{3} \frac{r' - r_{i-1+j}}{r_{i-1+k} - r_{i-1+j}} \tag{23}$$

The form of the Lagrangian interpolating polynomial used in this program is given by

$$Z_e (r') = a_o (r' - r_i)(r' - r_{i+1})(r' - r_{i+2})$$

$$+ a_1 (r' - r_{i-1})(r' - r_{i+1})(r' - r_{i+2})$$

$$+ a_2 (r' - r_{i-1})(r' - r_i)(r' - r_{i+2})$$

$$+ a_3 (r' - r_{i-1})(r' - r_i)(r' - r_{i+1}) \tag{24}$$

where

$$a_o = \frac{Z_e (r_{i-1})}{(r_{i-1} - r_i)(r_{i-1} - r_{i+1})(r_{i-1} - r_{i+2})}$$

$$a_1 = \frac{Z_e (r_i)}{(r_i - r_{i-1})(r_i - r_{i+1})(r_i - r_{i+2})}$$

$$a_2 = \frac{Z_e (r_{i+1})}{(r_{i+1} - r_{i-1})(r_{i+1} - r_i)(r_{i+1} - r_{i+2})}$$

$$a_3 = \frac{Z_e (r_{i+2})}{(r_{i+2} - r_{i-1})(r_{i+2} - r_i)(r_{i+2} - r_{i+1})}$$

The base interval, Δr, is always constant for a particular range increment mode, so that the programming steps are greatly simplified. The off-diagonal elements of the matrix used to calculate the value of

$Z_e(r')$ are constant and thus only the diagonal elements of the matrix need be computed. If a linear interpolation is required, then only the two points immediately adjacent to r' are used.

6. Once the value of $Z_e(r',h)$ is known, the value of h is tested to determine whether $Z_e(r',h)$ is to be added into the lower (0-deg to 15 kft), the middle (15 to 35 kft), or the upper (35 to 50 kft) PVSZ layer.

If the range increment is 2 km instead of 1 km, then all the increments in this scheme are simply doubled (Ex. r_{i+1} becomes r_{i+2}, r_{i+2} becomes r_{i+4}, etc.); the interpolation scheme itself remains unchanged. This interpolation along the data radial is accomplished by a subroutine called INTRP2, which also accomplishes the vertical integration of liquid water content (VIL). This procedure uses an algorithm developed by Greene (1971) and is based on the relationship

$$M* = 3.44 \times 10^{-6} \int_{h_{bottom}}^{h_{top}} Z_e^{4/7} \, dh \tag{26}$$

where M* is the VIL in units of kgm^{-2} and h is the height in meters.

Conversion to Rectangular Coordinate System

The other major interpolation scheme is used to map the reflectivity values from cylindrical coordinates into a rectangular coordinate system (x,y,h) where x and y are the rectangular coordinates on a flat Earth's surface and h is held constant. The technique is termed a quadratic interpolation scheme but is basically a finite-difference form of the Taylor series expansion in two dimensions, truncated after

the second-order terms. _Greene_ (1971) presents a complete discussion of the technique. Briefly, however, the scheme entails selection of the nearest six $(r,\alpha)_h$ grid points from the nine possible grid points closest to the $(x,y)_h$ point in question. For example, in Figure 5, the ith point is the closest to the desired point $(x,y)_h$. Therefore, the points (r_i,α_i), (r_{i+1},α_i), (r_{i-1},α_i) are always selected along with (r_i,α_{i+1}) and (r_i,α_{i-1}). The sixth point is determined by the sign of δx and δy. The sixth point, in any case, will always be such that the point $(x,y)_h$ is encompassed by the nearest four points. With $\delta x = \alpha' - \alpha_i$ and $\delta y = r' - r_i$, the sixth point is chosen based on the following conditions:

1. $\delta x \geq 0$

    $\delta y \geq 0$ $\qquad\qquad\qquad\qquad (r_{i+1},\alpha_{i+1})$

2. $\delta x \geq 0$

    $\delta y < 0$ $\qquad\qquad\qquad\qquad (r_{i-1},\alpha_{i+1})$

3. $\delta x < 0$

    $\delta y \geq 0$ $\qquad\qquad\qquad\qquad (r_{i+1},\alpha_{i-1})$

4. $\delta x < 0$

    $\delta y < 0$ $\qquad\qquad\qquad\qquad (r_{i-1},\alpha_{i-1})$

The quadratic interpolation function is given by

$$Z_e(x,y) = a_1 + a_2\delta x + a_3\delta y + a_4\delta x^2 + a_5\delta y^2 + a_6\delta x\delta y \qquad (27)$$

where δx is the percentage of distance from the azimuth of the (x,y) grid point to the nearest data azimuth, and δy is the percentage of
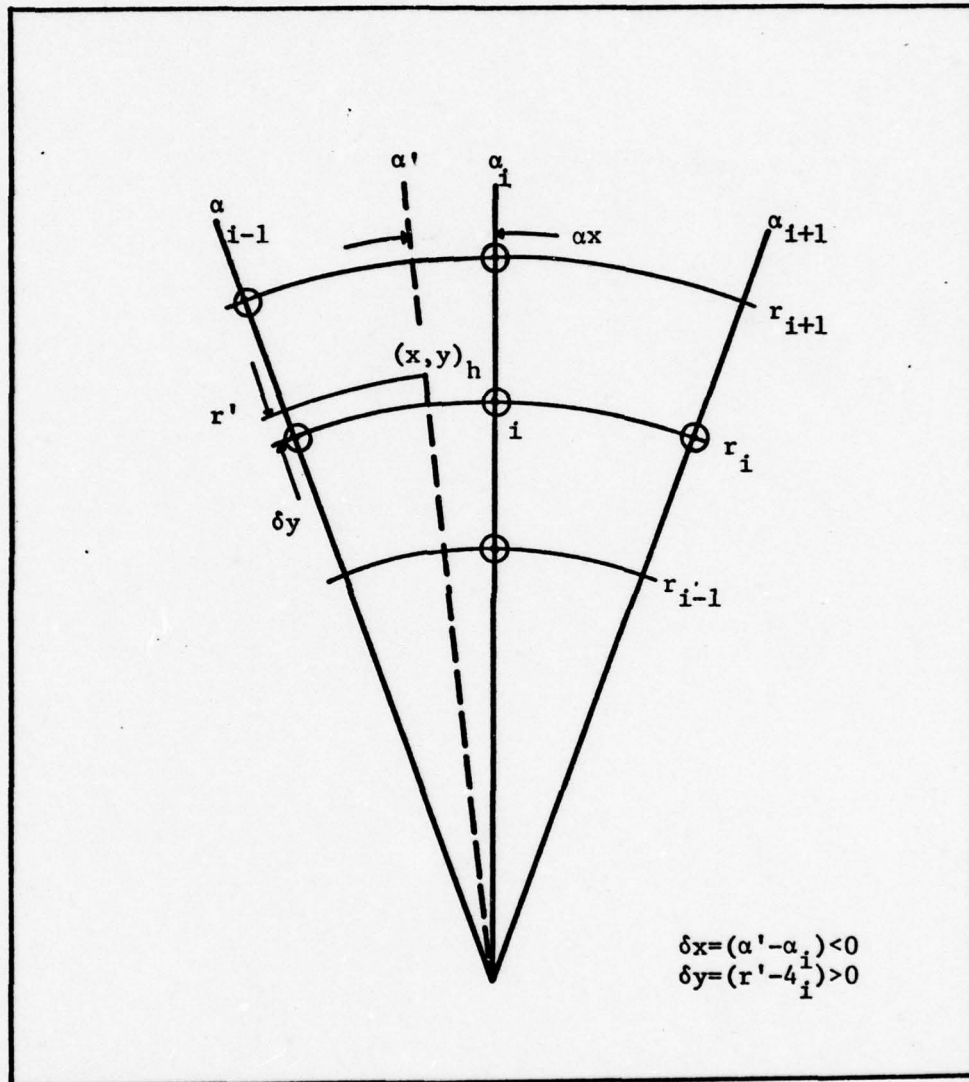
Fig. 5. Selection of the six grid points used in the interpolation of $Z_e(x,y)$ in the horizontal plane of h.

distance from the grid point to the nearest range gate.

The a_i coefficients are defined as

$$a_1 = Z_e (r_i, \alpha_i)$$

$$a_2 = [Z_e(r_i, \alpha_{i+1}) - Z_e(r_i, \alpha_{i-1})] / 2$$

$$a_3 = [Z_e(r_{i+1}, \alpha_i) - Z_e(r_{i-1}, \alpha_i)] / 2$$

$$a_4 = Z_e(r_i, \alpha_{i+1}) - a_i - a_2$$

$$a_5 = Z_e(r_{i-1}, \alpha_i) - a_1 + a_3$$

and a_6 is determined according to the sign of δx and δy to be

1. $\delta x \geq 0$ $a_6 = Z_e(r_{i+1}, \alpha_{i+1}) - a_1 - a_2$

    $\delta y \geq 0$ $- a_3 - a_4 - a_5$

2. $\delta x \geq 0$ $a_6 = a_1 + a_2 - a_3 + a_4 + a_5$

    $\delta y < 0$ $- Z_e(r_{i-1}, \alpha_{i+1})$

3. $\delta x < 0$ $a_6 = a_1 - a_2 + a_3 + a_4 + a_5$

    $\delta y \geq 0$ $- Z_e(r_{i+1}, \alpha_{i-1})$

4. $\delta x < 0$ $a_6 = Z_e(r_{i-1}, \alpha_{i-1}) - a_1 + a_2$

    $\delta y < 0$ $+ a_3 - a_4 - a_5$ (28)

If, however, the quadratic interpolation results in a negative value for $Z_e(x,y)$, then a linear interpolation scheme which uses the

four data points immediately surrounding (x,y) is employed to obtain the interpolated value of $Z_e(x,y)$. This linear interpolation takes the form

$$A = Z_e(r_{i+1}, \alpha_{i-1}) + [Z_e(r_{i+1}, \alpha_i) - Z_e(r_{i+1}, \alpha_{i-1})] (\delta x)$$

$$B = Z_e(r_i, \alpha_{i-1}) + [Z_e(r_i, \alpha_i) - Z_e(r_i, \alpha_{i-1})] (\delta x)$$

$$Z_e(x,y) = B + (A - B)(\delta y) \tag{29}$$

If the grid point falls on a data radial, then a linear interpolation is performed along that radial between the range gates on either side of the grid point.

If either 2 deg or 2 km data are being processed, the appropriate increments (α_{i+1} or r_{i+1}, etc.) are all doubled, as they were in the Lagrangian cubic interpolation scheme. The interpolations involved in this conversion from cylindrical to rectangular coordinates are performed by a subroutine called QD2.

Mechanics of the Computer Program

This computer program takes digital radar reflectivity data from the TAMU digital weather radar system, which has been recorded on 9-track tape, and uses these data to compute and produce:

1. Zero-degree tilt reflectivity maps;

2. Partial vertically-summed reflectivity (Z) maps (PVSZ) for three layers (sfc to 15 kft, 15 to 35 kft, and 35 to 50 kft); and

3. Vertically integrated liquid water content (VIL) maps.

The program will process data recorded in all four modes possible with

this radar system: 1 deg by 1 km, 1 deg by 2 km, 2 deg by 1 km, and 2 deg by 2 km.[5] However, it will only process data from one radar at a time, either the 3 cm or the 10 cm radar. The complete program, including comments and job control language (JCL), is provided in Appendix A for reference.

Program Inputs

The program requires three inputs, two on punch cards and one on magnetic tape. The first data card is the radar calibration data. It is used by the subroutine LOAD to reproduce the radar calibration curve, which converts each of the 256 digital integers of the raw reflectivity data (numbered from 0 to 255) to equivalent dBm values. The data card contains eight integers and one real number, all positive, as in the example below:

32 27 60 98 139 171 201 233 107.5

The real number is the radar's minimum detectable signal (MDS) in dBm. The first integer is the number of digital integers that are assigned the MDS for their equivalent dBm value (32). The next integer is the total number of digital integers assigned values before the equivalent dBm value increases to 10 dBm above MDS (from -107.5 to -97.5 dBm)(37). The third integer is the total number of digital integers assigned values before the equivalent dBm value increases another 10 dBm (total

---

[5]When first encountered by this investigator, this computer program would only process data recorded in the 1 deg by 1 km mode. This investigator made all subsequent modifications to the program to enable it to process data recorded in the other three modes of collection.

from -107.5 to -87.5)(60). This process continues until all eight
integer locations on the data card have been filled.

The second data card provides the initializing information for the
radar scan sequence. One of these cards is required for each complete
scan sequence that is to be processed. An example is

162-3826935106402002321008200515

which is broken up into its individual components and defined below
(see Figure 6).

(162)(-38)(269)(351)(06)(40)(200232)(10)(08)(200515)

ILEFT is the distance east (-) or west (+) from TAMU to the
lower left corner of the 100 x 100 km grid, plus two. For example, 160
km west = 162.

JDOWN is the distance north (-) or south (+) from TAMU to the
lower left corner of the 100 x 100 km grid, plus two. For example,
40 km north = -38.

KAZ is the desired starting azimuth for data processing to load
the grid box, moving clockwise. KAZ may be several degrees short of
the grid box, but may not err on the long side. Example is 269 deg.

LASTAZ is the last azimuth needed to load the grid box, and it
may be several degrees beyond the end of the box, but not short of it.
Example is 351 deg.

NTLT is the last elevation angle incremented by 1 deg in the tilt
sequence. Example is 6 deg.
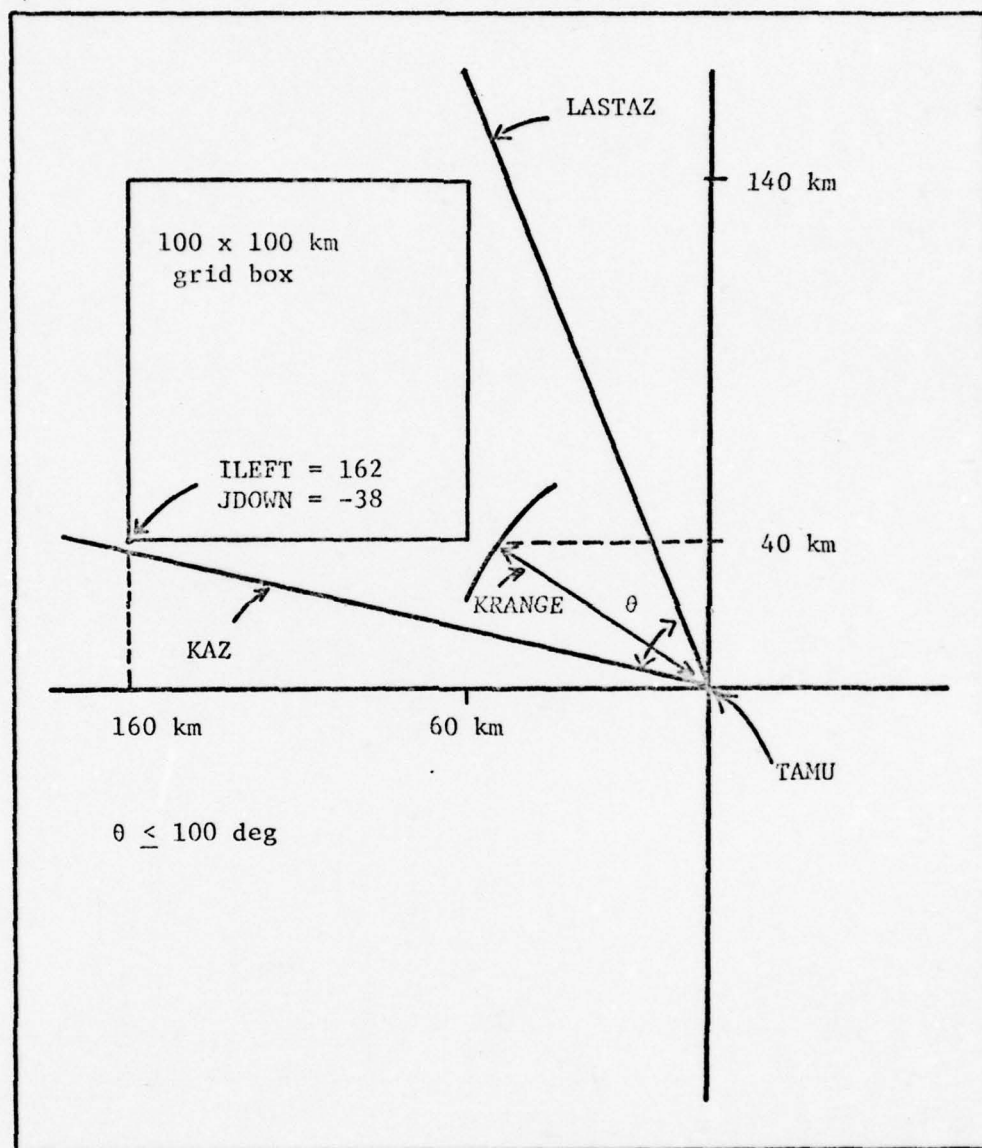
Fig. 6. Computer program initialization parameters.

KRANGE is the radial distance to the nearest point in the grid box. It also may err on the short side, but not on the long side. Example is 40 km.

ISTRT is the starting time of the scan sequence, local time, in hours, minutes, and seconds. Example is 20:02:32.

IRIT is the tape unit onto which the output data are written, defined in the JCL. Example is 10.

IRR is the tape unit from which the input data are read, defined in the JCL. Example is 08.

NENDT is the end time of the scan sequence, as above. Example is 20:05:15.

There are several important input limitations that must be observed. These are:

1. KAZ and LASTAZ must both be odd azimuths.

2. KRANGE must be an even range.

3. The angle described by KAZ and LASTAZ must not exceed 100 deg.

4. The program only processes data out to a range of 200 km.

The final form of input is the magnetic data tape itself. It is a nine track tape with data recorded in sequential logical records, each record being composed of 1744 eight-bit words (bytes). The first 24 words comprise the header group (see Figure 7) and the last 1720 contain the 860 words of DVIP data, which are recorded in every other word. The 1720 word array on the tape is called (LOGC(I), I = 1,1720), and when the tape is read, only every other word is read (I = 2,1720,2) and the resulting 860 values of raw reflectivity data are placed in the array IHWORD(I).

MAGNETIC TAPE DATA FORMAT (ONE RECORD)

	TRACK NUMBER (LOGICAL TRACKS)	1 2 3 4 5 6 7 8 9
		1 1 1 1 DATE 100's
		1 1 1 1 DATE 10's
		1 1 1 1 DATE 1's
		1 1 1 1 HOUR 10's
		1 1 1 1 HOUR 1's
		1 1 1 1 MIN 10's
		1 1 1 1 MIN 1's
		1 1 1 1 SEC 10's
		1 1 1 1 SEC 1's
		1 1 1 1 SPARE
		1 1 1 1 SPARE
		1 1 1 1 SPARE
RADAR BEING RECORDED (3 or 10)	1 1 1 1 ID
DEGREES (AZ)	1 1 1 1 DS
RANGE BIN SELECTION	1 1 1 1 RI
NUMBER OF PULSES INTEGRATED	1 1 1 1 SA
RATE ERROR	1 1 1 1 RE
PARITY ERROR	1 1 1 1 PE
	1 1 1 1 AZ 100's
AZIMUTH INFORMATION	1 1 1 1 AZ 10's
	1 1 1 1 AZ 1's
	1 1 1 1 EL 10's
ELEVATION INFORMATION	1 1 1 1 EL 1's
	1 1 1 1 EL 0.1's

CODE	1	2	
ID	3	10 cm	**
DS	1°	2°	
RI	1 Km	2 Km	
SA	15	31	

** ID code shall be
hard wired to indi-
cate either 3 or 10
cm radar recorder.
Playback shall be on
the 3 cm radar tape
recorder.

8-BIT DVIP DATA
- - - - - - - - - -

RECORDED AT EITHER 1° OR
2° OF AZIMUTH. IN 1 Km
RANGE MODE: 2 DATA SETS
PER RECORD. IN 2 KM
RANGE MODE: 4 DATA SETS
PER RECORD

Fig. 7. Magnetic tape data recording format.

Each logical record contains either two or four radials of data,
depending on the range increment selected, and from two to eight
degrees of azimuthal area coverage, depending on the azimuth increment
selected. In the 1 km mode, the first radial of data is contained in
IHWORD (1-430) and the second in IHWORD (431-860). In the 2 km mode,
the first radial is contained in IHWORD (1-215), the second in IHWORD
(216-430), the third in IHWORD (431-645), and the fourth in IHWORD
(646-860). Likewise, in the 1 deg mode, the first radial of data
represents α, the second $\alpha + 1$, the third and fourth (in the 2 km mode)
$\alpha + 2$ and $\alpha + 3$ deg. In the 2 deg mode, the radials represent α, $\alpha + 2$,
$\alpha + 4$, and $\alpha + 6$ deg, each increment being two degrees wide, for a
total areal coverage of eight degrees.

Main Program

The first thing the main program does is assign a value to WAVEC,
which represents the radar constant, and is different for each radar
(see pg. 14). This value must match that of the radar that generated
the data being processed.

The next thing accomplished is the reconstruction of the radar
calibration curve and the assignment of equivalent dBm values to the
256 digital integers by the subroutine LOAD.

Then the initializing data card is read, and most of the values
contained on it printed out below the radar calibration curve for
reference.

The program then calls the subroutine DIVIDE, which computes the
number of interpolation points contained in each PVSZ layer above each

range gate, and stores them in the arrays IDIV1(I), IDIV2(I), and IDIV3(I).

Then the first logical record of data is read from tape and the time of the record ITIME is tested against the desired start time ISTRT. If ITIME is less than ISTRT, another record is read and tested, until one is found that is within the desired time. This data record is then tested for range and azimuth increments, and the appropriate increments (IADD for azimuth and IADDR for range) are assigned for use throughout the remainder of the program. The next test is to see if the azimuth of the first data radial falls within the area of interest, that is, between KAZ and LASTAZ. If so, processing begins, but if not, the azimuth of the second radial is tested, etc. If the last radial in that record does not fall within the required bounds, then another record is read, and the procedure continues until the first data radial is found that falls within the area of interest.

Once a radial is found that lies between KAZ and LASTAZ, it is converted from azimuth to coded form II, where KAZ is II = 1, and II increases sequentially clockwise. Then the elevation angle is tested, first by a library subroutine ATOI, and then against a reference angle, PTILT. ATOI checks to ensure that the integer to binary conversion of the elevation angle was done correctly. A non-zero result returned from this test ends the program. PTILT is a reference angle that is initialized at 0.0 deg at the start of the program. If the elevation angle, TILT, is larger than PTILT, it means that the zero-tilt portion of the scan is over, and the program prints out the zero-tilt reflectivity map, increments PTILT up to the current value of TILT, then

begins processing the data radials that go into the three PVSZ layers. If, however, TILT becomes more than 0.5 deg smaller than PTILT, then the program assumes that the scan sequence is over, and it terminates processing data radials, prints out all the remaining maps, and prepares to start a new scan sequence.

Now the actual processing of the reflectivity data begins. The first 180 elements of the first data radial, IHWORD(1-430) or (1-215), are loaded into the array ICLASS(I) in positions 21-200, since the first 20 km of range are blanked out by the DVIP, and the first element recorded is the 21st range gate. Then the reflectivities for 100 km of range are computed, beginning at KRANGE plus one range increment. If the digital value in ICLASS is less than or equal to 34, the reflectivity ZW(II,I), is set to 0.0, since values of 34 or less represent reflectivities below the MDS of the radar. The reflectivity is computed according to Eq (10) on pg. 13. If the tilt angle is less than 0.5 deg, then the interpolated reflectivity data are added into the lower PVSZ layer after being divided by the appropriate IDIV1 divisor. The interpolated reflectivity factors at each range gate in a layer cannot simply be summed vertically, because there are a different number of factors to be summed in each layer. The results would be erroneous gradients of reflectivity. Thus the value of each reflectivity factor is divided by the number of tilt angles of data that are actually available in the applicable layer for that range. If the tilt angle is greater than 0.5 deg, then the program waits until all 100 reflectivities have been computed, and then sends them to the INTRP2 subroutine. INTRP2 interpolates the reflectivities along the radial, converts the data to cylindrical coordinates, and assigns the

reflectivities to the appropriate PVSZ layer, where they are summed and divided by the appropriate IDIV divisor. INTRP2 also accomplishes the vertical integration of liquid water content (VIL). This completes the processing of the first data radial. The remaining radials in that record are processed, and another record read, etc., until all the data for that scan sequence have been read. When either a time is read that exceeds the end time of the sequence, or the tilt angle becomes more than 0.5 deg less than PTILT, the processing terminates and the output of the four remaining maps begins.

The three PVSZ arrays represent the three layers of the storm complex, and the value of the summed reflectivity factors at any given point in a PVSZ array represents the average reflectivity in the layer at that point. Since each PVSZ layer is made up of a distinct number of 5 kft CAZM levels, the elements of each PVSZ array are multiplied by the appropriate number of CAZM levels in each layer in order to provide a weighted average reflectivity. For example, the elements of the lower PVSZ array, PVSZ1, are multiplied by three, since that layer is made up of three CAZM levels (5 kft, 10 kft, and 15 kft). Likewise, the elements of PVSZ2 are multiplied by four, and PVSZ3 by three.

From this point, the sequence of events is nearly the same for generating all of the maps, including the zero-tilt map printed earlier. First, the PVSZ array is sent to the subroutine QD2, where it is transformed from a 100 x 100 array in cylindrical coordinates to a 51 x 51 array in rectangular coordinates, still representing a 100 x 100 km grid. The rectangular grid points are 2 km apart, rather than 1 km. Upon return from QD2, the reflectivity values are converted from dBm to dBZ by

$$Z_e \ (dBZ) = 10 \ \log_{10} Z_e \ (mm^6 \ m^{-3}) \tag{30}$$

The final 51 x 51 array of dBZ values is sent to the subroutine PLOTZ, which plots the dBZ values in a 25 in x 25 in square. The printer prints out first the left half, and then the right half of the map, and they then must be taped together. The final step is to write the array on the output tape.

The VIL map is produced in the same manner, except that the elements of the VIZ array are divided by 1000 to convert them to VIL in units of kgm^{-2} before they are plotted by PLOTZ.

Once the last of the five output arrays, the VIL map, has been written onto the output tape, an end-of-file mark is put on the tape, so that these five maps comprise one file.

This completed, the program sets all the array values and counters equal to zero, and goes back to read a new data card and begin processing a new scan sequence.

The JCL that is required to make this program run is also included in Appendix A, with the statements located where they must appear in the card deck. The comments included in Appendix A should suffice to explain adequately the use of and changes to the JCL cards that are required for successful operation of the program.

Contoured Output Maps

The final stage of the output procedure is accomplished by a library subroutine called CONREC, which produces contoured reflectivity maps of the output arrays on the CALCOMP plotter. The entire contouring program, named RDRMAP, including JCL and explanatory com-

ments, is provided in Appendix B. The values that are shown for the various parameters are the ones that were used to produce all of the maps contained in this investigation.

The RDRMAP program uses the output arrays of the RADAR program (Sieland's program) as recorded on magnetic tape, to produce contoured reflectivity maps. The program will plot the entire 51 x 51 reflectivity array, or any portion of it that is of interest to the programmer. The only input required by the program is the output tape from the RADAR program. All the plotting parameters are set or initialized inside the program. The JCL required for the program is contained and explained in Appendix B. The main points of the program are discussed briefly below.

All of the subroutines in this program make extensive use of coordinate locations. It is important to realize that the locations addressed by this program are based on a rectangular coordinate system, with the origin (0,0) in the lower left corner, and not the conventional Fortran two-dimensional variable addressing system. However, the array address of the lower left corner of the plot is (1,1). Coordinates may have two forms, either integer or real numbers. The integers have a range of 1 to 1024, where each unit represents 0.01 inch on the output map. The real numbers, on the other hand, refer to a specific coordinate position (x = 6.), and the correct distance down the axis in inches is determined internally by the program. The maximum size of the output plot, for these purposes, is 10.24 in x 10.24 in, including labels, and the programmer may utilize any portion of that field.

The first subroutine called is SET, which physically sets up the graph. The form is CALL SET (XA, XB, YA, YB, XC, XD, YC, YD, LTYPE), where the arguments are defined below.

The first four arguments (XA, XB, YA, YB) establish the size of the area to be plotted. XA and YA are the position of the origin of the field. For example, XA = 110, YA = 110 indicates that the origin of the plot is to be 1.10 in to the right and 1.10 in up from the lower left corner of the field. XB and YB indicate the length of the x and y axes, starting from the point (XA,YA). The second four arguments (XC,XD,YC,YD) define the range of x and y along their respective axes. XC determines the coordinate assigned to the lower left corner of the grid, and XD the lower right corner. For example, XC = 0., XD = 25. means the scale along the x axis will range from 0 to 25, for a total of 26 coordinate addresses. The same is true for the y axis and YC (bottom) and YD (top). The last argument, LTYPE, determines the type of mapping to be done, either log or linear, in the x and y directions. LTYPE = 1 is linear in both directions.

The next subroutine called is PERIM, which has the form CALL PERIM (MGRX, MINRX, MGRY, MINRY). This subroutine draws a box around the area specified by SET, and places tick marks around the outside perimeter of the box as determined by the arguments of PERIM. MGRX and MGRY determine the number of major divisions along the x or y axis. It is important to note that the divisions are the holes, and not the tick marks. Likewise, MINRX and MINRY determine the number of minor divisions per major division. Once again, these are the holes, and not the tick marks.

The next subroutine called is PWRX, which puts the labels on the map. This subroutine must be called once for each label. The form is CALL PWRX (X,Y,ID,N,ISIZE,ITHETA,ICNT). The first two arguments (X,Y) are the positioning coordinates for the characters to be drawn, and may be either integer or real. For example, $X = 15.$, $Y = 90$ indicates that the character is to be drawn .90 in up from the bottom of the field (y coordinate) and at a position corresponding to the coordinate $X = 15$ along the x axis of the graph.

The argument ID is the character string to be drawn and takes the form of this example: 8H'IRU'MAP, where 8H reserves eight spaces for hollerith code ('IRU'MAP), IRU specifies the type of printing, and MAP are the characters printed. The coding of IRU is:

I = .13 in	R = Roman	U = upper case
P = .21 in	G = Greek	L = lower case

The argument N is simply the number of hollerith characters in ID, ISIZE determines the size of the characters, and may be either integer or real. If it is real (floating point), then it is used as a multiplication factor of I or U in ID. If it is integer, it has a different function that is not relevant to this application of this program.

The argument ITHETA determines along which orientation the characters are printed. if ITHETA = 0, the character strings are printed in the x direction, oriented vertically (normal orientation). If ITHETA = 1, the character strings are printed in the y direction, oriented horizontally.

ICNT is the centering option and is defined as follows:

ICNT = 0   (X,Y) is the center of the first character.

ICNT = 1   (X,Y) is the center of the entire string.

ICNT = 2   (X,Y) is the left edge of the first character.

ICNT = 3   (X,Y) is the center of the last character.

ICNT = 4   (X,Y) is the right edge of the last character.

The next subroutine called by the program is the CONREC subroutine itself, and this is the one that actually does the plotting and con-touring of the data array. The form of this subroutine is CALL CONREC (Z(X,Y),L,M,N,FLO,HI,FINC,NSET,NHI,NDOT).

The first argument, Z(X,Y), is the array coordinate of the lower left corner of the field to be contoured. For example, Z(1,1) will fill the entire grid box, but Z(2,2) will leave a blank margin one grid unit wide around the inside of the box. The argument L is the first dimension of the array Z in the calling program. The next two argu-ments (M,N) are the number of data values to be plotted in the x and y directions. FLO and HI are the values of the lowest and highest contour levels to be drawn, respectively, and FINC is the increment between contour levels.

The last three arguments (NSET, NHI, NDOT) control scaling, extra information on the plot, and the line pattern, and should not be changed for use with this program.

The last subroutine called by this program is PLOT, and it pro-vides pen control, and is also used to signal end-of-plot. The form is CALL PLOT(X,Y,IPEN) where (X,Y) are the page coordinates in inches of the point to which the pen is to be moved. For example, (12., 0.) moves the pen 12 inches in the x direction. The magnitude of IPEN specifies the up or down condition of the pen during its movement to

(X,Y). IPEN = 2 is for pen down, and IPEN = 3 is for pen up. If the sign of IPEN is positive, the movement results in a normal plot entrance. However, if the sign of IPEN is negative, the movement is an end-of-plot entrance, and after the pen moves to (X,Y), the value x = 0, y = 0 is assigned to the new pen location, and the plot number is incremented by one. Additionally, IPEN = 99 is used to empty the output buffer at the completion of the plot, and this must be done prior to terminating the program.

The remainder of the RDRMAP program is explained by means of comments in the progrm as it appears in Appendix B.

Radar Volume in Space

It is easy to see from Figure 8 that the volume in space of the various range bins increases rapidly both as the range increases, and as the collection mode is changed from the 1 deg x 1 km mode to one of the other modes. The illuminated radar volume, which is one half the geometric volume, is given by

$$V = \pi \left(\frac{r\theta}{2}\right)^2 \frac{h}{2} \tag{31}$$

where θ is the beamwidth in radians (assumed to be circular and 1 deg in diameter), r is the range in km, h is the length of the range bin in km, and V is the volume in km^3. Table 3 shows the approximate illuminated radar volumes enclosed by range bins in each of the four collection modes, at ranges of 50 and 150 km. Note that the volume enclosed by the 2 deg x 2 km mode is four times that enclosed by the 1 deg x 1 km mode, and that the 1 deg x 1 km volume at 150 km is nine times the
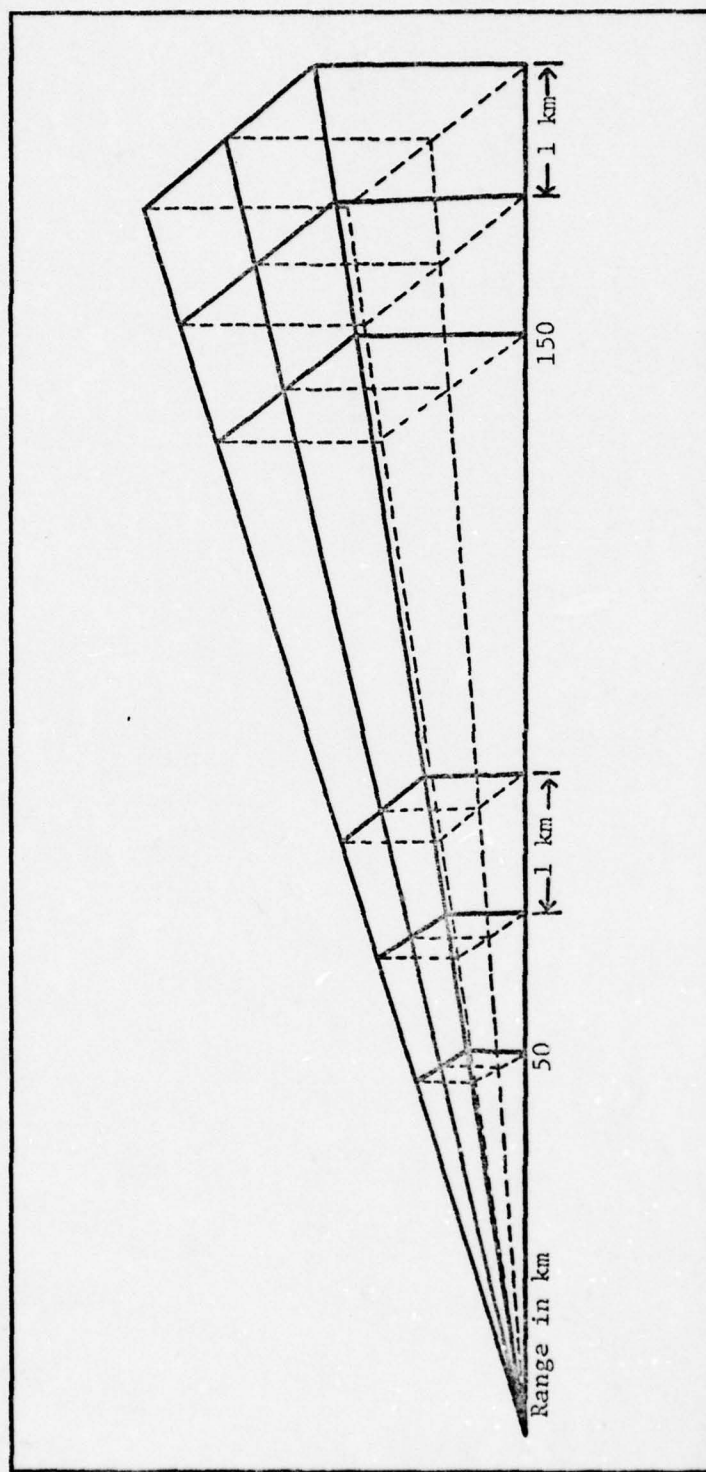
Fig. 8. Radar volume in space.

TABLE 3. Radar Volumes at Near and Far Ranges.

Collection Mode	Volume in km^3	
	50 km range	150 km range
1 deg x 1 km	0.30	2.70
2 deg x 1 km	0.60	5.40
1 deg x 2 km	0.60	5.40
2 deg x 2 km	1.20	10.80

1 deg x 1 km volume at 50 km. Even more dramatic is that the 2 deg x 2 km volume at 150 km is 36 times as large as the 1 deg x 1 km volume at 50 km, remembering that the physical volumes in space are twice the radar volumes shown in the table. Based on these considerations, it is only reasonable to suspect that a single digital value representing the mean reflectivity in a volume of 10.8 km^3 may not represent that volume as adequately as four digital values, each being the mean reflectivity of one fourth of that larger volume. The results of the investigation into this and other questions are presented in the next chapter.

CHAPTER IV

PRESENTATION AND DISCUSSION OF RESULTS

Data Acquisition and Reduction

The radar data used in this investigation were produced and recorded by the TAMU Digital Weather Radar System during the evening of 9 May 1977, as an area of light and moderate thunderstorm activity moved through the College Station area. Data were recorded simultaneously in both wavelengths (3 and 10 cm) and as near simultaneously as possible in all four modes of collection. Only zero-degree tilt data were recorded, and all the data were recorded within a period of only 3.5 minutes. The digital data were processed by Sieland's RADAR computer program, and then the final output arrays of zero-tilt reflectivity data were plotted on the CALCOMP plotter.[6] The contoured reflectivity maps presented here are reductions of the originals, which were approximately ten inches square.

Data Analysis

The data generated by this investigation were analyzed both qualitatively and quantitatively. The qualitative analysis consisted of physically superimposing the contoured reflectivity maps on one another and examining them over a light source.

---

[6]All contoured maps were produced using a library subroutine named CONREC and plotted on the CALCOMP plotter at the TAMU Data Processing Center. All isopleths on these maps are in units of dBZ.

The quantitative analysis consisted of a statistical comparison of corresponding points in two different data sets (reflectivity maps) to determine whether there was any significant difference between them. The test employed was the Student's t test, based on the assumptions discussed below.

The first assumption is that the data value assigned to each grid point in the 51 x 51 output arrays represents the mean reflectivity (sample mean, $\overline{X}_i$) for that grid square, and that each data point is derived from 31 samples. We also assume that the sample variance (s_i^2) is the same for each data set and is equal to $(5.57)^2$ dB. The null hypothesis is H_o: $\mu_1 = \mu_2$, or that there is no significant difference between the data values (means) of two corresponding grid points on different reflectivity maps (1 deg x 1 km map versus 2 deg x 2 km map, etc.). The test statistic is then given by

$$t = \frac{(\overline{X}_1 - \overline{X}_2)}{\left(\frac{s^2}{n_1} + \frac{s^2}{n_2}\right)^{1/2}} \tag{32}$$

where s^2 is the pooled variance since $s_1^2 = s_2^2$, and the critical region is defined by

$$|t| \geq t_{(1 - \alpha/2)(n_1 + n_2 - 2)} \tag{33}$$

The 1 deg x 1 km map served as the standard and the other three modes were tested against it. The test was applied stepwise to every individual pair of corresponding grid points in the two maps being compared, and the null hypothesis was either rejected or not rejected for each pair of points. The pairs of points were tested at three levels of

significance, α = .01, .05, and .10, where a significance level of α = .01 means that there is only a 1% chance of rejecting a true hypothesis; that is, there is only a 1% chance of saying that there is a significant difference between the two points, when in truth there is not. Finally, the percentages of pairs of points that were significantly different from one another were tabulated.

Comparison of 3 cm Data in the Near Range

The first analyses made were of the 3 cm data collected in all four modes within the near range, or from 20 to 60 km from the radar. The zero-tilt reflectivity maps for the four modes are shown in Figures 9 through 12. Additionally, the results of the statistical analyses of the different modes are also displayed in map form.

The 2 deg x 1 km Mode

The first comparison was between the 1 deg x 1 km mode (Figure 9), which was taken to be the standard mode in all the analyses, and the 2 deg x 1 km mode (Figure 10).[7] The 2 deg x 1 km map retains most of the features of the 1 deg x 1 km map, although there are a fair number of differences apparent. In the 2 deg x 1 km map, there is some smoothing of the details contained in the 1 deg x 1 km map, and a tendency to combine small, adjacent echo features into single features, most likely caused by the wider integration interval in the direction

---

[7]The apparent strong reflectivity gradients in the upper left hand corner of all the near range maps should be disregarded. This apparent gradient is due to the range blanking of the DVIP, which blanks out all data within 20 km of the radar.
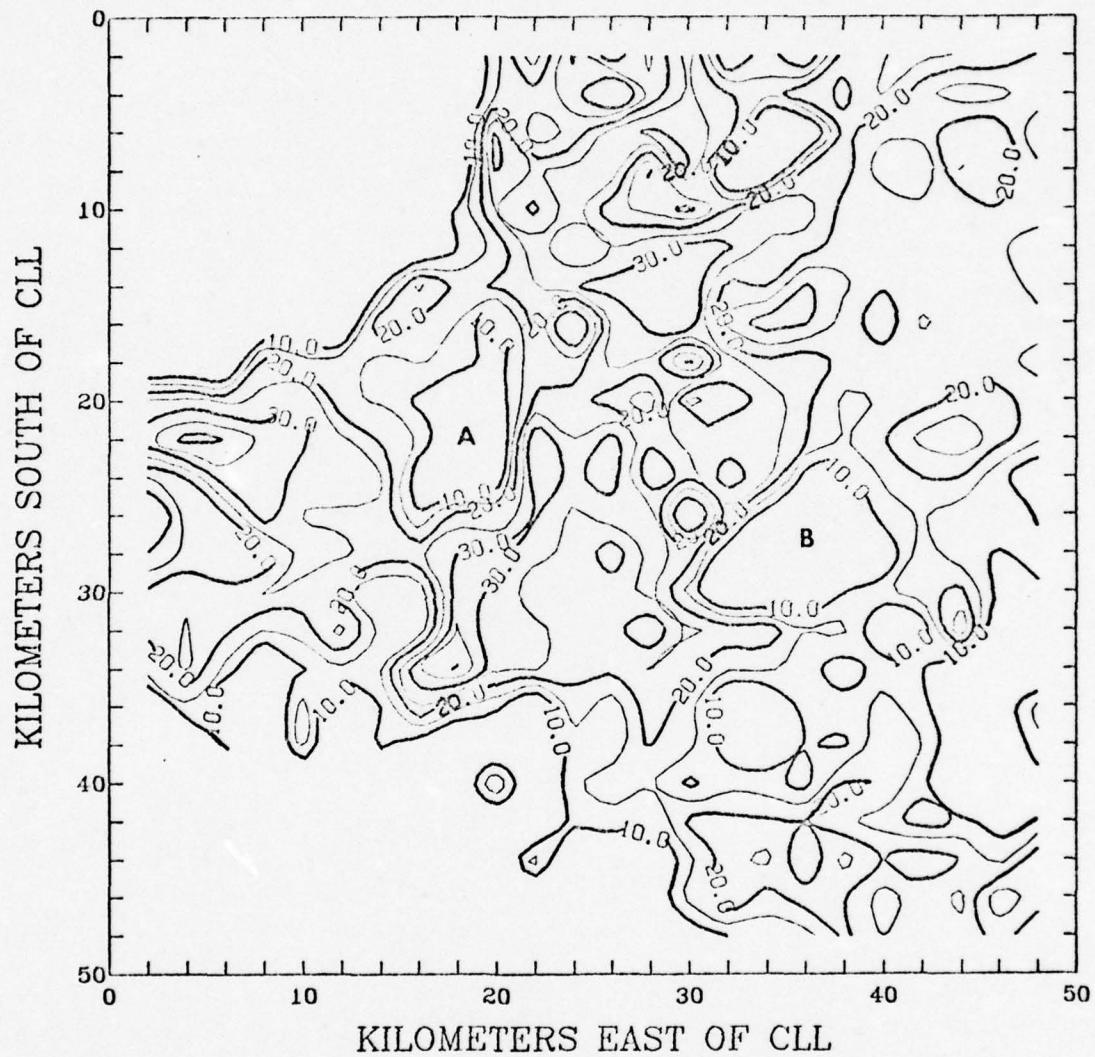
Fig. 9. Three cm reflectivity map in the near range, 1 deg x 1 km mode.
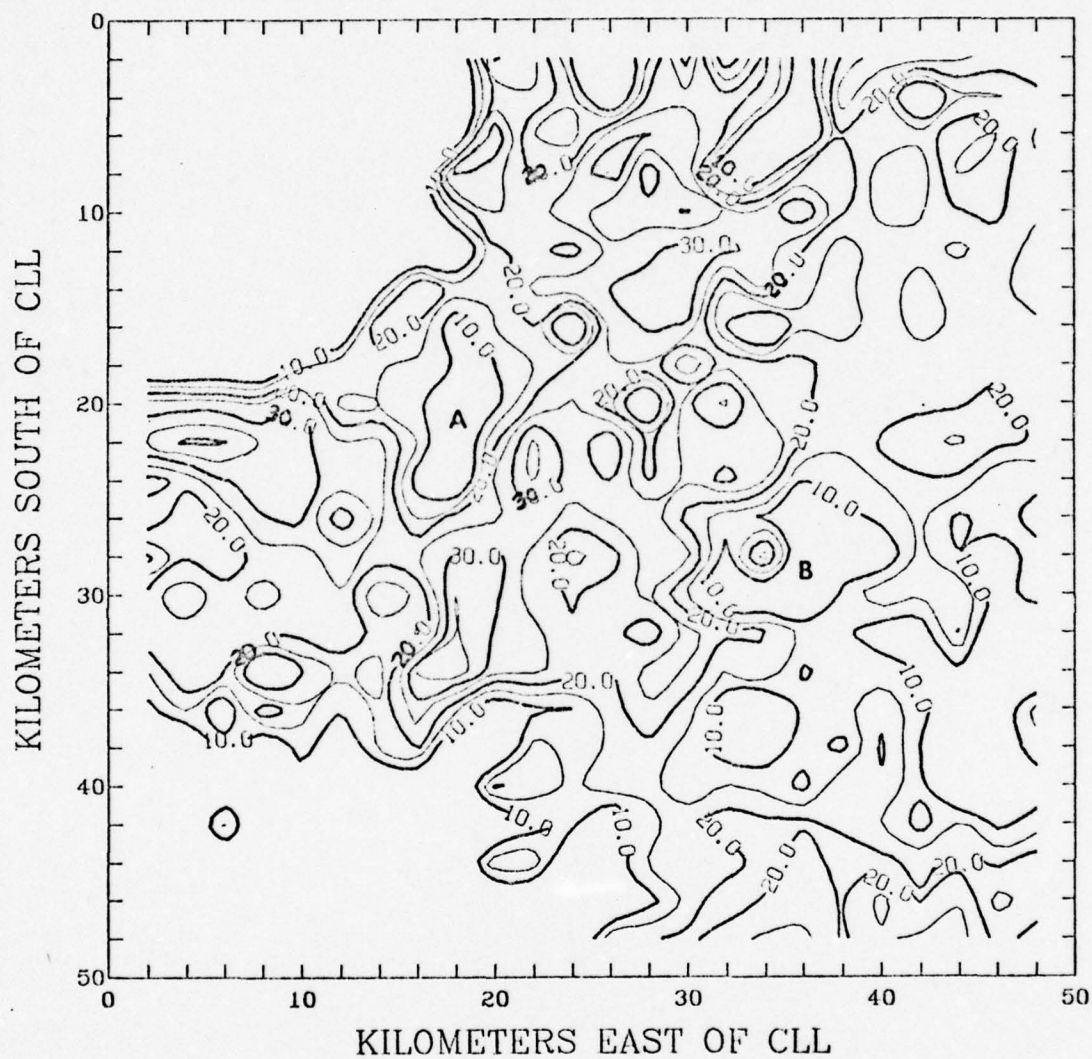
Fig. 10.   Three cm reflectivity map in the near range, 2 deg x 1 km mode.
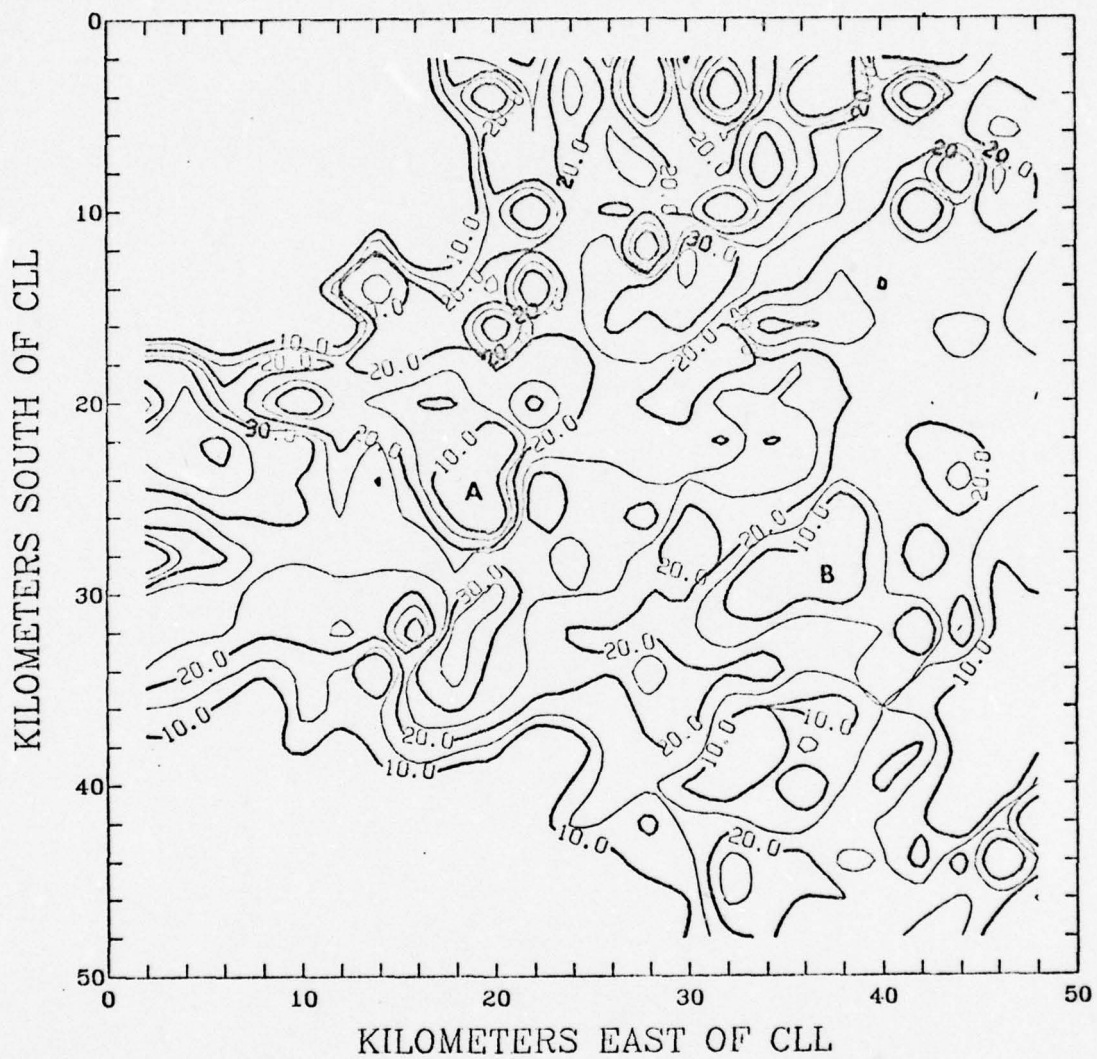
Fig. 11. Three cm reflectivity map in the near range, 1 deg x 2 km mode.
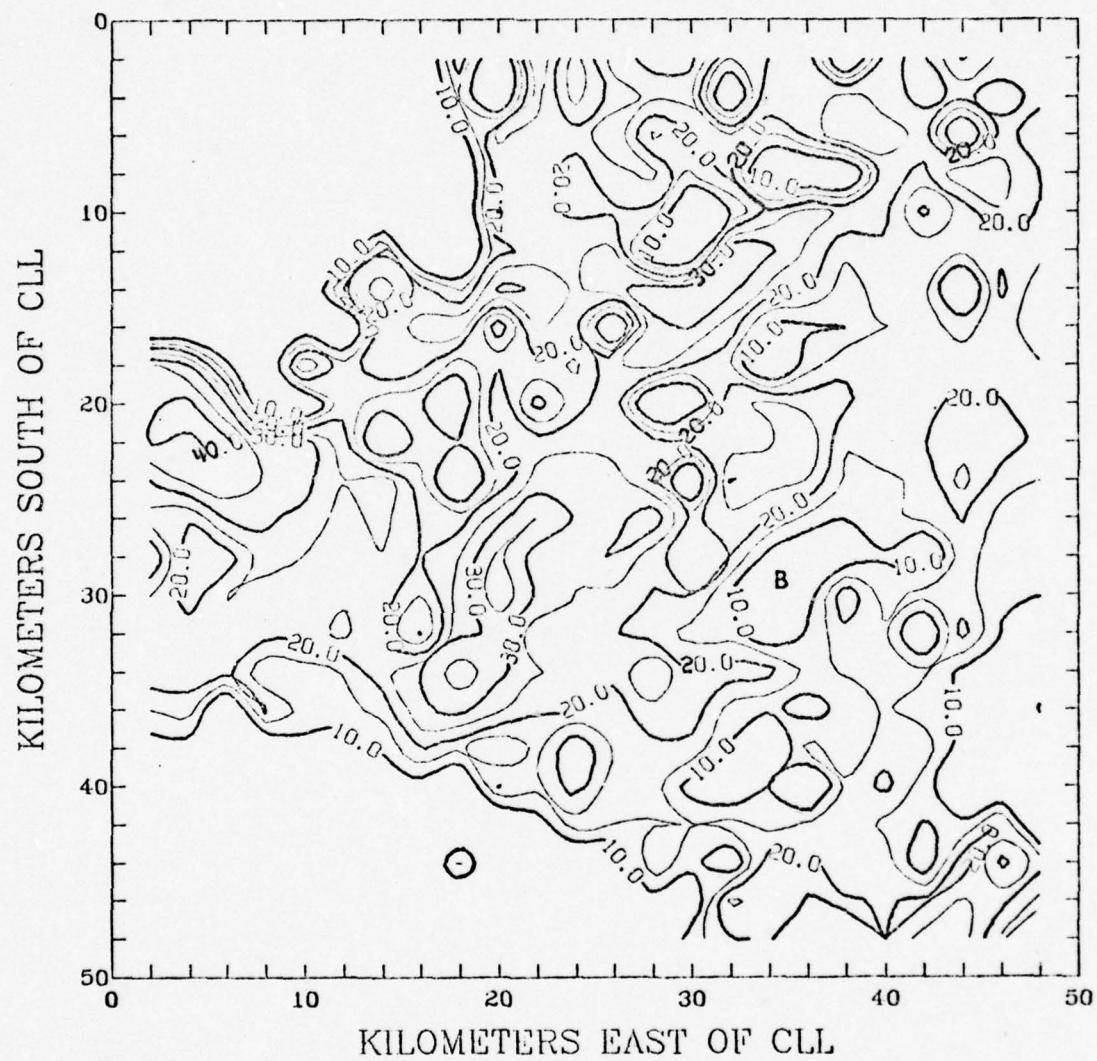
Fig. 12.   Three cm reflectivity map in the near range, 2 deg x 2 km mode.

of antenna rotation. This phenomena also results in the expansion or shift of some reflectivity features in the direction of antenna rotation (clockwise). Additionally, several of the reflectivity features with closed isopleths exhibit slightly higher dBZ values on the 2 deg x 1 km map, although not more than 5 dBZ higher, and the highest value on both maps is 40 dBZ. It also appears that the deeper a reflectivity feature is embedded inside the precipitation area, the greater the amount of smoothing and reduction in size of features that occur on the 2 deg x 1 km map, as shown in the southeast corner of these maps. The two maps do agree quite well on the two areas of significantly reduced reflectivity (near zero) shown at A and B. It is possible that these two areas represent BWERs, but a positive determination can not be made without the maps for the next several CAZM levels above these areas, or a complete lower level PVSZ map, integrated from the 0-deg tilt level to 15 kft.

The statistical comparisons of these two maps at three levels of significance (α = .01, .05, and .10) are shown in Figures 13 through 15.[8] Figure 13 shows that at a significance level of .01, 25.4 per cent of all the non-zero pairs of corresponding data points are significantly different from each other. This percentage increases to 35.4 percent for α = .05 (Figure 14) and to 43.2 percent for α = .10 (Figure 15). Examination of these figures shows that the differences

---

[8]On the statistical maps, a blank means that the two corresponding grid point values on the two maps being compared were both zero; a '.' means that there was no significant difference between the two corresponding grid points at that level of significance; an 'xx' means that the two corresponding grid points were significantly different from one another.
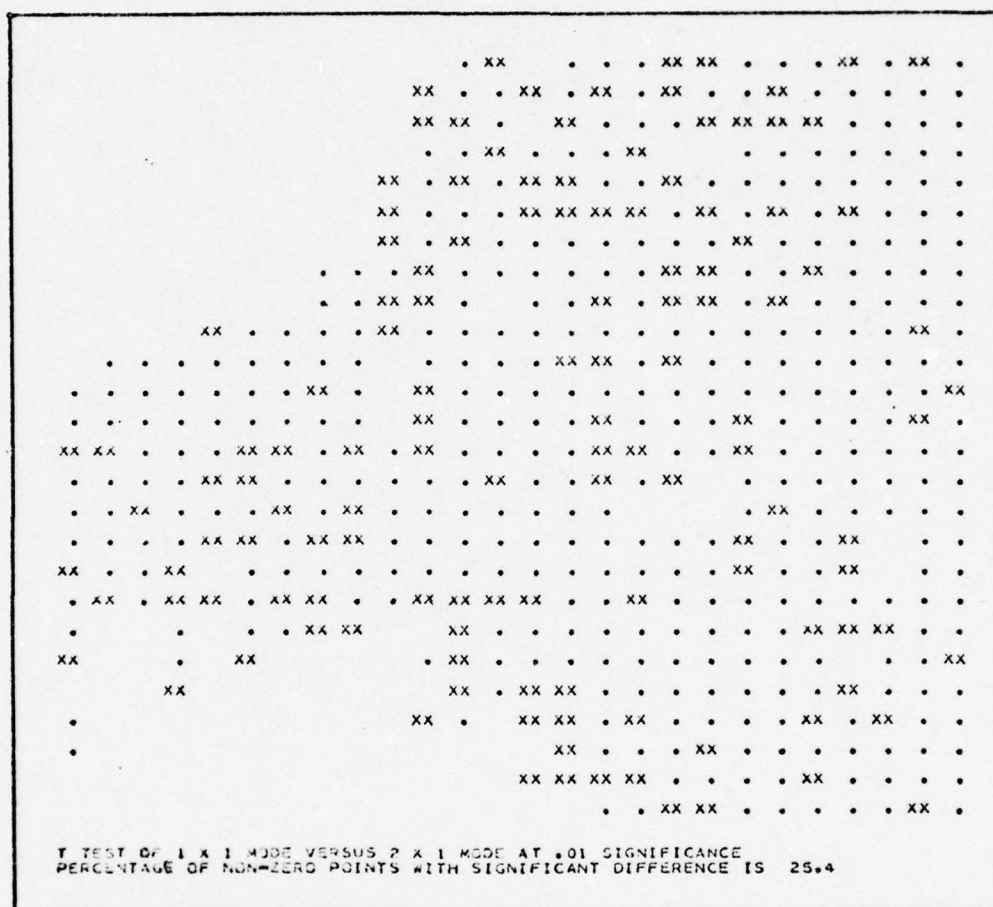
Fig. 13.   Statistical comparison of the 1 deg x 1 km and
2 deg x 1 km modes, 3 cm, near range, at .01 level of significance.
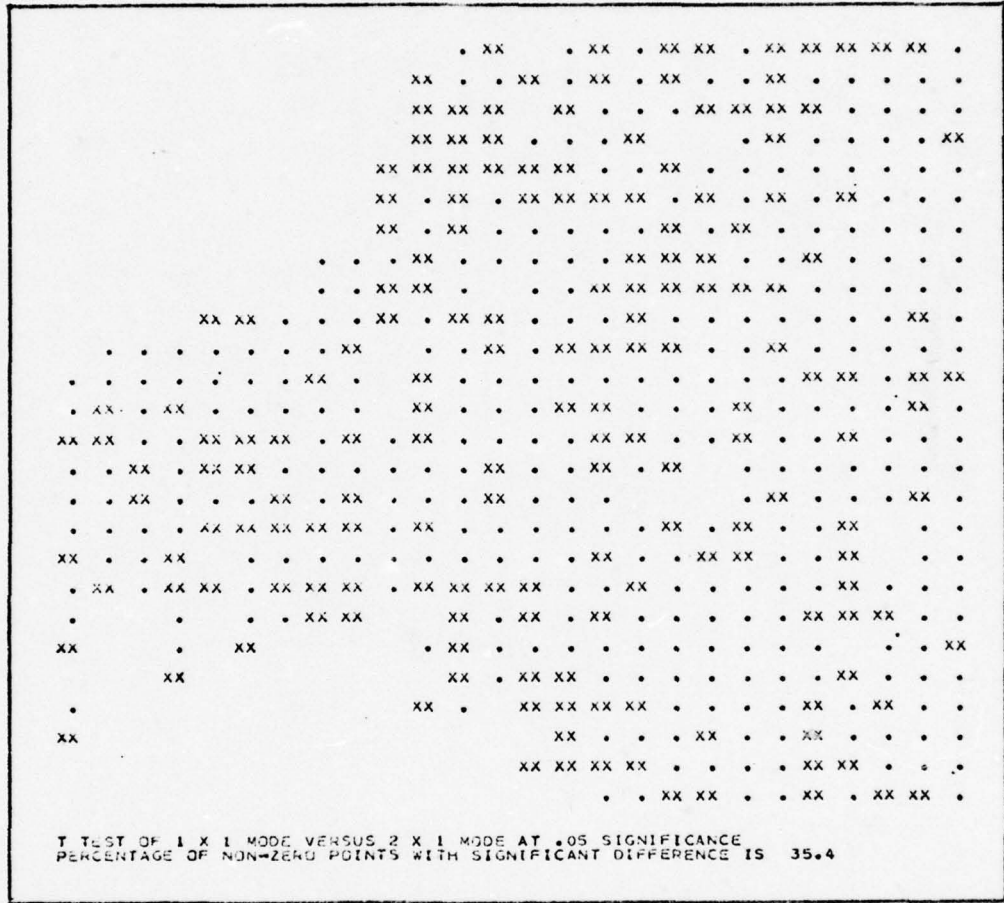
Fig. 14. Statistical comparison of the 1 deg x 1 km and 2 deg x 1 km modes, 3 cm, near range, at .05 level of significance.
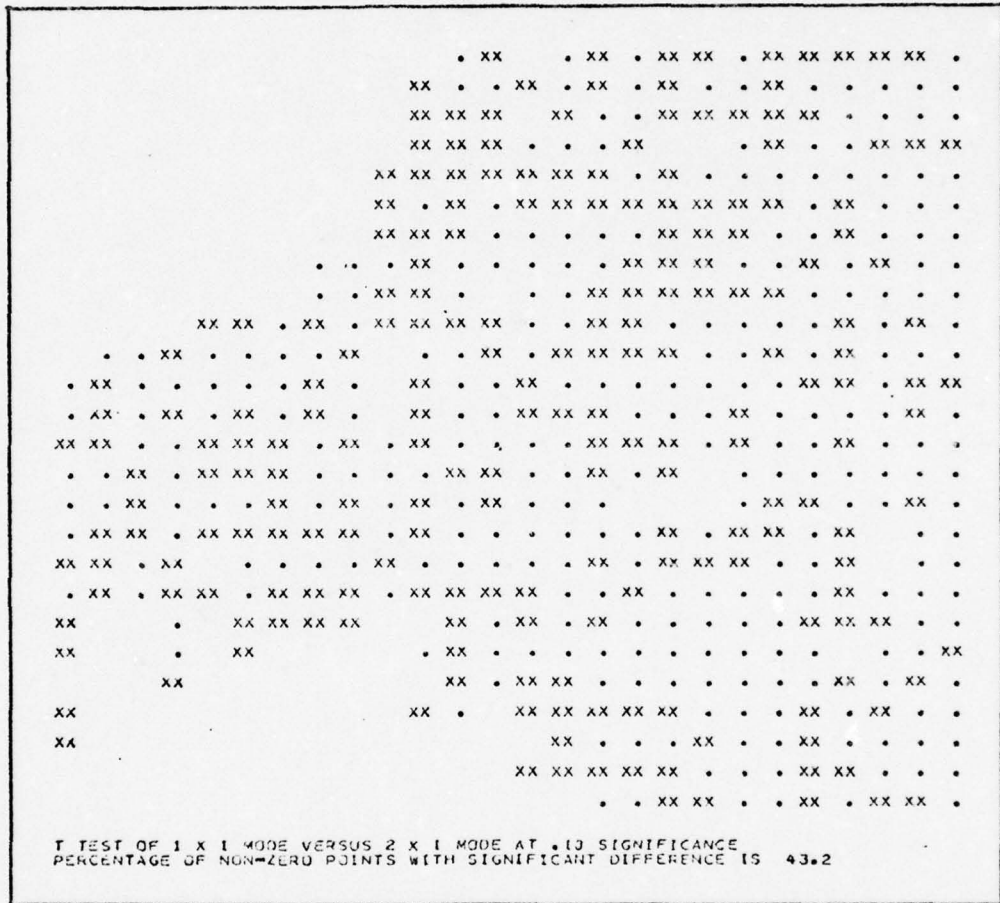
Fig. 15. Statistical comparison of the 1 deg x 1 km and 2 deg x 1 km modes, 3 cm, near range, at .10 level of significance.

occur primarily in areas with a pronounced reflectivity gradient and in the areas of maximum reflectivity values. This corresponds well with the smoothing of detail and shifting of reflectivity features observed on the contoured maps. The statistical analysis maps also show the two areas of zero reflectivity, A and B, quite well.

The 1 deg x 2 km Mode

The second comparison was made between the 1 deg x 1 km mode and the 1 deg x 2 km mode (Figure 11). The correlation between these two maps is poor, with most of the significant features of the 1 deg x 1 km map either lost or greatly distorted on the 1 deg x 2 km map. Additionally, many of the features appear to be shifted outwards in range several km, as might be expected with the longer range integration increment. The 1 deg x 2 km map also shows a considerable smoothing of the fine scale details of the reflectivity contours. The dBZ values on the two maps agree fairly well, however, and the highest observed dBZ value is once again 40 dBZ. Perhaps the best areas of agreement on the two maps are the two areas of zero reflectivity at A and B, although they are somewhat reduced in size on the 1 deg x 2 km map.

The statistical analysis at $\alpha = .05$ (Figure 16) shows that 66.2 percent of all the non-zero pairs of data points differ from one another significantly. The points that differ significantly are generally widespread everywhere except in the areas of low reflectivity. The areas A and B are just barely discernible in this map.

Fig. 16. Statistical comparison of the 1 deg x 1 km and 1 deg x 2 km modes, 3 cm, near range. Level of significance is .05.

The 2 deg x 2 km Mode

The final comparison in this group was made between the 1 deg x 1 km map and the 2 deg x 2 km map (Fig. 12). The correlation between these two maps is also quite poor, and most of the small scale detail has been washed out on the 2 deg x 2 km map. Most of the features appear to have been shifted outwards and clockwise slightly, and many of them have been stretched in the direction of antenna rotation. Although area B still shows up well, area A has lost its identity. Many of the dBZ values on the 2 deg x 2 km map are 5 dBZ lower than the corresponding values on the 1 deg x 1 km map; however, the maximum dBZ value observed is still 40 dBZ.

The statistical analysis at $\alpha = .05$ (Figure 17) shows that 66.9 percent of the pairs of non-zero data points are significantly different from one another. Once again, the only areas where the points generally do not differ are the areas of lower reflectivity. Although small, both areas A and B can be seen on this map.

Table 4 summarizes the statistical comparisons of all four modes at each of the three levels of significance.

Comparison of 10 cm Data in the Near Range

The zero-tilt reflectivity maps for the 10 cm data in the near range that were recorded simultaneously with the 3 cm data are shown in Figures 18 through 21. Once again, the 1 deg x 1 km mode was used as the standard for comparison in all the analyses.

Fig. 17. Statistical comparison of the 1 deg x 1 km and 2 deg x 2 km modes, 3 cm, near range. Level of significance is .05.
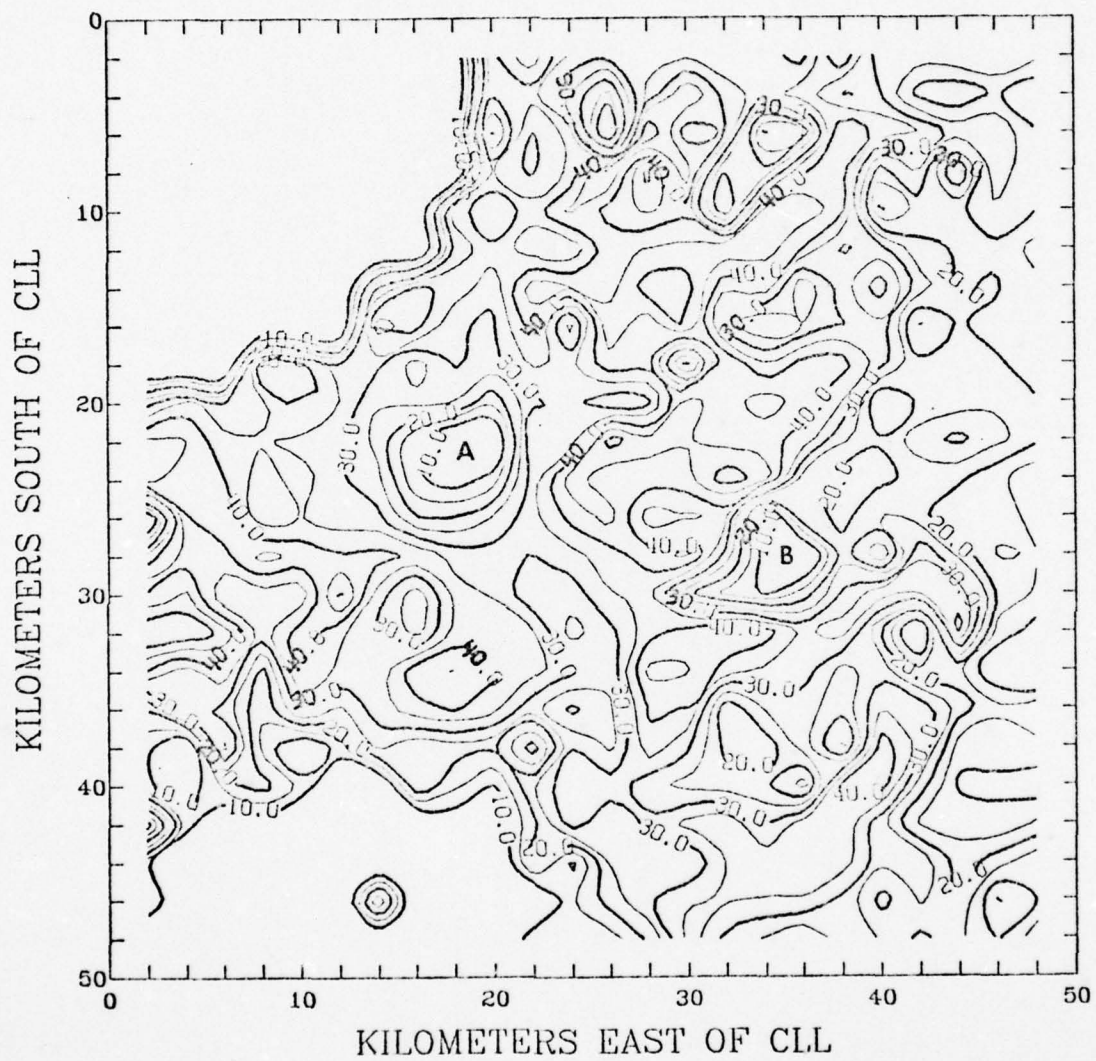
Fig. 18. Ten cm reflectivity map in the near range, 1 deg x 1 km mode.
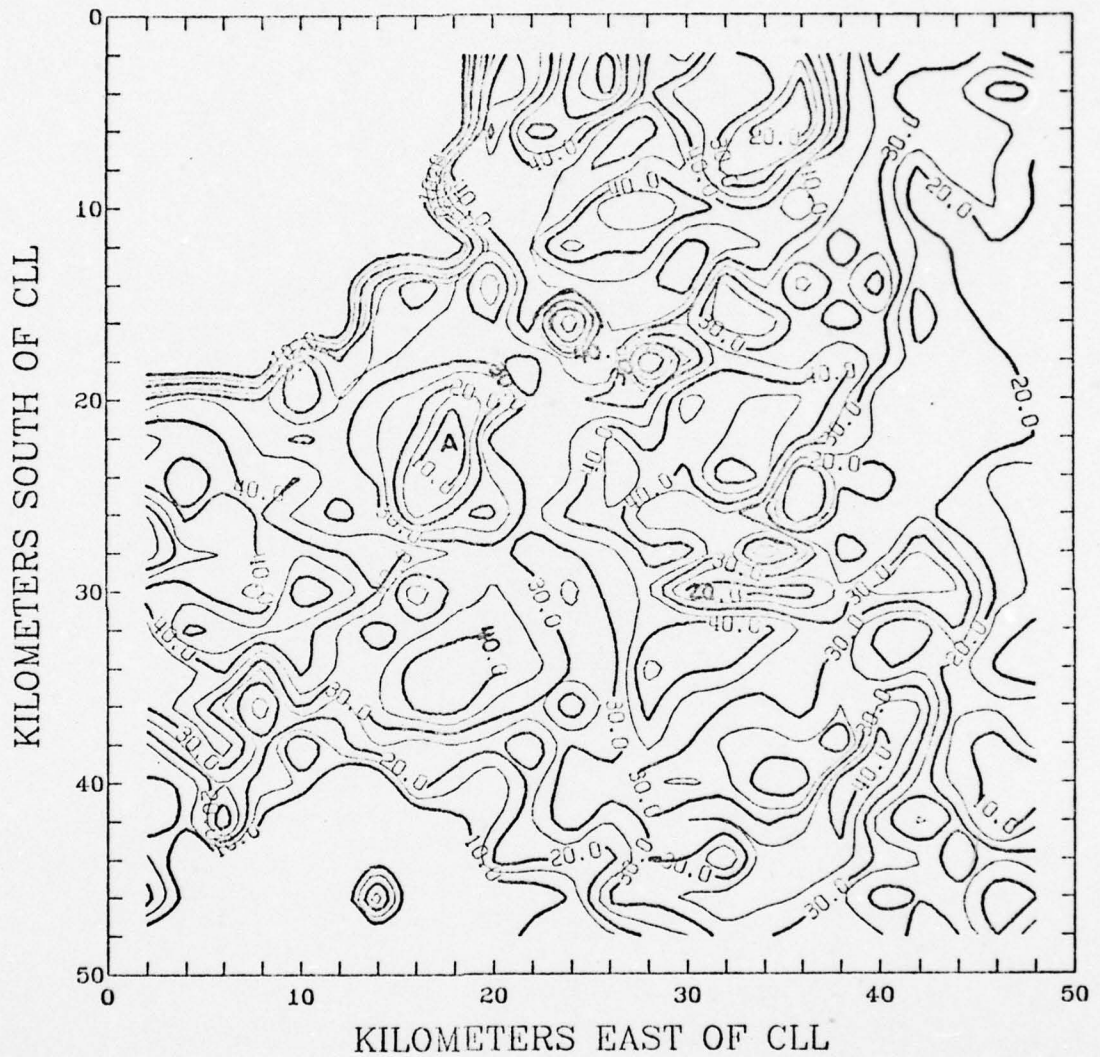
Fig. 19. Ten cm reflectivity map in the near range, 2 deg x 1 km mode.
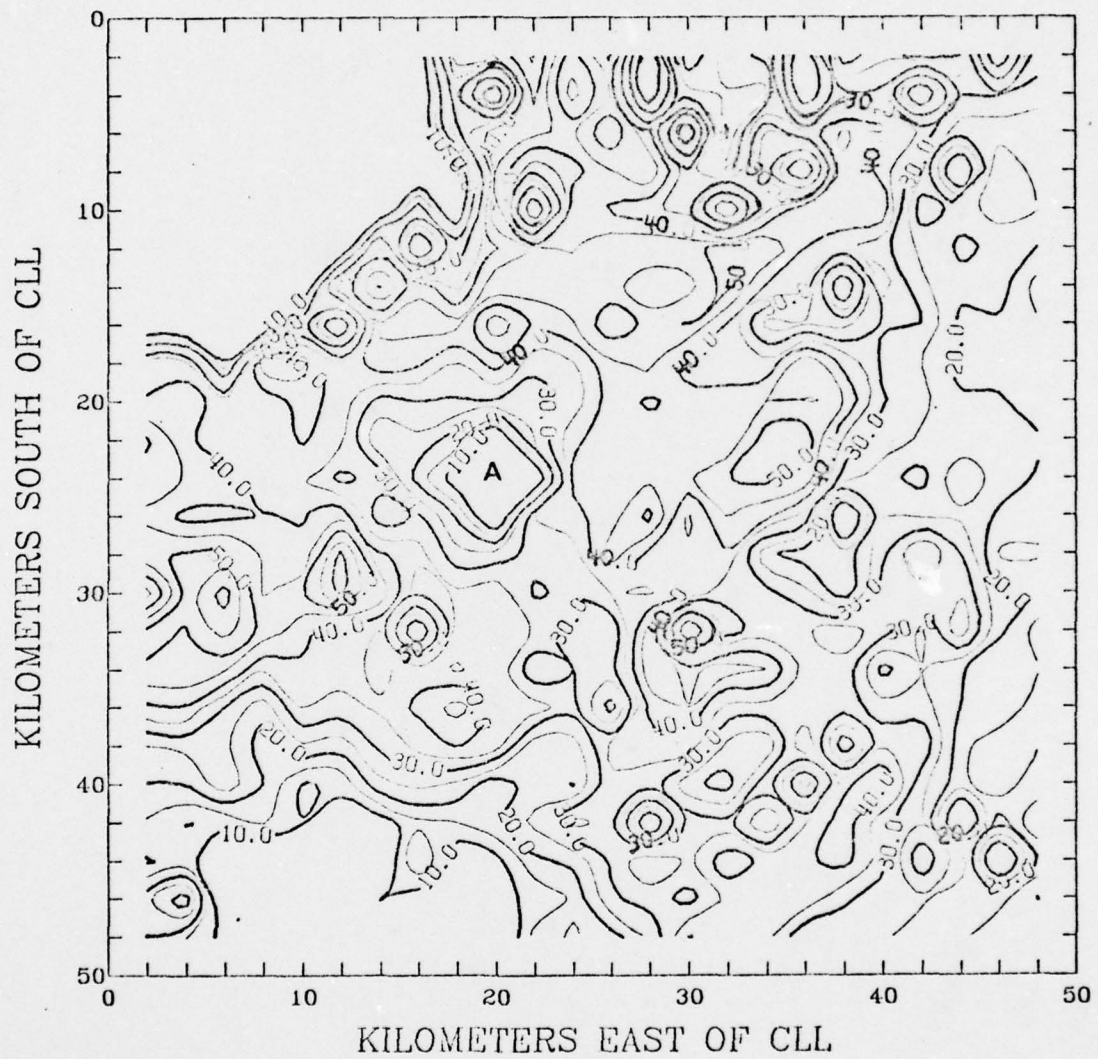
Fig. 20. Ten cm reflectivity map in the near range, 1 deg x 2 km mode.

Fig. 21. Ten cm reflectivity map in the near range, 2 deg x 2 km mode.

TABLE 4. Summary of Statistical Analyses of Collection Modes, 3 cm, Near Range.

Percentage of non-zero pairs of points with significant difference at significance level α.			
1 deg x 1 km mode compared to	α = .01	α = .05	α = .10
2 deg x 1 km	25.4	35.4	43.2
1 deg x 2 km	56.6	66.2	71.3
2 deg x 2 km	58.2	66.9	72.4

The 2 deg x 1 km Mode

The first comparison made was between the 1 deg x 1 km map (Figure 18) and the 2 deg x 1 km map (Figure 19). The most notable feature at first glance is the fact that the dBZ values of many of the reflectivity features are 10 to 20 dBZ higher than the corresponding features shown on the 3 cm maps. This is good tangible evidence of the increased attenuation by precipitation of microwave energy at wavelengths shorter than 10 cm. The correlation between these two maps is fair and the 2 deg x 1 km map retains most of the features of the 1 deg x 1 km map, although some of the detail is smoothed over. Many of the low reflectivity features have been shifted slightly in the direction of antenna rotation, and in general, the extreme low reflectivity points on the 2 deg x 1 km map tend to be 5 to 10 dBZ higher than the corresponding points on the 1 deg x 1 km map. The two large zero

reflectivity areas, A and B, show up well on the 1 deg x 1 km map
again, but only A is well defined on the 2 deg x 1 km map. Area B
is almost completely masked by a single high reflectivity point that
is located at the front edge of the area, relative to the direction of
antenna rotation. The highest reflectivity value observed on both maps
is 50 dBZ.

The statistical comparison between these two maps (Figure 22) at
the α = .05 significance level shows that 45.2 percent of all the pairs
of non-zero points differ from one another significantly. Most of the
differences occur in areas of high reflectivity gradients and small
scale high reflectivity features. This agrees well with the smoothing
of features observed in the 2 deg x 1 km map. Neither area A nor B
show up on this map.

The 1 deg x 2 km Mode

The next comparison was between the 1 deg x 1 km map and the 1 deg
x 2 km map (Figure 20). Correlation between these two maps is poor.
Most of the detail is either lost or significantly altered, and only
the most prominent reflectivity features retain their identity. There
is a noticeable shift radially outwards of many of the high and low
reflectivity features, and many of the low values are 5 dBZ higher
than those on the 1 deg x 1 km map. Additionally, many of the high
reflectivity features are 10 dBZ higher than on the 1 deg x 1 km map,
as is the maximum observed value on this map of 60 dBZ. Once again,
the zero reflectivity area at A shows up quite well, even though it
is shifted outwards almost 3 km, while that at B is not readily
apparent.
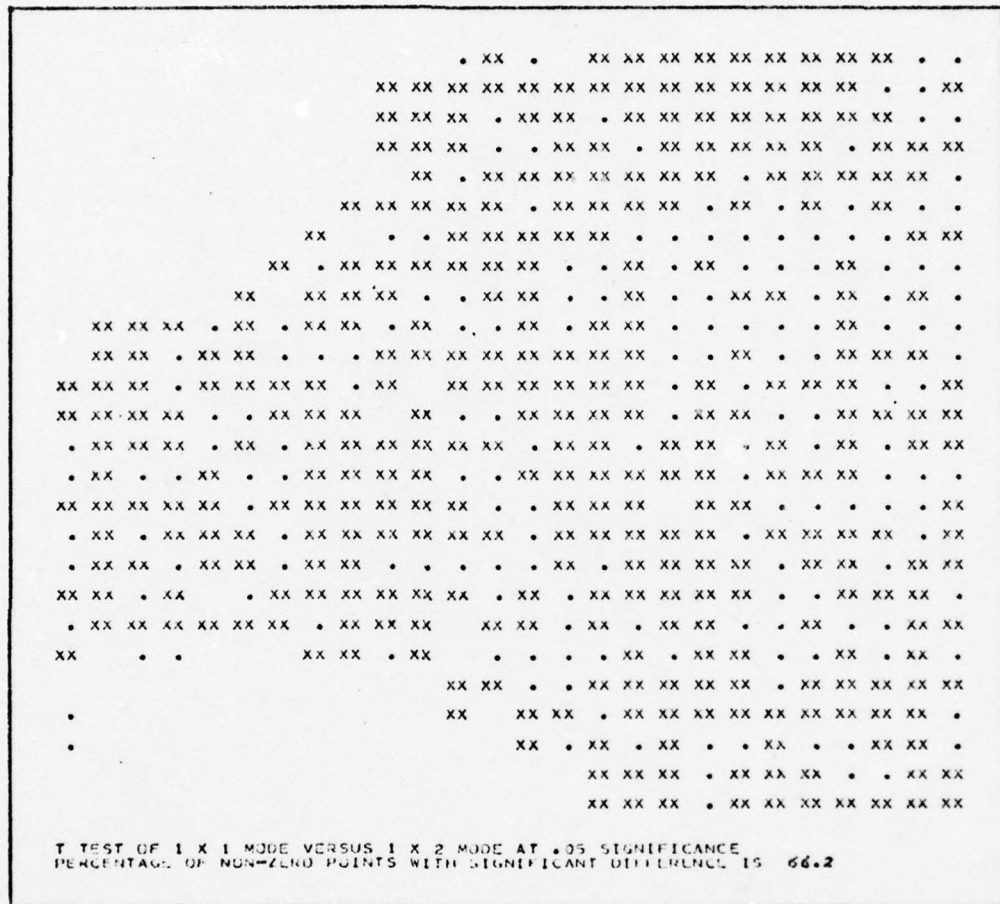
Fig. 22. Statistical comparison of the 1 deg x 1 km and 2 deg x 1 km modes, 10 cm, near range. Level of significance is .05.

The statistical analysis of these two maps (Figure 23) shows that 70.1 percent of all the non-zero pairs of points are significantly different from one another at the $\alpha = .05$ level of significance. The only areas where almost all of the points do not differ are several of the areas of generally low reflectivity. Neither area A nor B show up on this map.

The 2 deg x 2 km Mode

The final comparison in this section was between the 1 deg x 1 km map and the 2 deg x 2 km map (Figure 21). The correlation between these two maps is also very poor. There is a great deal of smoothing of detail and altering of the shape, size, and position of the various reflectivity features. Once again, both the high and low reflectivity points tend to be 5 to 10 dBZ higher on this map than on the 1 deg x 1 km map; however, the maximum observed dBZ value on both maps is 50 dBZ. Many of the features are shifted radially outwards one or more km, and there is also some elongation of features in the direction of antenna rotation, due no doubt to the longer integration intervals in both range and azimuth. The zero reflectivity area at A is very apparent, but once again, the area at B has been lost.

The statistical comparison of these two maps (Figure 24) shows that 72.9 percent of all the non-zero pairs of points were significantly different from one another at the $\alpha = .05$ level of significance. Once again, only in the areas of generally low reflectivity was there any substantial correlation between the data points, and neither area A nor area B was apparent on this map.
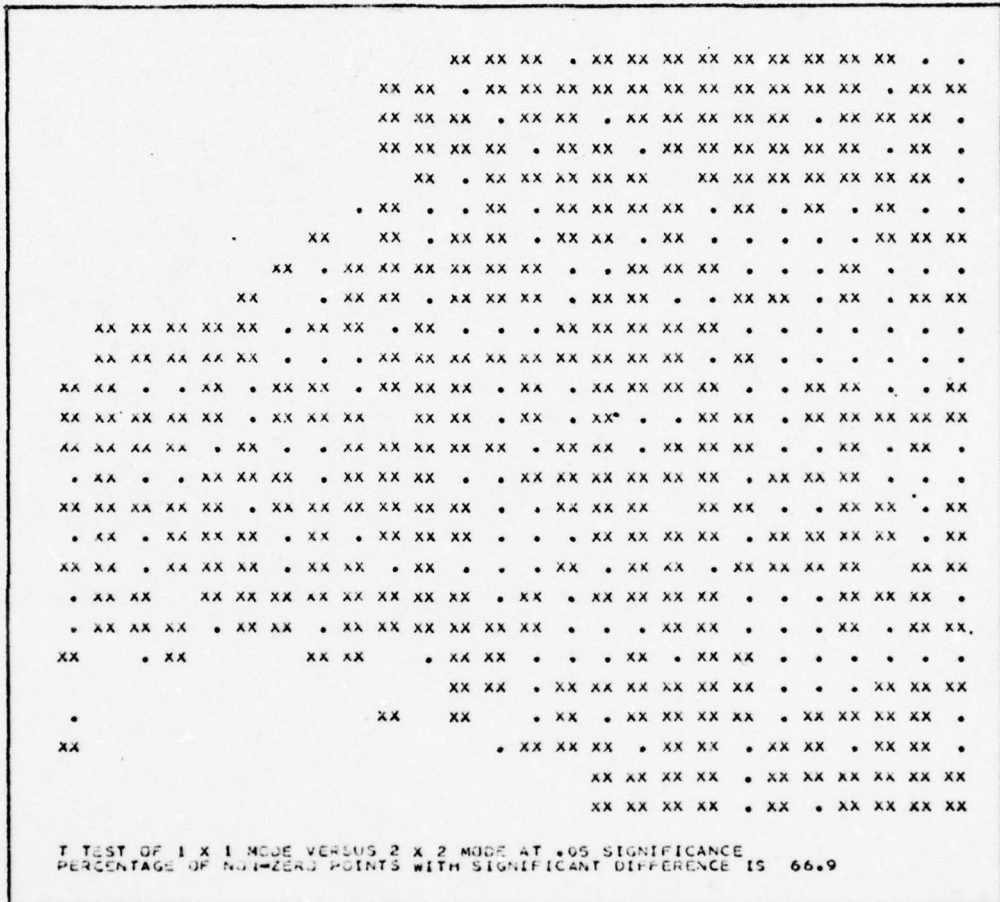
Fig. 23. Statistical comparison of the 1 deg x 1 km and 1 deg x 2 km modes, 10 cm, near range. Level of significance is .05.

Fig. 24. Statistical comparison of the 1 deg x 1 km and 2 deg x 2 km modes, 10 cm, near range. Level of signifcance is .05.

1.0

1.1

1.25 1.4 1.6

2.8 2.5
3.2
3.6 2.2
4.0 2.0

1.8
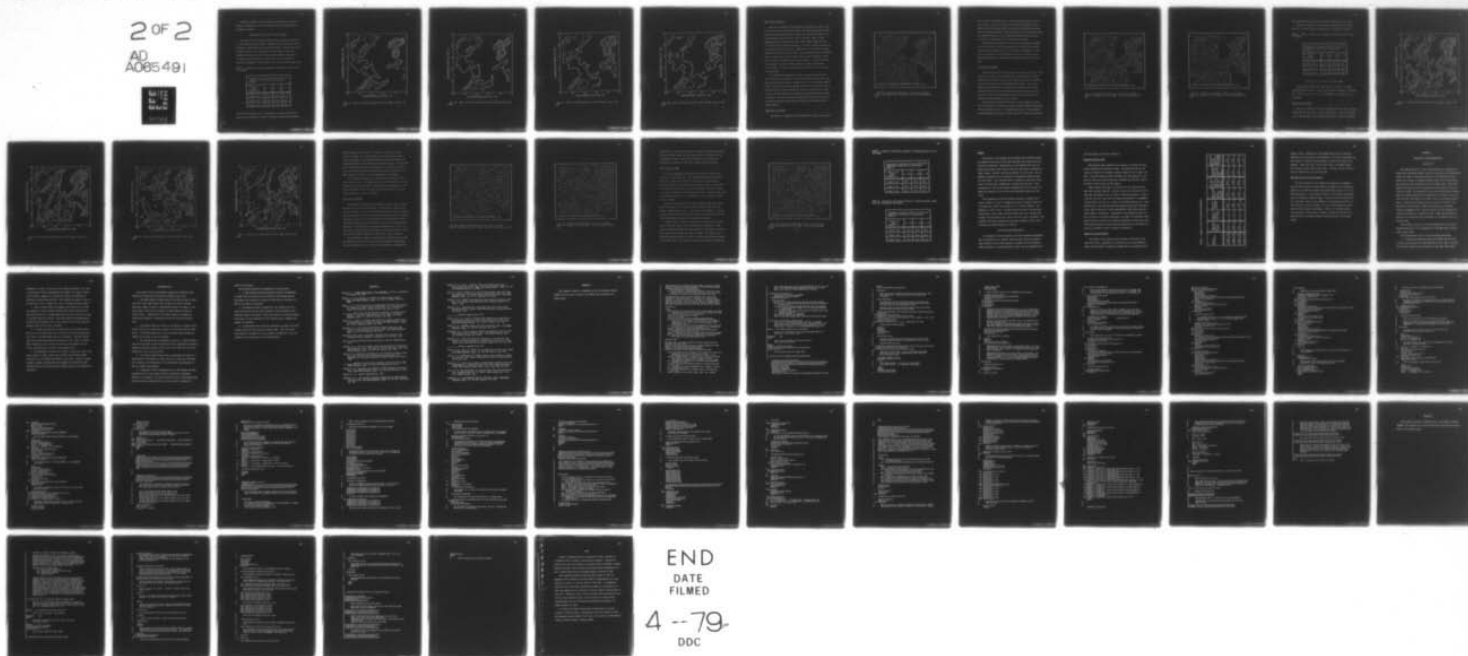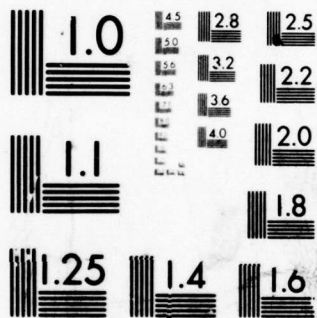
MICROCOPY RESOLUTION TEST CHART
NATIONAL BUREAU OF STANDARDS-1963-A

Finally, a summary of the statistical comparisons of all four modes of collection at each of the three levels of significance is presented in Table 5.

Comparison of 3 cm Data in the Far Range

The next set of analyses was made of the 3 cm data collected in all four modes in the far range. Initially, the far range was to be distances of approximately 150 km from the radar. However, there were no radar returns of any significance at that range, so the area farthest from the radar that had any clearly defined reflectivity features was chosen instead, and that is the area presented in Figures 25 through 28. These figures cover the area which ranges from

TABLE 5. Summary of Statistical Analyses of Collection Modes, 10 cm, Near Range.

Percentage of non-zero pairs of points with significant difference at significance level α.			
1 deg x 1 km mode compared to	$\alpha = .01$	$\alpha = .05$	$\alpha = .10$
2 deg x 1 km	36.5	45.2	51.5
1 deg x 2 km	63.5	70.1	75.7
2 deg x 2 km	64.9	72.9	76.9

75 to 140 km from the radar. Specifically, the major reflectivity feature in the northeast corner of the maps is 106 km from the radar.

Fig. 25. Three cm reflectivity map in the far range, 1 deg x 1 km mode.

Fig. 26. Three cm reflectivity map in the far range, 2 deg x 1 km mode.

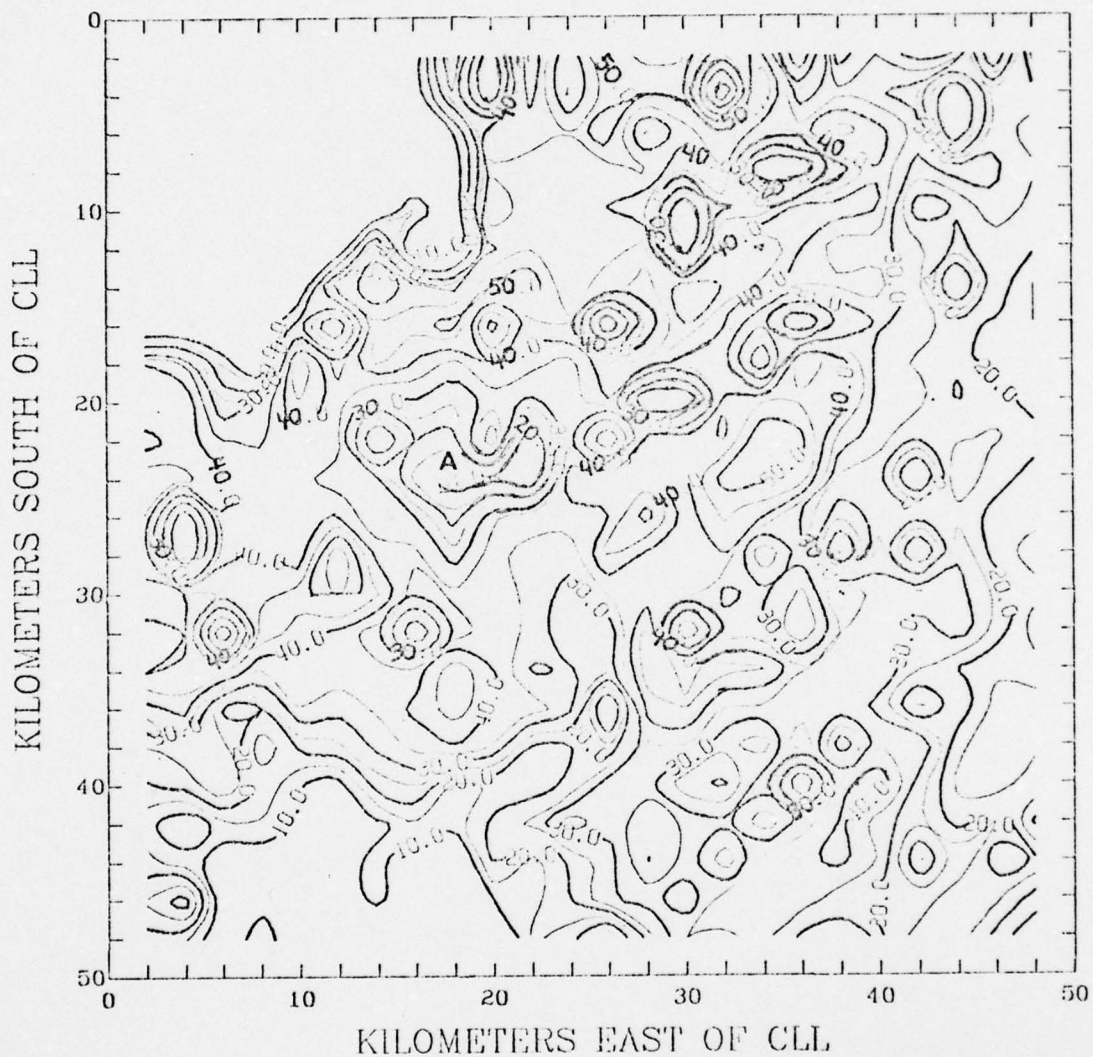Fig. 27. Three cm reflectivity map in the far range, 1 deg x 2 km mode.

Fig. 28. Three cm reflectivity map in the far range, 2 deg x 2 km mode.

The 2 deg x 1 km Mode

The first comparison of this series was between the 1 deg x 1 km map and the 2 deg x 1 km map (Fig. 26). The correlation between these two maps is quite good, and the 2 deg x 1 km map retains almost all of the significant features of the 1 deg x 1 km map. There is some smoothing of fine scale details and a slight shift of some features in the direction of antenna rotation, as well as a slight elongation of some features in that direction. Additionally, three small, adjacent reflectivity features on the 1 deg x 1 km map (location A) are combined into one larger area on the 2 deg x 1 km map, and the extent of that area's region of highest reflectivity is smaller. A different situation prevails in cell B, however, where the maximum reflectivity on the 2 deg x 1 km map is 30 dBZ, whereas on the 1 deg x 1 km map it is only 25 dBZ.

The statistical comparison of these two maps (Figure 29) indicates that only 26.2 percent of the non-zero pairs of points were significantly different from one another at the $\alpha = .05$ level of significance. This pair of maps corresponds better statistically than any of the other pairs of maps analyzed, but this is no doubt due, at least in part, to the relatively low reflectivity values that comprise most of the map. The areas of greatest disagreement are cell B and area A, as could be expected, where almost 55 percent of the points differ significantly.

The 1 deg x 2 km Mode

The next set of comparisons was between the 1 deg x 1 km map and
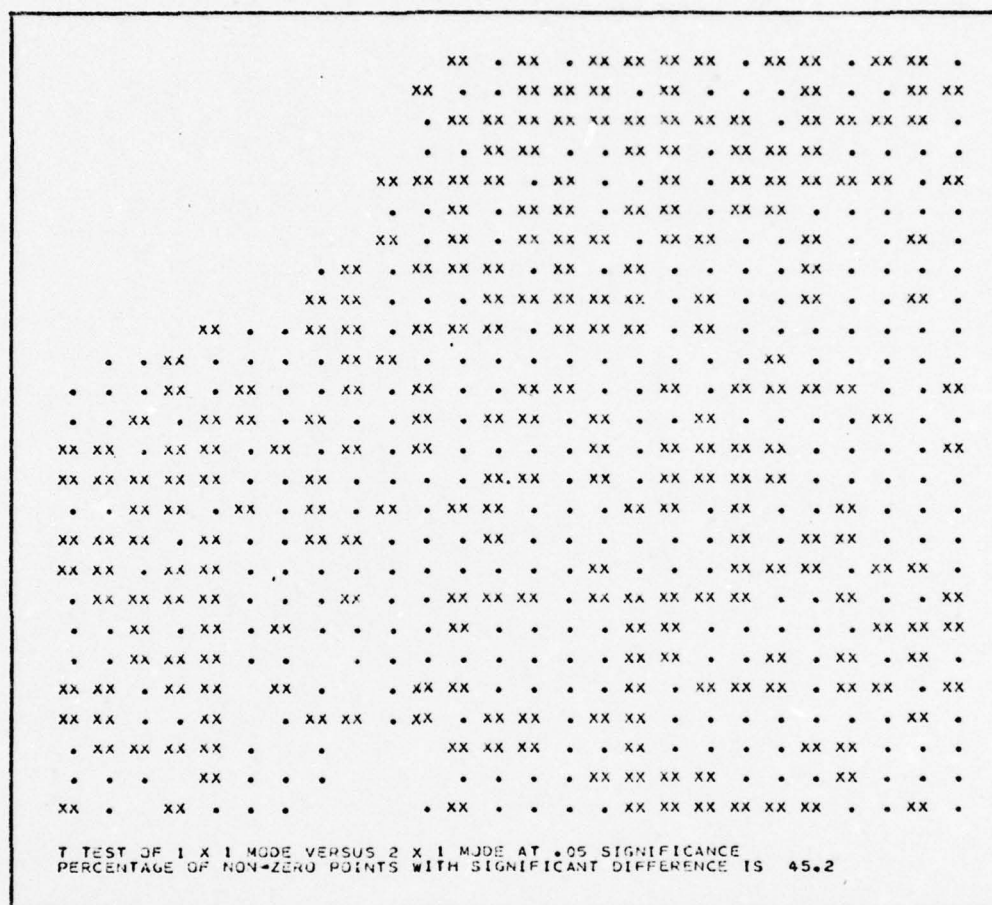
Fig. 29. Statistical comparison of the 1 deg x 1 km and 2 deg x 1 km modes, 3 cm, far range. Level of significance is .05.

the 1 deg x 2 km map (Figure 27). The correlation between these two maps is poor. Most of the detail has either been smoothed over or altered, and the trailing edges of most of the reflectivity features have been shifted outwards. Area A and cell B have been combined into one elongated feature, and once again, the maximum reflectivity of this area is 5 dBZ higher than on the 1 deg x 1 km map.

The statistical comparison of these two maps (Figure 30) shows that 48.5 percent of all the non-zero pairs of points vary significantly from one another at the α = .05 level of significance. Once again, the region of greatest difference is in the areas A and B, although differences are widespread throughout the rest of the map, also.

The 2 deg x 2 km Mode

The final comparison in this section was between the 1 deg x 1 km map and the 2 deg x 2 km map (Figure 28). The correlation between these maps is also poor. Most of the detail is lost and the shape of many of the features has been substantially altered. Many of the features, particularly the low reflectivity features, are shifted slightly outwards and in the direction of antenna rotation. Area A and cell B have been combined into a feature that bears little resemblance to those on the 1 deg x 1 km map.

The statistical comparison of these two maps (Figure 31) shows that 45.7 percent of the non-zero pairs of points differ significantly from one another at the α = .05 significance level. The percentage is much higher in the region of area A and cell B (almost 66 percent),
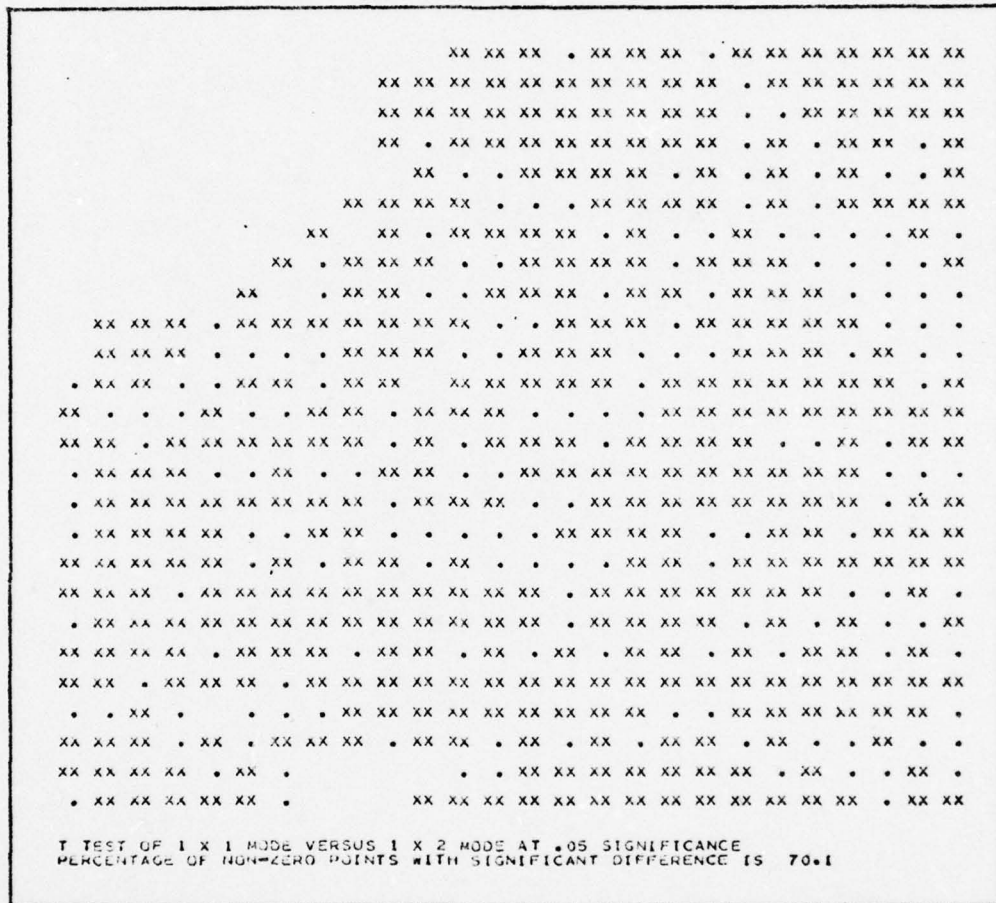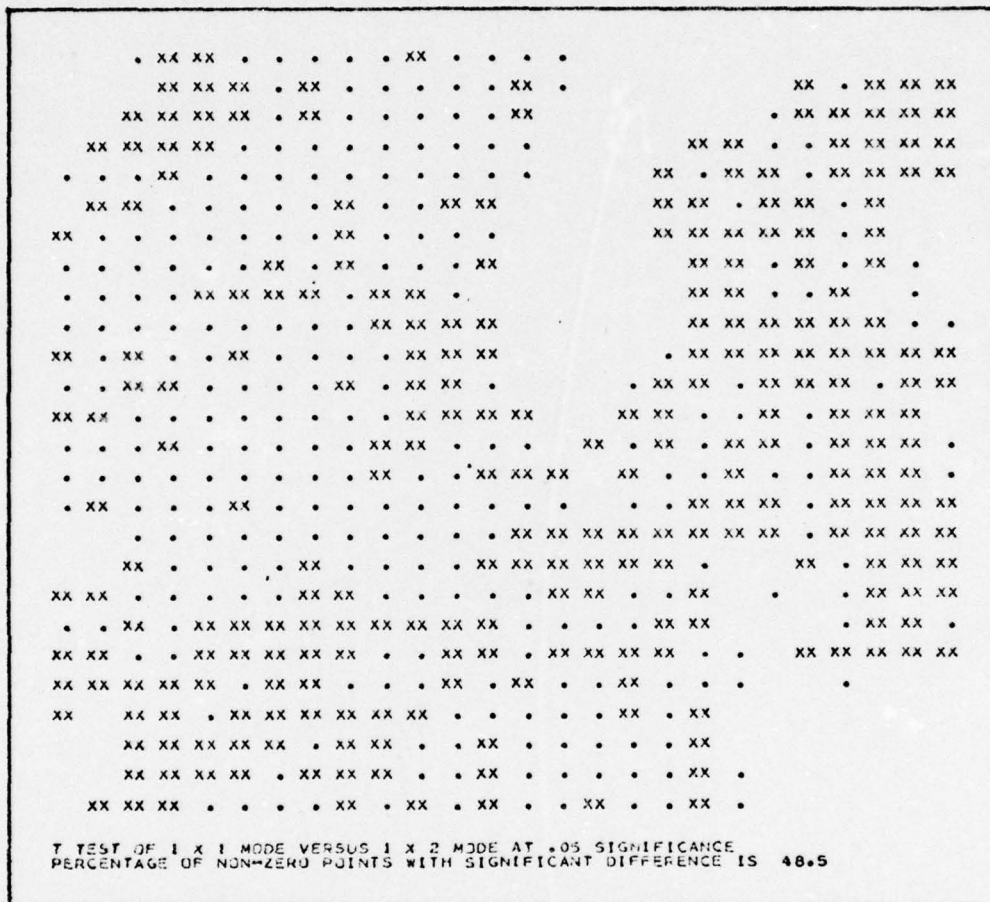
Fig. 30. Statistical comparison of the 1 deg x 1 km and 1 deg x 2 km modes, 3 cm, far range. Level of significance is .05.
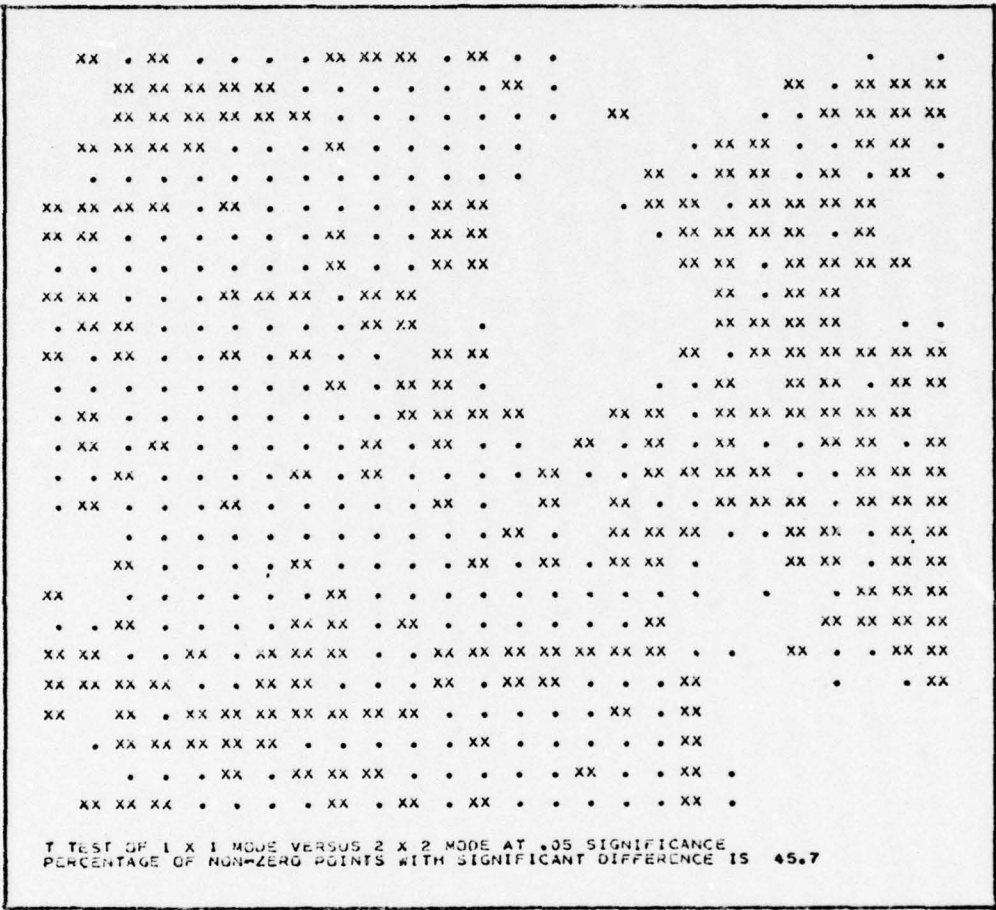
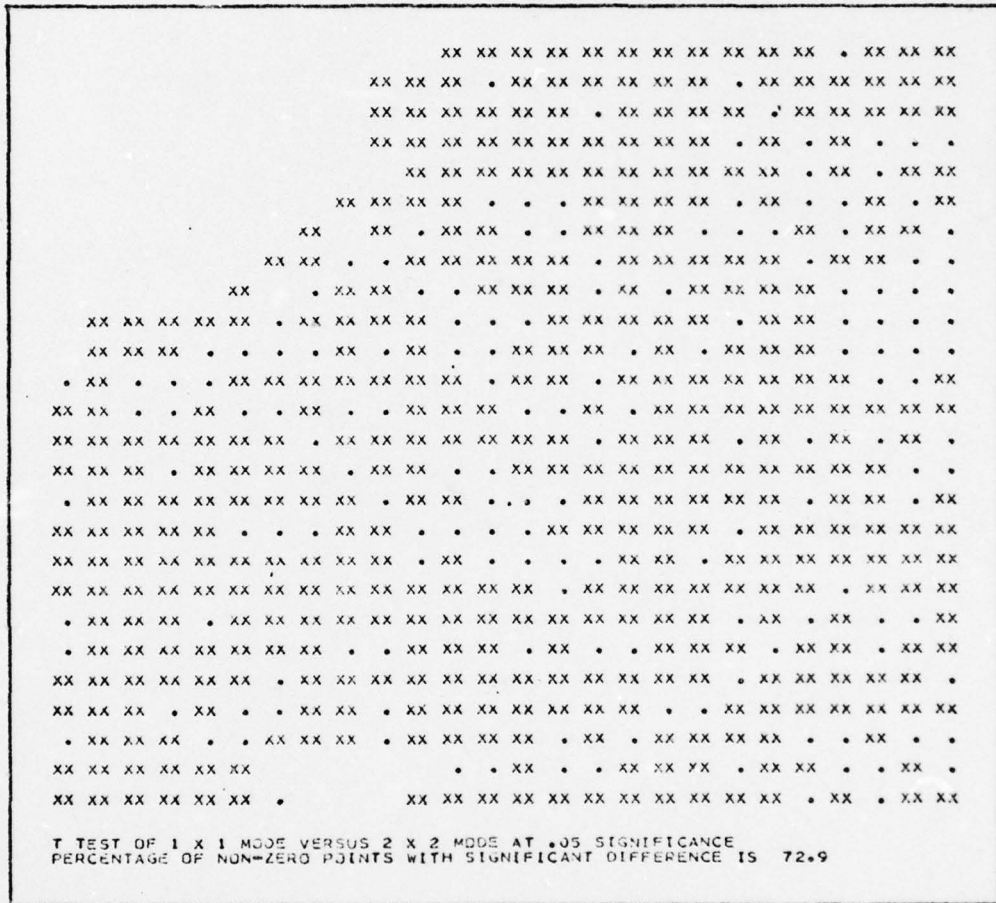Fig. 31. Statistical comparison of the 1 deg x 1 km and 2 deg x 2 km modes, 3 cm, far range. Level of significance is .05.

but the differences are still widespread throughout the entire map.

Lastly, the summary of the statistical comparisons of all four

modes at all three levels of significance is presented in Table 6.

TABLE 6. Summary of Statistical Analyses of Collection Modes, 3 cm,
Far Range.

Percentage of non-zero pairs of points with significant differences at significance level α			
1 deg x 1 km mode compared to	$\alpha = .01$	$\alpha = .05$	$\alpha = .10$
2 deg x 1 km	17.7	26.2	31.9
1 deg x 2 km	37.3	48.5	55.9
2 deg x 2 km	34.8	45.7	53.0

Comparison of 10 cm Data in the Far Range

The zero-tilt reflectivity maps for the 10 cm data, recorded

simultaneously with the 3 cm data, are presented in Figures 32 through

35. As before, the 1 deg x 1 km map was used as the standard for

comparison.

The 2 deg x 1 km Mode

The first comparison in this set was between the 1 deg x 1 km map

(Figure 32) and the 2 deg x 1 km map (Figure 33). The correlation be-

tween these two maps is fairly good, and most of the detail and shape
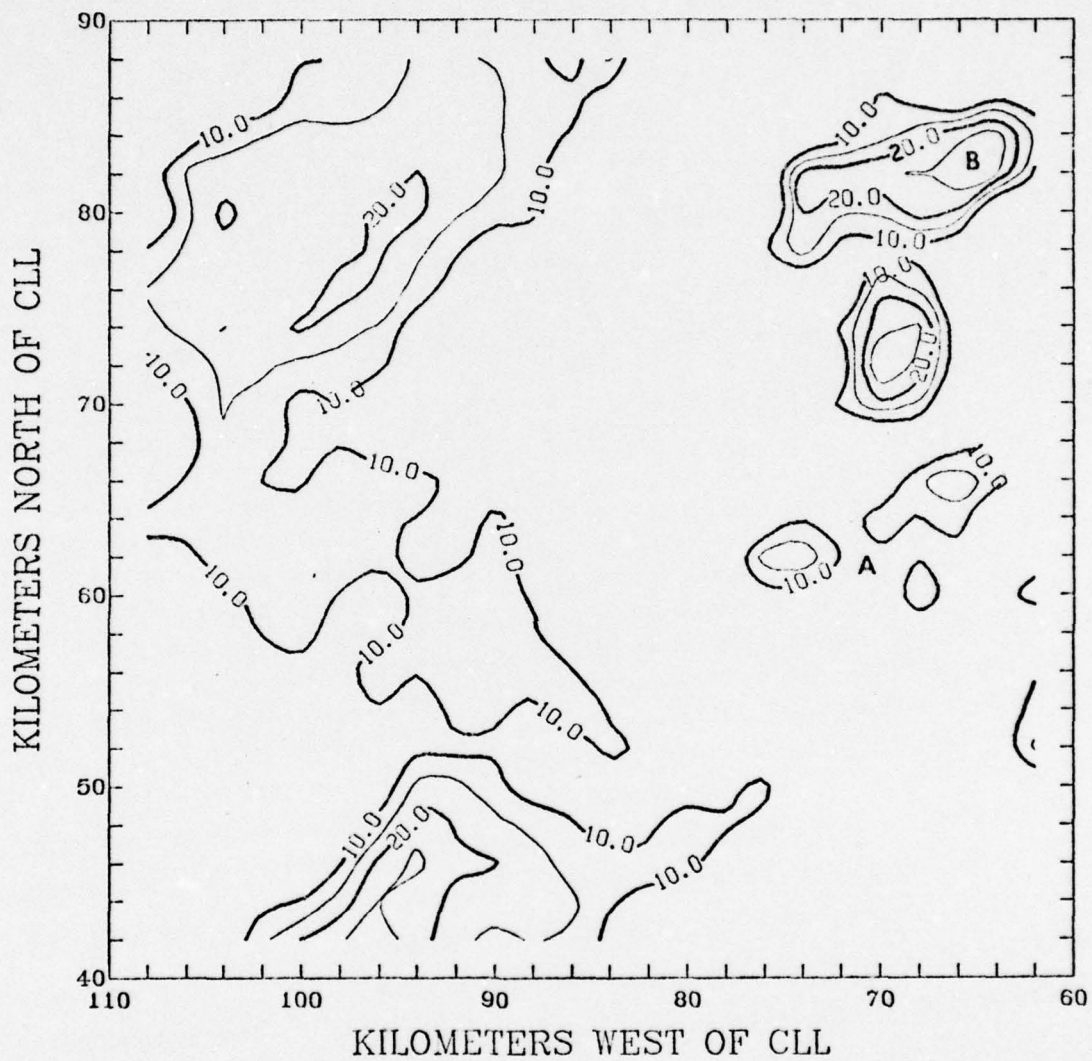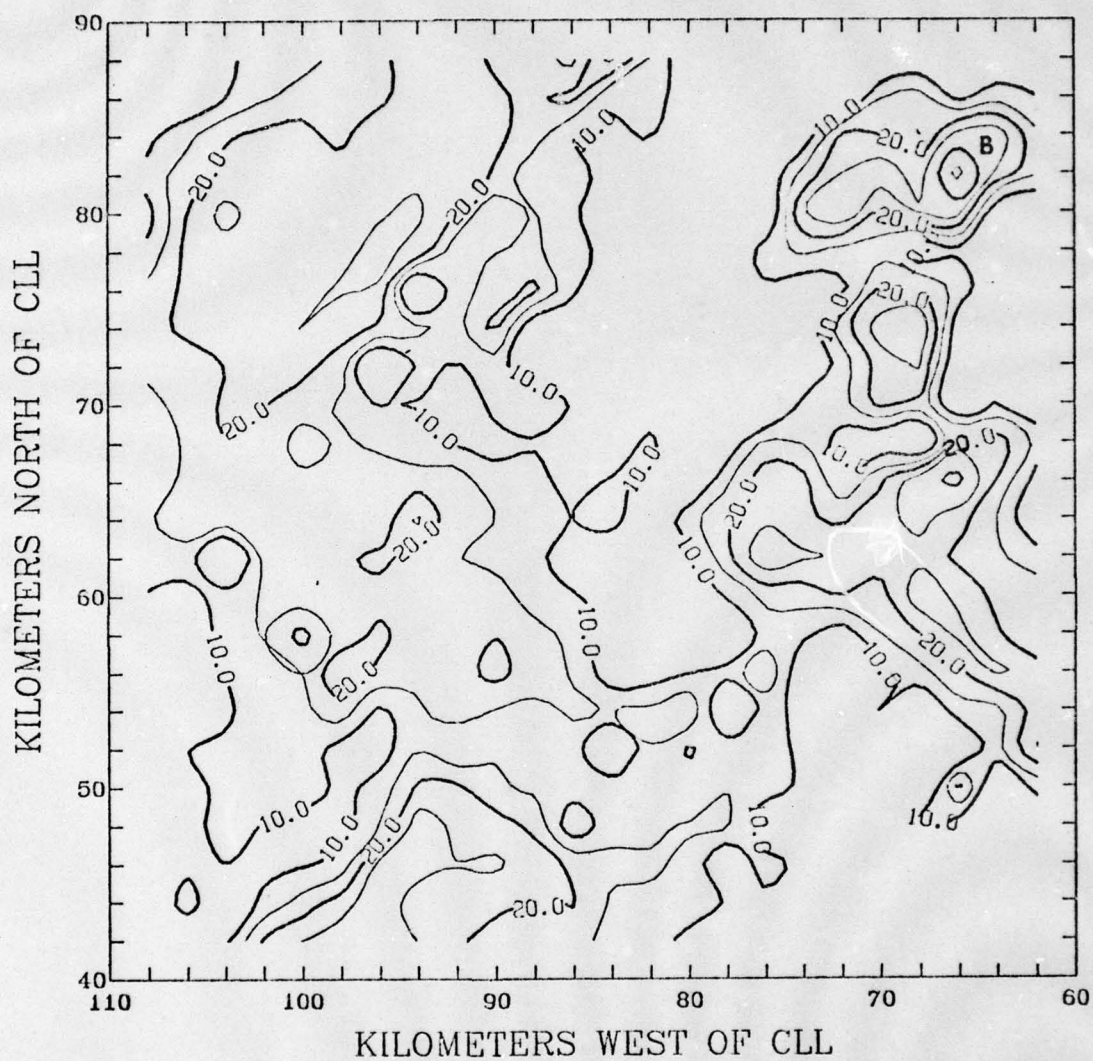
Fig. 32. Ten cm reflectivity map in the far range, 1 deg x 1 km mode.
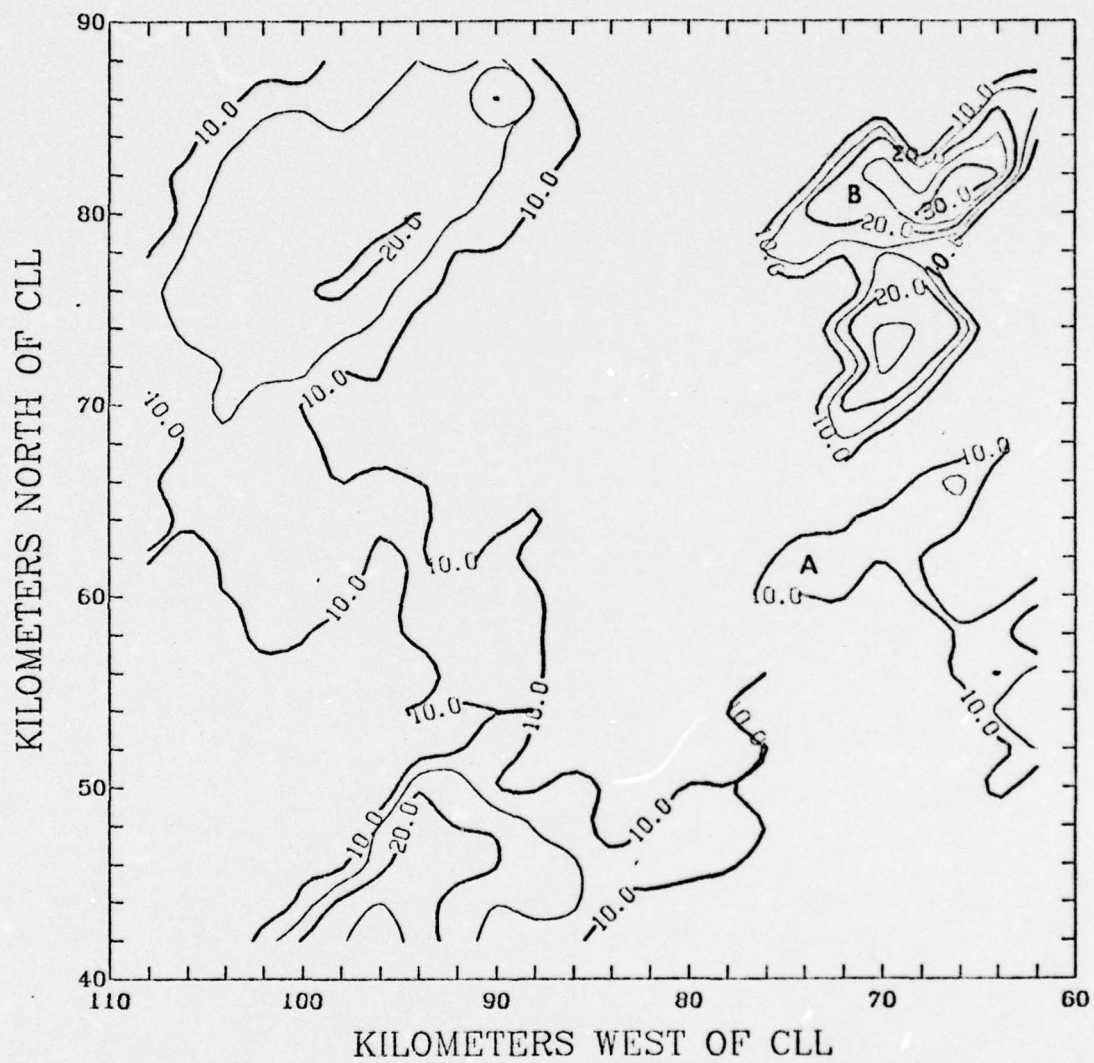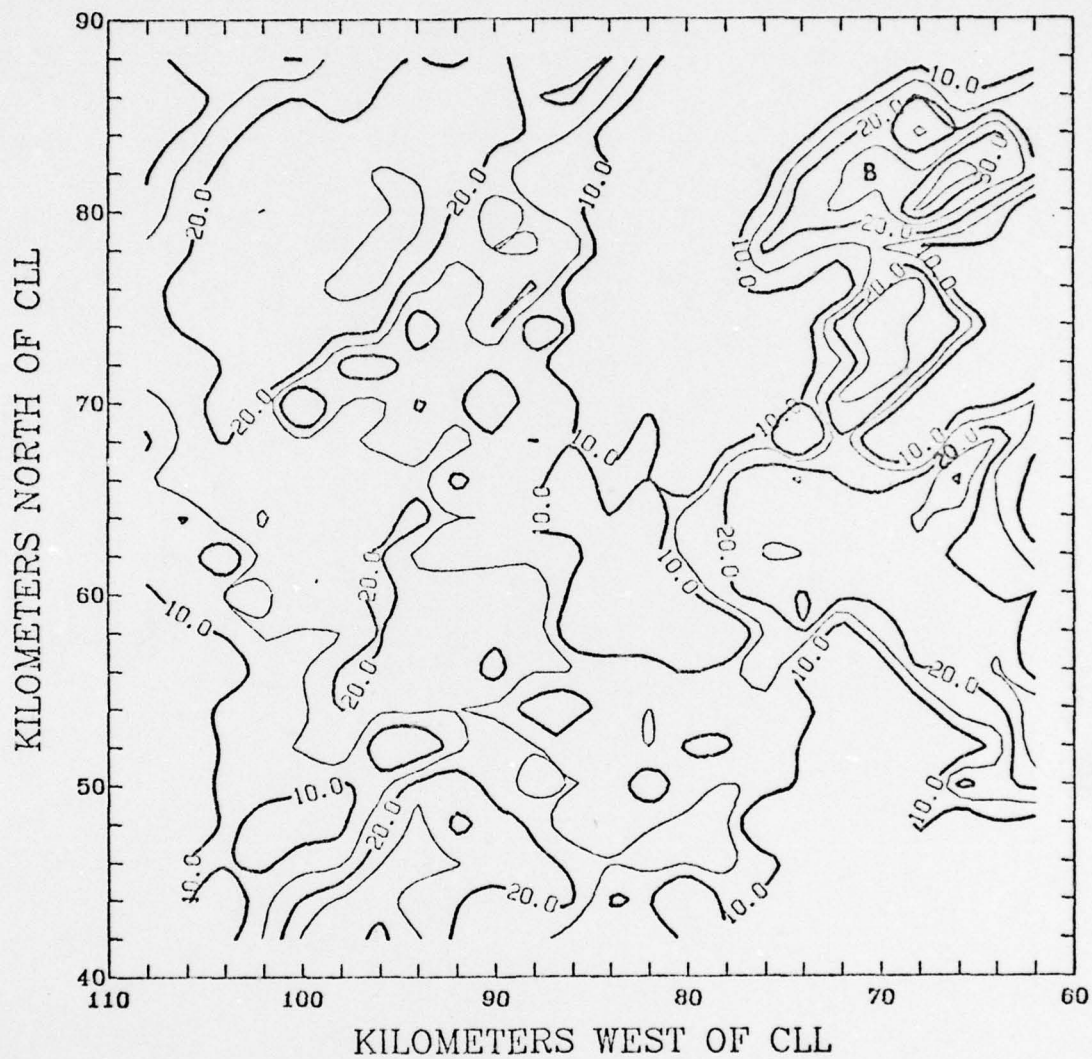
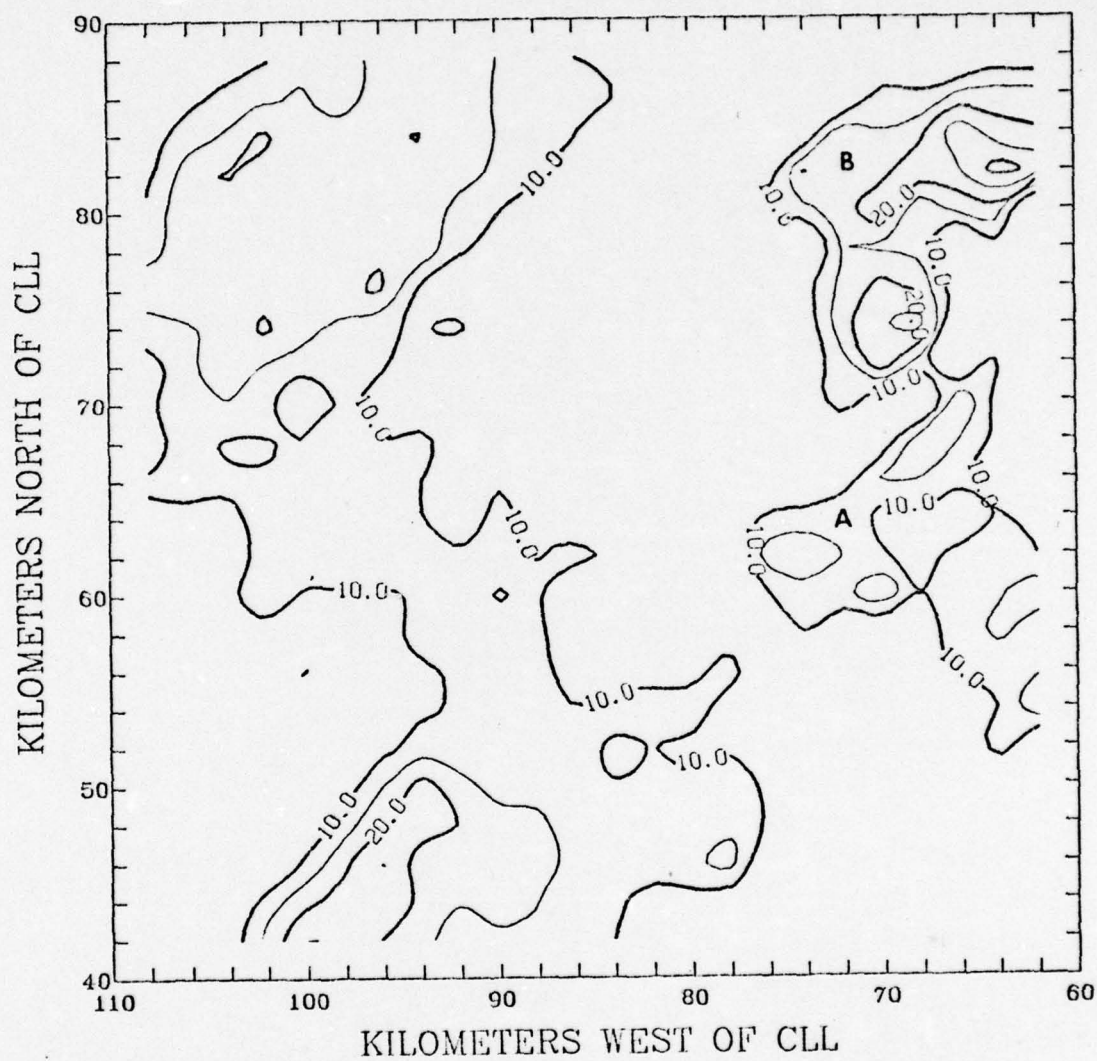Fig. 33.   Ten cm reflectivity map in the far range, 2 deg x 1 km mode.
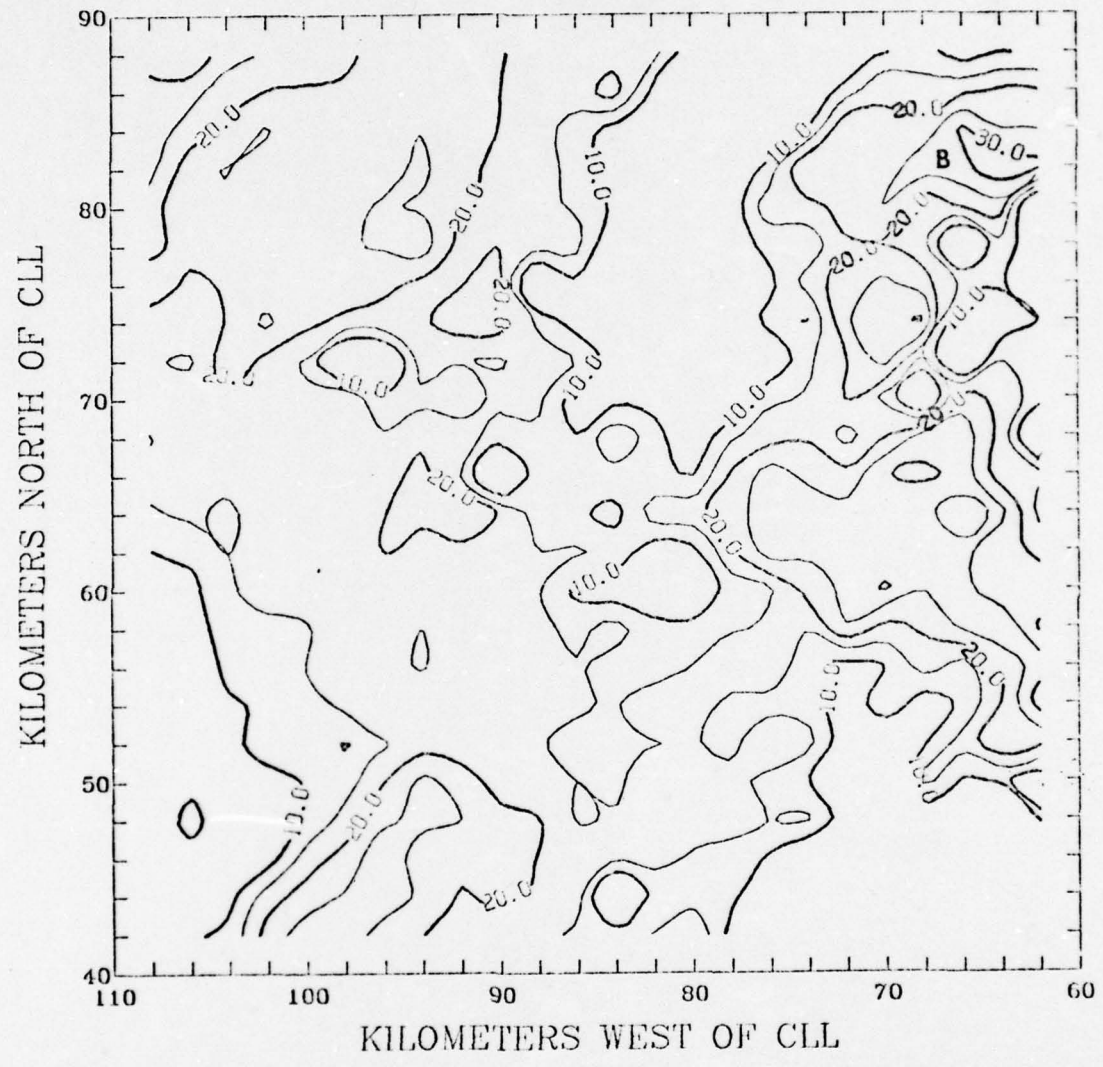
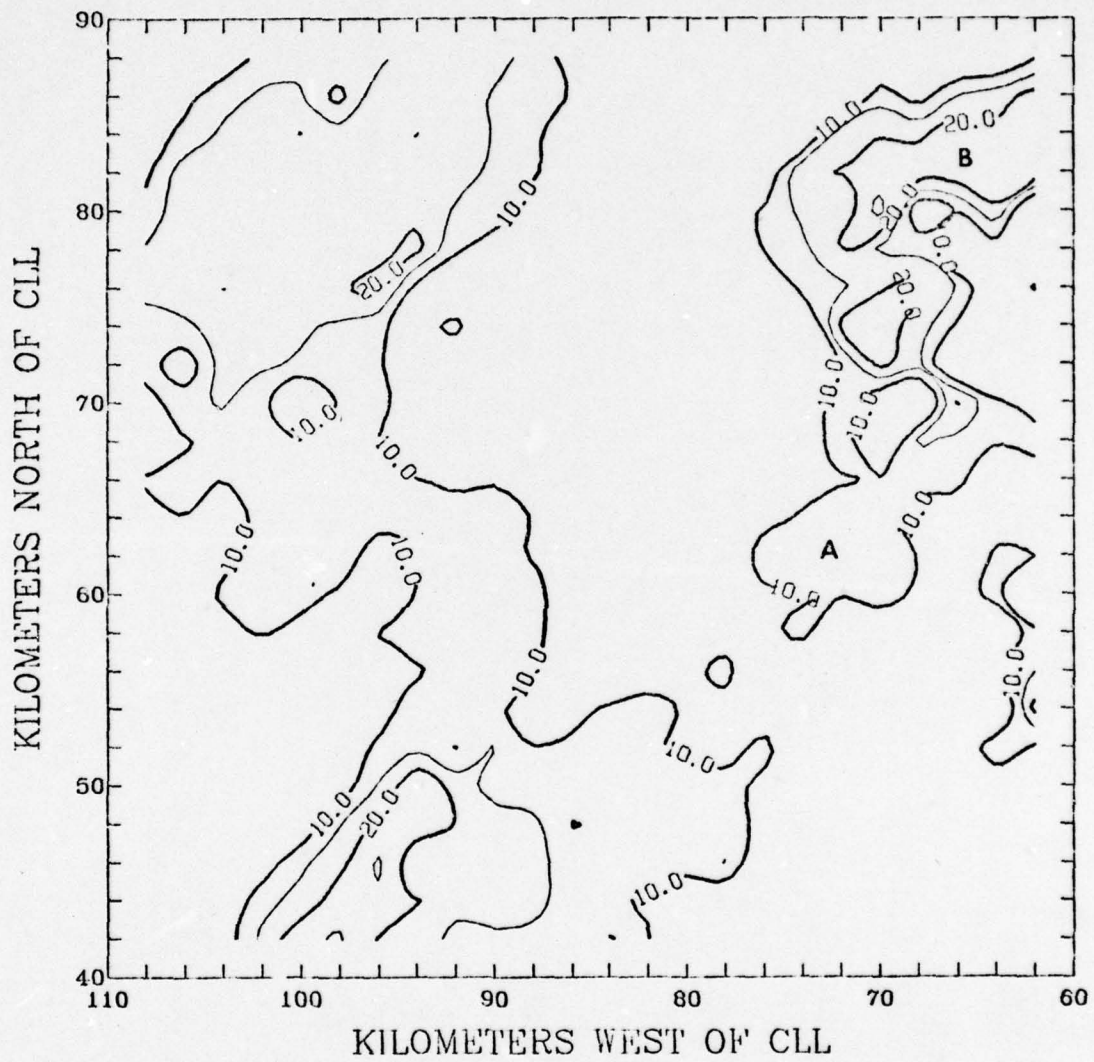Fig. 34. Ten cm reflectivity map in the far range, 1 deg x 2 km mode.
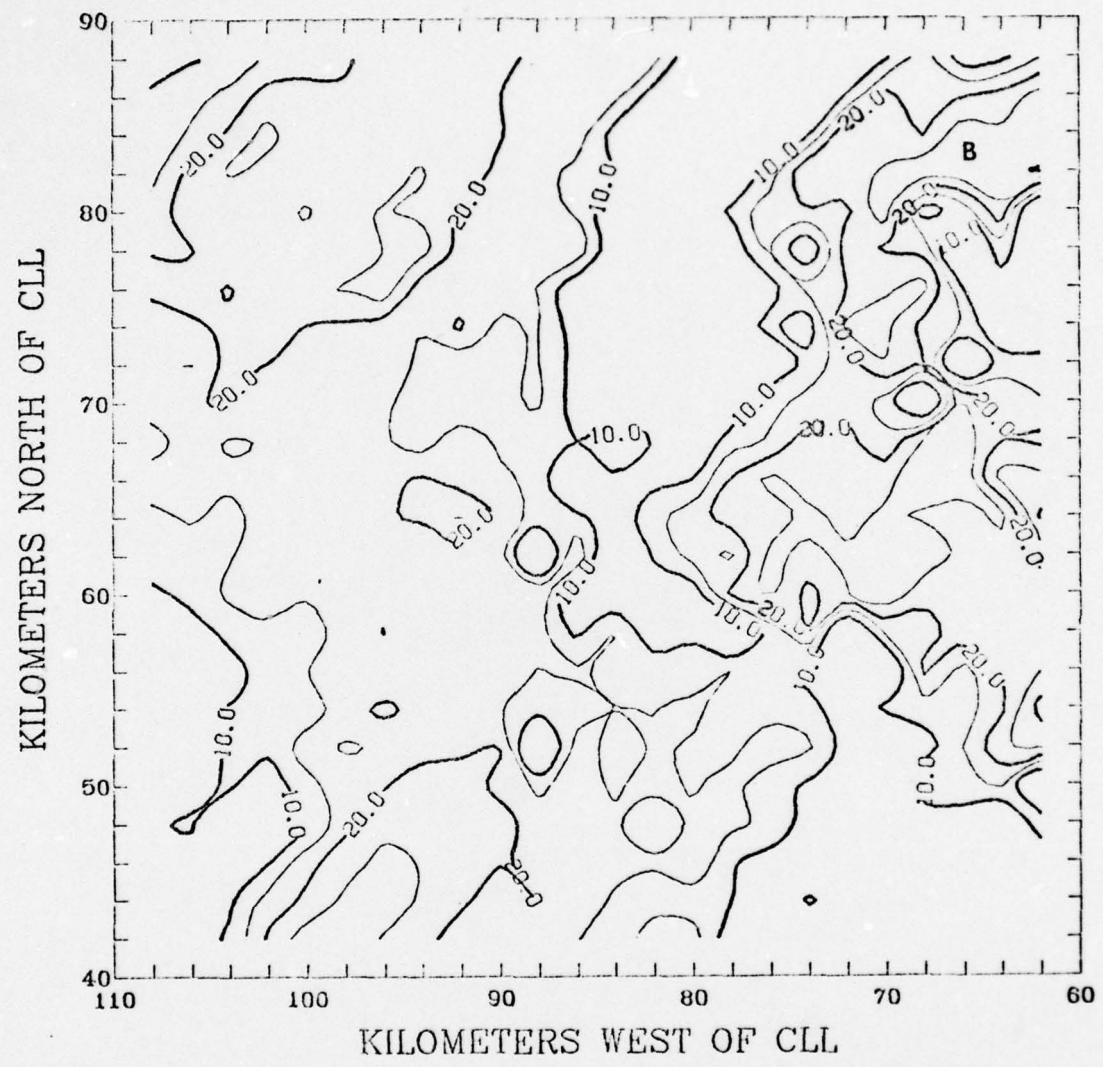
Fig. 35. Ten cm reflectivity map in the far range, 2 deg x 2 km mode.

of the features on the 1 deg x 1 km map are carried over to the 2 deg x 1 km map. The correspondence of cell B on the two maps is particularly good, even though the point of maximum reflectivity is elongated somewhat in the direction of antenna rotation. The high and low reflectivity values match quite well in all regions of the two maps, and the maximum observed reflectivity value on both maps is 35 dBZ, compared to 30 dBZ on the corresponding 3 cm data maps.

The statistical comparison of these two maps (Figure 36) indicates that, at the $\alpha = .05$ significance level, 29.0 percent of all the non-zero pairs of points differ from one another significantly. Most of the differences occur in regions of high reflectivity or reflectivity gradient, as is to be expected.

The 1 deg x 2 km Mode

The next pair of maps analyzed consisted of the 1 deg x 1 km map and the 1 deg x 2 km map (Figure 34). The correlation between these two maps is poor, as much of the detail has been lost and the shapes of many reflectivity features have been altered substantially. The trailing edges of most and the leading edges of many reflectivity features have been shifted radially outward two km or more, and many features with small, closed isopleths have been expanded in size. Cell B has lost some of its identity, and the maximum reflectivity value of that cell is only 30 dBZ, compared to 35 dBZ on the 1 deg x 1 km map.

The statistical analysis of these two maps (Figure 37) shows that 52.2 percent of the non-zero pairs of points differed significantly from one another at the $\alpha = .05$ level of significance. Although the
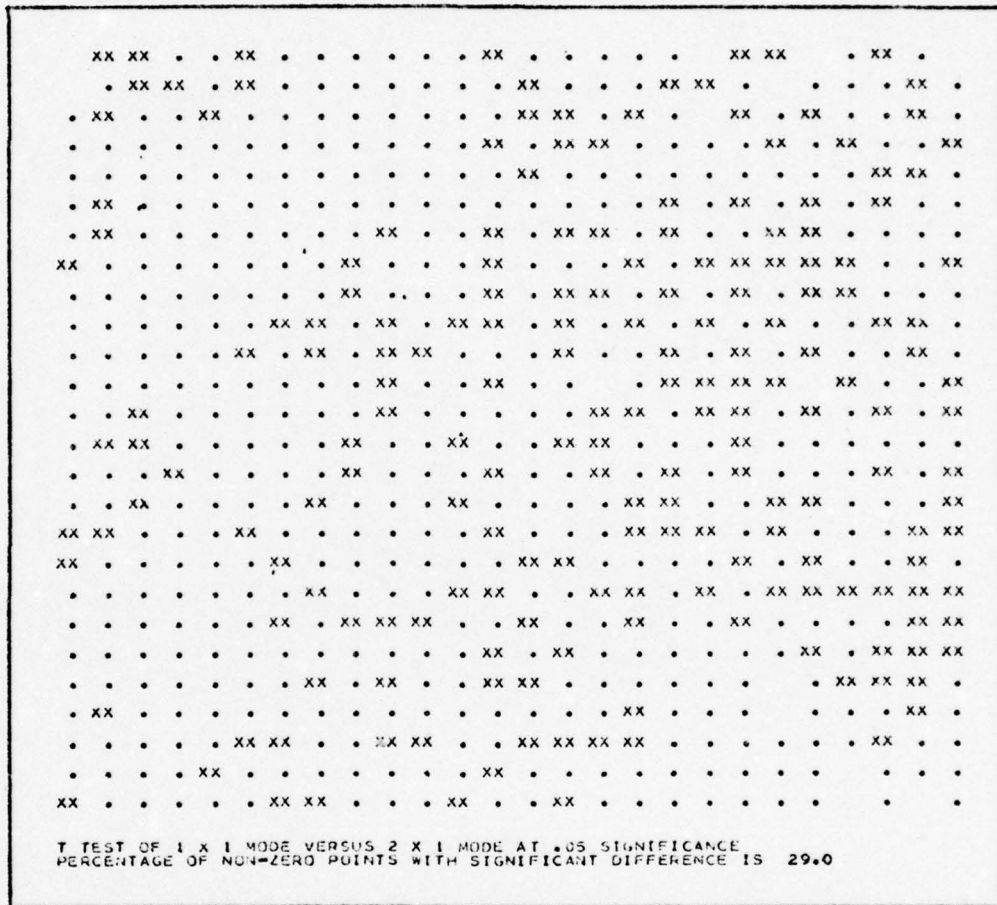
Fig. 36. Statistical comparison of the 1 deg x 1 km and
2 deg x 1 km modes, 10 cm, far range. Level of significance is .05.
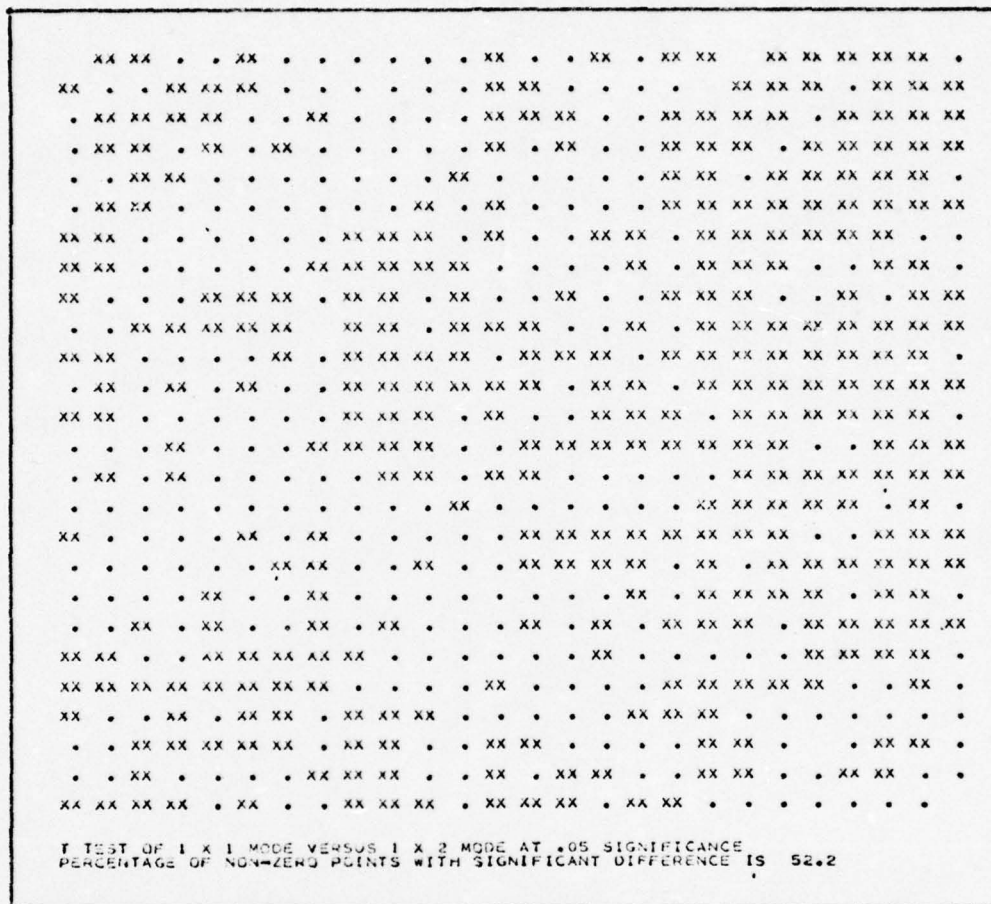
Fig. 37. Statistical comparison of the 1 deg x 1 km and 1 deg x 2 km modes, 10 cm, far range. Level of significance is .05.

differences are more concentrated in the regions of high reflectivity gradient and dBZ values, the only regions where differences are not widespread are those broad areas of generally low reflectivity. Elsewhere, differences are the rule, rather than the exception.

The 2 deg x 2 km Mode

The final comparison was between the 1 deg x 1 km map and the 2 deg x 2 km map (Figure 35). The correlation between these maps is quite poor. Most of the detail is either lost or significantly altered, and many of the features are shifted outwards. Reflectivity values over the entire map tend to be 5 dBZ lower than on the 1 deg x 1 km map, including the maximum observed values. Cell B on the 2 deg x 2 km map bears little or no resemblance to its counterpart on the 1 deg x 1 km map.

The statistical comparison of these two maps (Figure 38) shows that 50.4 percent of the non-zero pairs of points differ from one another significantly at the $\alpha = .05$ level of significance. The only regions where differences are not the rule are the broad areas of low reflectivity where the values are relatively constant.

Finally, Table 7 presents a summary of the statistical comparisons of all four modes at all three levels of significance. Additionally, Table 8 presents the same summary, but averaged over all the data, both 3 and 10 cm and near and far ranges. The analyses consistently show that while the 2 deg x 1 km mode data correspond fairly well to the 1 deg x 1 km mode data, neither of the other two modes do.
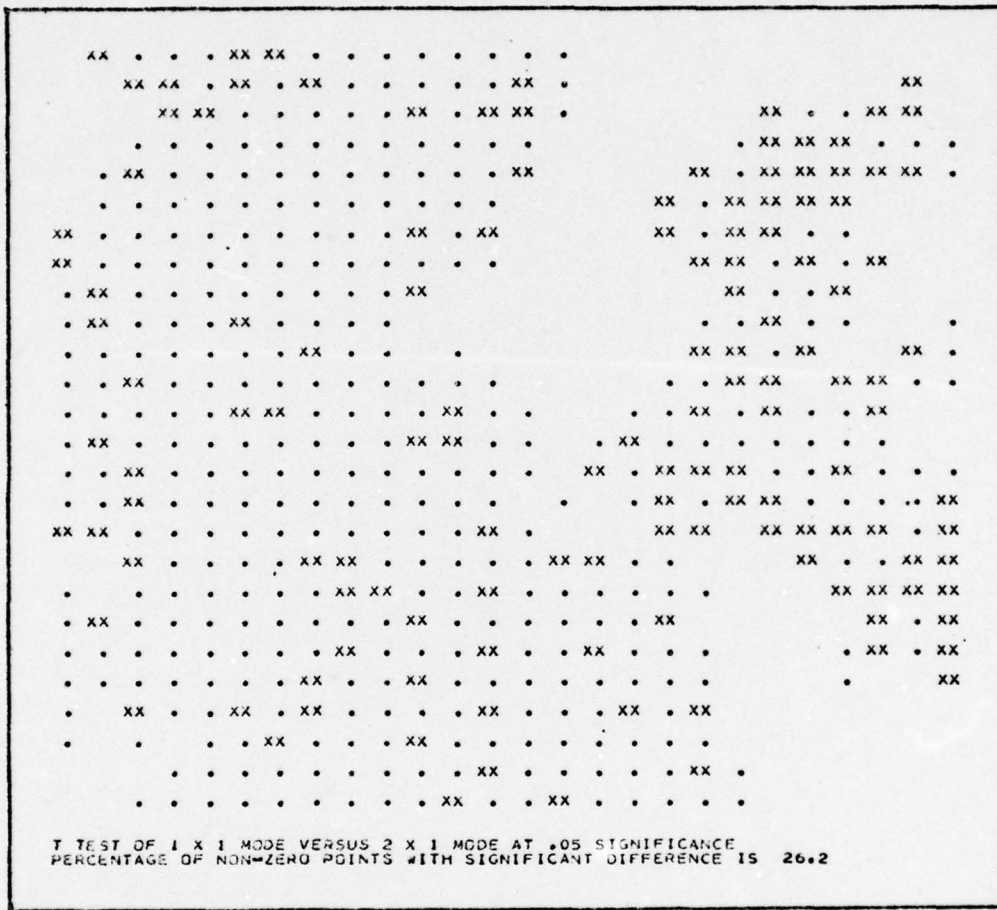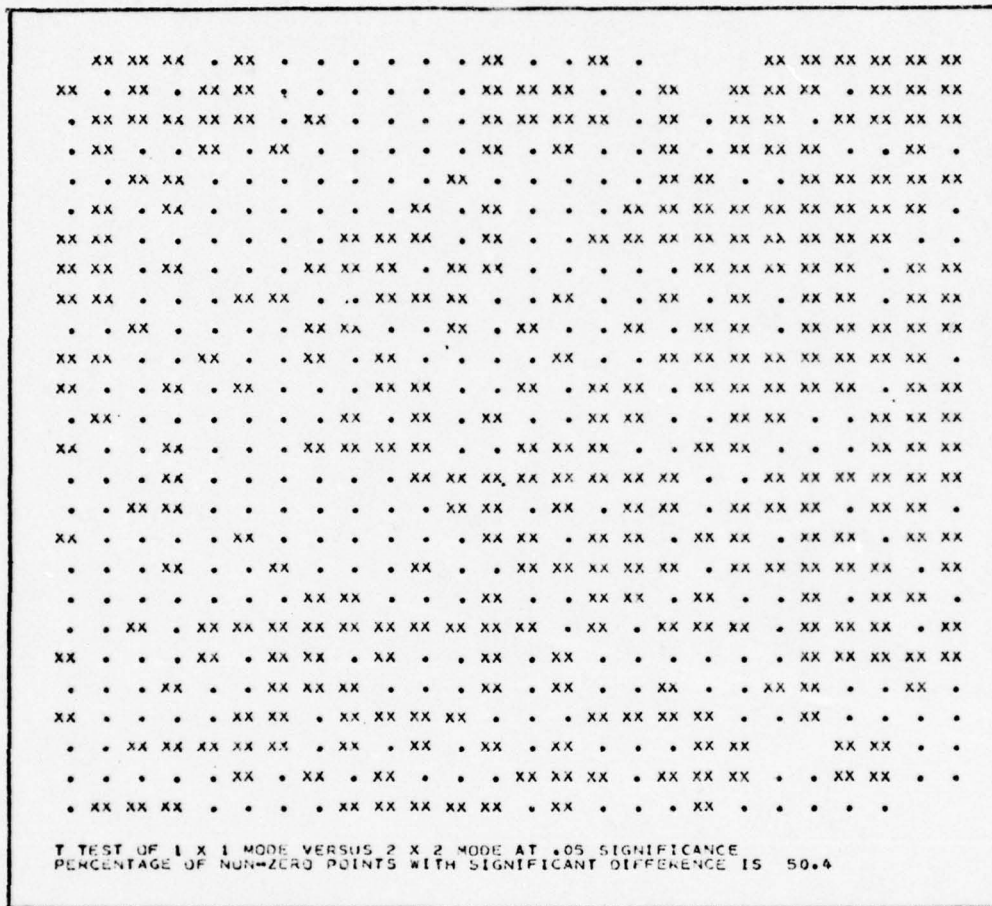
Fig. 38. Statistical comparison of the 1 deg x 1 km and 2 deg x 2 km modes, 10 cm, far range. Level of significance is .05.

TABLE 7. Summary of Statistical Analyses of Collection Modes, 10 cm, Far Range.

Percentage of non-zero pairs of points with significant difference at significance level α.			
1 deg x 1 km mode compared to	α = .01	α = .05	α = .10
2 deg x 1 km	20.7	29.0	35.2
1 deg x 2 km	40.7	52.2	57.0
2 deg x 2 km	39.9	50.4	56.1

TABLE 8. Averages of Statistical Analyses of Collection Modes, Taken Over Both Wavelengths and Ranges.

Percentage of non-zero pairs of points with significant difference at significance level α.			
1 deg x 1 km mode compared to	α = .01	α = .05	α = .10
2 deg x 1 km	25.1	34.0	40.4
1 deg x 2 km	49.5	59.3	65.0
2 deg x 2 km	49.5	59.0	64.6

Summary

The results of the analyses of the various data collection modes are somewhat surprising in that they contradict the results that were initially anticipated. Specifically, it was expected that the 2 km modes would produce better results than the 2 deg modes, especially at longer ranges. However, such has not proven to be the case. The explanation probably lies in the method of integration employed along the data radial. The 2 km mode uses the average of eight 250 m increments of return power, whereas the 1 km mode uses only four. This averaging over 2 km may be enough to substantially alter or mask the shape and intensity of any but the most prominent reflectivity features.

The integration across the azimuth increment is slightly different, however, in that it integrates the last 31 average values for that range bin, either over a space of 1 or 2 deg of azimuth. Consequently, in the 2 deg x 1 km mode, it uses the last 31 one-km range bin averages, each of which is more accurate than the 2 km range bin averages that are used by the 1 deg x 2 km and 2 deg x 2 km modes. The resultant differences between the modes when compared to the 1 deg x 1 km mode are readily apparent in Table 8.

Data Processing Requirements

For purposes of this discussion, the data processing requirements may be considered to be computer execution time, amount of magnetic tape required, and the time required to complete one scan sequence. These parameters are discussed briefly below, and then summarized for

all four modes of collection in Table 9.

Computer Execution Time

The execution time required by the computer to process the data varies substantially from mode to mode. The execution time for the 1 deg x 1 km mode is the lowest, followed closely by the 2 deg x 1 km mode. The times shown in Table 9 represent the time required to produce one 0-deg tilt reflectivity map, averaged over both the 3 and 10 cm data at both the near and far ranges.

These results also appear to conflict with the execution times that were initially expected. However, this is most likely due to the fact that the simplest mode, in terms of computer execution, (1 deg x 1 km) was run first, and then the program was modified to accommodate the next mode to be run, etc., until all the modes had been run. Each modification of the program introduced numerous additional executable steps, many of which fell inside computational loops which required a great number of iterations. Consequently, even though the number of bits of data to be processed decreased, the number of executable statements increased, and hence the apparent discrepancy in execution times. This problem should not exist when processing data with the RADAR program in its general form as it appears in Appendix A.

Magnetic Tape Requirements

The length of each logical record recorded on the tape is the same (1744 bytes), regardless of the mode in use, so the difference comes from the number of degrees of azimuth that are covered by each

TABLE 9. Summary of Data Processing Requirements.

Mode of Collection	Execution time per map in seconds	Degrees of azimuth coverage per record	Records per scan sequence	Antenna RPM req'd for 1.0 db accuracy (31 time samples)	Time req'd for one scan sequence (31 time samples in minutes)	Antenna RPM req'd for 1.0 db accuracy (15 time samples)	Time req'd for one scan sequence (15 time samples in minutes)
1 deg x 1 km	4.77	2	1800	1.00	10.00	2.07	4.83
2 deg x 1 km	5.84	4	900	2.00	5.00	4.13	2.42
1 deg x 2 km	7.51	4	900	1.00	10.00	2.07	4.83
2 deg x 2 km	6.46	8	450	2.00	5.00	4.13	2.42

logical record. Knowing this, and assuming that each scan sequence consists of ten revolutions of the antenna, it is easy to determine the total number of logical records required to record one complete scan sequence. Both the 2 deg x 1 km and the 1 deg x 2 km modes require only one half as much tape as the 1 deg x 1 km mode, and the 2 deg x 2 km mode requires only one fourth as much.

Time Required for One Scan Sequence

The time required for one complete scan sequence is dependent upon the radar antenna rpm which should correspond to the antenna rpm required by the DVIP to maintain the desired data accuracy of 1.0 dB. This assumes that a scan sequence consists of ten antenna revolutions, each at a different elevation angle. Note that the time required for the 1 deg modes (using 31 time samples) is ten minutes, whereas it is five minutes for the 2 deg modes. If only 15 time samples are used, then the times decrease accordingly. However, it should be noted that operation of the antenna at speeds in excess of 3.00 rpm is undesirable due to the added physical stresses placed on the antenna system.

CHAPTER IV

CONCLUSIONS AND RECOMMENDATIONS

Conclusions

The primary objective of this investigation was to examine and compare dual wavelength digital radar data collected near-simultaneously in the four modes of collection possible by the TAMU weather radar system, in an effort to determine whether there is an optimum mode of data collection for operational use of the radar system. This determination was based on such considerations as resolution of data, retention of detail, and smoothing of fine scale meteorological features. These were weighed against such considerations as range of the storm from the radar, wavelength of the radar, and data processing requirements. Digital data collected from the 3 and 10 cm radars of the Department of Meteorology at TAMU were processed by a modified version of Sieland's (1977) computer program, and then displayed as contoured zero-deg tilt reflectivity maps. These maps provided the basis for the comparisons and evaluations of the different data collection modes.

The secondary objective of this investigation was to provide a detailed description of the composition of the TAMU digital weather radar system itself.

This investigation has led to the following conclusions.

1. A significant difference does exist between the zero-tilt reflectivity map produced by data collected in the 1 deg x 1 km mode and the maps produced by data collected in the other three modes.

Assuming the 1 deg x 1 km map to be the reference standard, the 2 deg x 1 km map most closely approximates the standard, in terms of retention of detail, magnitude of reflectivity values, and shifting or altering of reflectivity features. The remaining two modes, 1 deg x 2 km and 2 deg x 2 km, resemble the 1 deg x 1 km map much less closely.

2. For all cases wherein the digital radar data are to be used for research or other scientific applications, where resolution and fine scale detail are of utmost importance, but time is not, the 1 deg x 1 km mode should be utilized. This mode affords the maximum amount of detail and resolution, but it also requires twice as much time and magnetic tape as the 2 deg x 1 km mode.

3. In those cases wherein the application of the digital radar data is to be an operational one, and time is of much more importance, the 2 deg x 1 km mode should prove to be adequate. This mode retains most of the detail and significant features of the 1 deg x 1 km mode, while completing a scan in only one half the time required for the latter, and using only one half as much magnetic tape.

4. The remaining two modes, the 1 deg x 2 km and the 2 deg x 2 km modes, appear to suffer enough loss of detail and introduce enough distortion to be of limited usefulness at this point. However, further research, perhaps utilizing data from complete scan sequences taken through storms with pronounced severe weather features, may negate this conclusion.

Recommendations

The results of this investigation suggest the following recommendations concerning the processing of digital radar data.

1. The RADAR computer program should be revised so that it packs data with return power values that are below the radar's minimum detectable signal in order to substantially reduce the amount of computer memory utilized and the amount of time required to read the various arrays. Additionally, the program should be streamlined, eliminating redundant or unnecessary steps that increase execution time.

2. The program should be revised to incorporate a variable sized box for the area to be analyzed, instead of the current 100 deg x 100 km box. The current memory size could be retained, while making the lengths of the sides of the box flexible.

3. The program should be permanently stored as a library program that could be called up and initialized with the appropriate parameters, instead of manually reading a deck of more than 1,000 cards for every program run, as is now the practice.

4. The revised program should then be programmed and tested on a mini-computer to determine the time required to produce the PVSZ maps, and ultimately, the feasibility of the operational implementation of this or similar type programs.

5. A comparison of data integrated over 15 time samples and data integrated over 31 time samples should be conducted to determine whether it is feasible to use data collected in the 15 time sample mode, and hence decrease substantially the time required to complete an

entire scan sequence.

The following additional recommendations are also made.

1. A radar standard operating procedure should be established to insure that all radar data are recorded at the antenna rpm and time sample rate required to produce the same level of accuracy (1.0 dB) for all modes of collection.

2. An analysis should be conducted of the rainfall rate of a storm derived from the VIL values produced by data obtained in the different modes of collection. This would require a relatively steady state storm, as the computation of VIL requires that a complete scan sequence be recorded.

3. A continuing effort should be undertaken to observe and study tornadic storms in this region of central Texas. Data from such a storm should be recorded in all four modes of collection to test the validity of the conclusions of this investigation.

REFERENCES

Battan, L. J., <u>Radar</u> <u>Observation</u> <u>of</u> <u>the</u> <u>Atmosphere</u>, 324 pp., University of Chicago, IL, 1973.

Bigler, S. G., An analysis of tornado and severe weather echoes, <u>Proc.</u> <u>5th</u> <u>Radar</u> <u>Meteorol.</u> <u>Conf.</u>, pp. 167–175, Asbury Park, NJ, 1955.

Canipe, Y. J., On the structure and development of severe local storms as revealed by digital radar observations, Ph.D. Dissertation, Texas A&M University, College Station, TX, 142 pp., 1973.

_____, and P. Das, Partial vertical integration of liquid water (PVIL), an improved radar-analytical tool, <u>Proc.</u> <u>16th</u> <u>Radar</u> <u>Meteorol.</u> <u>Conf.</u>, pp. 328–332, Houston, TX, 1975.

Clark, R. A., and Y. J. Canipe, Applications of digital radar data in both meteorology and hydrology, <u>Proc.</u> <u>15th</u> <u>Radar</u> <u>Meteorol.</u> <u>Conf.</u>, pp. 93–98, Champaign-Urbana, IL, 1972.

Elvander, R. C., The relationship between digital radar data and reported severe weather occurrences, <u>Proc.</u> <u>16th</u> <u>Radar</u> <u>Meteorol.</u> <u>Conf.</u>, pp. 333–336, Houston, TX, 1975.

Enterprise Electronics Corporation, Digital Video Integrator and Processor (DVIP), Appendix I, Enterprise, AL, 127 pp., 1975.

Ford, R., Enterprise Electronics Corporation, Private communication, 1978.

Freeman, L. E., and P. M. Austin, Sizes and intensities of mesoscale precipitation areas as depicted by digital radar data, <u>Proc.</u> <u>17th</u> <u>Radar</u> <u>Meteorol.</u> <u>Conf.</u>, pp. 486–491, Seattle, WA, 1976.

Greene, D. R., Numerical techniques for the analysis of digital radar data with applications to meteorology and hydrology, Ph.D. Dissertation, Texas A&M University, College Station, TX, 124 pp., 1971.

_____, Hydrologic application of digital radar data, <u>Proc.</u> <u>16th</u> <u>Radar</u> <u>Meteorol.</u> <u>Conf.</u>, pp. 353–360, Houston, TX, 1975.

Hudlow, M. D., Collection and handling of GATE shipboard radar data, <u>Proc.</u> <u>16th</u> <u>Radar</u> <u>Meteorol.</u> <u>Conf.</u>, pp. 186–193, Houston, TX, 1975.

Huebner, G. L., Private communication, 1978.

Marshall, J. S., The constant altitude presentation of radar weather patterns, <u>Proc.</u> <u>6th</u> <u>Radar</u> <u>Meteorol.</u> <u>Conf.</u>, pp. 321–324, Cambridge, MA, 1957.

Morgan, M. M., and E. A. Mueller, The total liquid water mass of large convective storms, Proc. 15th Radar Meteorol. Conf., pp. 39-40, Champaign-Urbana, IL, 1972.

Pautz, M., and F. Doloresco, On the relation between radar echo tops, the tropopause, and severe weather occurrences, Proc. 10th Radar Meteorol. Conf., pp. 51-56, Washington DC, 1963.

Pittman, D. W., Tornado identification from analyses of digital radar data, M.S. Thesis, Texas A&M University, College Station, TX, 93 pp., 1976.

Radlein, R. A., Digitized dual wavelength radar data from a Texas thunderstorm, M.S. Thesis, Texas A&M University, College Station, TX, 95 pp., 1977.

_____, Private communication, 1977.

Riley, G. F., Jr., and P. M. Austin, Some statistics of gradients of precipitation intensity derived from digital radar data, Proc. 17th Radar Meteorol. Conf., pp. 492-497, Seattle, WA, 1976.

Saffle, R. E., D/RADEX products and field operation, Proc. 17th Radar Meteorol. Conf., pp. 555-559, Seattle, WA, 1976.

Schroeder, M. J., and L. Brueni, Computer processing of digital radar data gathered during HIPLEX, Proc. 17th Radar Meteorol. Conf., pp. 453-461, Seattle, WA, 1976.

Sieland, T. E., Real time computer techniques in the detection and analysis of severe storms from digital radar data, Ph.D. Dissertation, Texas A&M University, College Station, TX, 141 pp., 1977.

_____, Private communication, 1977.

Silver, W. M., and S. G. Geotis, On the handling of digital data, Proc. 17th Radar Meteorol. Conf., pp. 462-467, Seattle, WA, 1976.

Vogel, J. E., Applications of digital radar in the analysis of severe local storms, M.S. Thesis, Texas A&M University, College Station, TX, 94 pp., 1973.

Whiton, R. C., On the use of radar in identifying tornadoes and severe thunderstorms: a diagnostic guide for radar scope interpretations, USAF Technical Report 243, 18 pp., Scott AFB, IL, 1971.

Yates, J. M., The association of vertical radar echo protrusions with hail, Progress Report No. 12, WSR-57 radar program, pp. 47-51, U.S. Weather Bureau, 1963.

Yeager, K. C., A programmable digital integrator, Proc. 16th Radar Meteorol. Conf., pp. 200-201, Houston, TX, 1975.

APPENDIX A

This appendix contains a commented copy of the computer program (RADAR) that was used to process the digital data recorded by the radar system.

```
C     THIS PROGRAM USES DIGITIZED RADAR DATA FROM THE TEXAS A&M RADAR
C     SYSTEM.  THESE DATA, WRITTEN ON MAGNETIC TAPE, ARE READ AND USED
C     TO COMPUTE AND PRODUCE THE FOLLOWING:
C          1. ZERO DEGREE TILT REFLECTIVITY MAPS
C          2. PARTIAL VERTICALLY SUMMED REFLECTIVITY(Z) MAPS (PVSZ) FOR
C             3 LAYERS (SFC - 15 KFT, 15 KFT - 35 KFT, & 35 KFT - 50 KFT)
C          3. VERTICALLY INTEGRATED LIQUID WATER CONTENT (VIL) MAP
C
C     THE PROGRAM WILL OPERATE ON DATA RECORDED IN ALL FOUR MODES
C     POSSIBLE BY THIS RADAR SYSTEM:  1 DEG BY 1 KM, 1 DEG BY 2 KM,
C     2 DEG BY 1 KM, AND 2 DEG BY 2 KM.  HOWEVER, IT WILL ONLY PROCESS
C     DATA FOR ONE RADAR (3 CM OR 10 CM) AT A TIME.  TO PROCESS DATA
C     FROM THE OTHER RADAR, YOU MUST CHANGE THE RADAR CONSTANT (WAVEC),
C     THE RADAR CALIBRATION DATA CARD, AND THE JCL FOR THE INPUT TAPE.
C
C     DEFINITIONS:
C
C     ARRAYS
C        ZW - CONTAINS RAW REFLECTIVITY DATA VIA CODED AZIMUTH AND RANGE
C        Z - CONTAINS A PVSZ OR VIL ARRAY AFTER IT IS RETURNED FROM QD2.
C            THE ARRAY WILL BE IN X, Y COORDINATES
C        PVSZ1, 2, 3 - THE THREE PVSZ LAYERS
C        VIZ - THE VIL ARRAY
C        A - THE MATRIX USED FOR THE LAGRANGIAN INTERPOLATION
C        IDIV1, 2, 3 - THE DIVISORS USED FOR OBTAINING THE AVERAGE
C            REFLECTIVITY IN A LAYER.  THIS CONSISTS OF THE NUMBER OF
C            DATA RADIALS IN A GIVEN LAYER AT A GIVEN RANGE.  SEE
C            SUBROUTINE DIVIDE.
C        ZP - A DUMMY ARRAY USED FOR THE QD2 SUBROUTINE WHICH GIVES THE
C            PVSZ ARRAYS BACK TO THE MAIN PROGRAM IN X, Y COORDINATES
C        ICLASS - CONTAINS RAW DIGITIZED REFLECTIVITY DATA
C        CALIB - CONTAINS THE EQUIVALENT DBM VALUES FOR 256 DIGITAL
C            INTEGERS NUMBERED FROM 0 TO 255
C        CORECT - CONTAINS THE EARTH CURVATURE CORRECTION BASED ON RANGE
C        HT1, HT2 - THE HEIGHT ARRAYS TO COMPUTE DH IN THE VIL ROUTINE
C        PZ - CONTAINS THE REFLECTIVITY FACTORS FOR THE PREVIOUS
C            TILT ANGLE USED FOR COMPUTATION OF VIL
C
C     FOR DATA CARDS
C
C     THE FIRST DATA CARD READ CONTAINS THE RADAR CALIBRATION DATA,
C     DIFFERENT FOR EACH RADAR.
C     THE NEXT DATA CARD CONTAINS THE INITIALIZING INFORMATION LISTED
C     BELOW, IN THE ORDER GIVEN, STARTING IN COL. 1.
C     EXAMPLE:   10200226900102201940221008185430
C     EACH LELMENT LISTED IS CONTAINED IN PARENTHESES BELOW.
C
C        ILEFT - DISTANCE EAST (-) OR WEST (+) OF TAMU TO THE LOWER LEFT
C            CORNER OF THE 100 X 100 KM GRID, PLUS TWO.
C            FOR EXAMPLE, 80 WEST = +82, 80 EAST = -78 EX. (102)
C        JDOWN - DISTANCE NORTH (-) OR SOUTH (+) OF TAMU  TO THE LOWER
C            LEFT CORNER OF THE 100 X 100 KM GRID, PLUS TWO
C            FOR EXAMPLE, 15 SOUTH = +17, 15 NORTH = -13. EX. (002)
C        KAZ - DESIRED STARTING AZIMUTH TO LOAD THE GRID BOX- MOVING
C            CLOCKWISE EX. (269).
C        LASTAZ - THE LAST DATA AZIMUTH REQUIRED TO LOAD THE GRID BOX
C            EX. (001)
C        NTLT - THE LAST TILT ANGLE INCREMENTED BY 1 DEGREE IN THE TILT
C            SEQUENCE  EX. (02)
C        KRANGE - THE DISTANCE TO THE NEAREST POINT IN THE GRID BOX
C            EX. (20)
C        ISTRT - STARTING TIME OF SCAN (LOCAL TIME)  EX. (184822)
```

```
C             IRIT - FILE ONTO WHICH DATA IS WRITTEN. DEFINED IN JCL EX. (10)
C             IRR - FILE FROM WHICH DATA IS READ. DEFINED IN JCL EX. (08)
C             NENDT - END TIME OF THE SCAN SEQUENCE EX. (185430)
C
C
C     ********* NOTE ***********
C           KAZ AND LASTAZ MUST BE ODD NUMBERS
C           KRANGE MUST BE AN EVEN NUMBER
C     ***********************
C
C       OTHER VARIABLES
C           WAVEC - LOG OF RADAR CONSTANT IN DBM M**3 MM**(-6) KM**(-2)
C           KII AND KKII - CONSTANTS USED FOR CODING THE AZIMUTH PARAMETER
C                OF THE ARRAYS
C           IAZ1 AND IAZ2 - AZIMUTHS AS READ FROM DATA TAPE (TWO RADIALS
C                OF 1 KM DATA AND FOUR RADIALS OF 2 KM DATA ARE CONTAINED
C                IN EACH RECORD)
C           LVL - A COUNTER USED WHEN PLOTTING MAPS TO INDICATE WHICH LEVEL
C                IS BEING CALCULATED
C           II - AZIMUTH PARAMETER IN CODED FORM
C           MM - COUNTER USED FOR MAP CAPTIONS
C           PTILT - A REFERENCE LEVEL USED TO MONITOR THE ELEVATION ANGLE
C
C
C     ****** JCL - JOB CONTROL LANGUAGE *****
C           WITH THIS JCL, THE PROGRAM RUNS IN 'FORTRAN H EXTENDED'.
C           THE JCL WILL REQUIRE SOME CHANGES, BUT  NONE SIGNIFICANT, FOR
C           EACH PROGRAM RUN.  NOTE THAT THE FIRST CHARACTER ON ALL JCL
C           CARDS (COL. 1) SHOULD BE A '/', REPRODUCED HERE AS AN 'X'.
C
X/RADAR    JOB (X999.006D.009.015.XX).'YOUR NAME              '
C
C           009 IS TIME IN MINUTES. 015 IS LINES OF PRINTED OUTPUT IN
C           THOUSANDS.  DON'T CHANGE THESE
C
X*PASSWORD      XXXX
X*SETUP
C
C           THIS TELLS THE MACHINE NOT TO RUN UNTIL THE
C           TAPES HAVE BEEN MOUNTED.
C
X*LEVEL         X
X*JOBPARM K=0.R=512.T=9.TAPE9=2
X/ EXEC FORTXCLG.GOREGN=512K.FXLNSPC='3120.(100.10)'
X/FORT.SYSIN DD *
C
C           DO NOT CHANGE THESE LAST THREE CARDS
C
C
C     ********* THE MAIN PROGRAM CARD DECK BEGINS HERE
C
C
      DIMENSION ICLASS(200).CALIB(255)
      COMMON/BLOCKA/ZW(100.100).PVIZ1(100.100).PVIZ2(100.100).PVIZ3(100.
     1100).VIZ(100.100).KRANGE.A(4.4).IDIV1(150).IDIV2(150).IDIV3(150).
     2ZP(100.200).PZ(100.100).Z(51.51).CORECT(150).ICOUNT.HT1(100).
     3HT2(100).IADD.IADDR
      LOGICAL*1 LOGC(1720)
      INTEGER*2 IHWORD(860)
      EQUIVALENCE(LOGC(1).IHWORD(1))
      DIMENSION IEL2(3)
      DATA IZRO/'1'/.IONE/'2'/.NINE/'9'/.IHWORD/860*0/.ICHECK/'57'/.IZER
```

```
      *0/'0'/
       DATA ICLASS/200*0/,CALIB/255*0.0/
C
       WAVEC=6.0
C
C          THIS VALUE MUST BE CHANGED TO MATCH THE RADAR THE DATA  CAME
C          FROM, OR WHENEVER A NEW RADAR CONSTANT IS COMPUTED FOR
C          THE RADARS
C
       CALL LOAD(CALIB)
C
C          THIS RECONSTRUCTS THE CALIBRATION CURVE OF THE RADAR AND
C          CONVERTS THE 256 DIGITAL INTEGERS TO EQUIVALENT DBM VALUES.
C          IT ALSO PRINTS OUT THE ENTIRE CALIB ARRAY
C
C          READ DATA CARD FOR THE GRID BOX, STARTING TIME, DATA FILES,
C          AND PRINT THEM OUT BELOW THE CALIB ARRAY.
C
1      READ(5,100,END=99999)ILEFT,JDOWN,KAZ,LASTAZ,NTLT,KRANGE,ISTRT,IRIT
     1,IRR,NENDT
  100 FORMAT(4I3,2I2,I6,2I2,I6)
       WRITE(6,111) KAZ,LASTAZ,KRANGE,ILEFT,JDOWN
  111 FORMAT('0',' 1ST AZ = ',I3,' LAST AZ = ',I3,' KRANGE = ',I3,' LEFT
     C = ',I3,' DOWN = ',I3)
       WRITE(6,1000)IRIT,IRR
 1000 FORMAT('0','WRITE ON FILE ',I2,', READ FROM TAPE ',I2)
C
C          INITIALIZE OR DEFINE COUNTERS
C
       NCOUNT=0
       ICOUNT=0
       KII=KAZ-1
       KKII=(361-KAZ)
       PTILT=0.0
C
       CALL DIVIDE (NTLT)
C
C          DIVIDE IS A SUBROUTINE WHICH CALCULATES THE VALUES OF THE
C          DIVISORS NEEDED TO OBTAIN A MEAN REFLECTIVITY IN A LAYER.
C
C          READ DATA FROM FILE IRR
C
   15 READ(IRR,177,ERR=999,END=99999)IDATE,ITIME,ID,IDS,IRI,ISA,IRE,IPE,
     *IAZ1,IEL1,IEL2,(LOGC(I),I=2,1720,2)
  177 FORMAT(A3,1I6,3X,6A1,I3,A3,T22,3A1,4(215A1))
C
C          TEST TIME AGAINST ISTRT.  IF NOT AT STARTING TIME, READ
C          MORE DATA.  IF TIME HAS EXCEEDED NENDT, BEGIN PRINTING
C          OUT THE REMAINING MAPS.
C
       IF(ITIME.LT.ISTRT)GO TO 15
       IF(ITIME.GT.NENDT) GO TO 99
       INDEX=0
C
C          TEST RANGE INTERVAL.  IF IRI=2 KM, THEN IADDR=2
C          TEST DEGREE SELECT.  IF IDS=2 DEG, THEN IADD=2
C
       IADD=1
       IADDR=1
       IF(IDS.EQ.IONE)IADD=2
       IF(IRI.EQ.IONE)IADDR=2
C
```

```
        IAZ2 = IAZ1 + IADD
        IAZ3=IAZ2+IADD
        IAZ4=IAZ3+IADD
C
C         TEST AZIMUTH TO SEE IF IAZ IS BETWEEN KAZ AND LASTAZ.
C
        IF(KAZ.LT.LASTAZ) GOTO48
        IF(IAZ1.LT.KAZ.AND.IAZ1.GT.LASTAZ)GOTO58
        IF(IAZ1.LT.180) GOTO51
        GO TO 49
     48 IF(IAZ1.LT.KAZ.OR.IAZ1.GT.LASTAZ) GOTO58
     49 II=IAZ1-KII
        GO TO 52
     51 II=IAZ1+KKII
     52 CONTINUE
C
C         CALCULATE TILT AND TEST AGAINST PTILT.  IF TILT IS MUCH MORE
C         THAN PTILT, THEN THE SCAN HAS BEEN INCREMENTED UPWARDS AND THE
C         PROGRAM PRINTS OUT THE ZERO LEVEL MAP, THEN PTILT IS ADJUSTED
C         UPWARDS TO MATCH TILT, AND THE PROCESSING CONTINUES.  IF TILT
C         IS MUCH LESS THAN PTILT, THEN THE PROGRAM ASSUMES A NEW SCAN
C         HAS BEEN READ, AND IT TERMINATES PROCESSING THE DATA, AND
C         PRINTS OUT ALL THE MAPS.
C
C         IEL2(1), (2), AND (3) ARE THE TENS, UNITS, AND TENTHS DIGITS
C         OF THE ELEVATION ANGLE.
C         ATOI IS A SUBROUTINE THAT CHECKS TO ENSURE THAT THE DIGITS OF
C         IEL1 WERE CORRECTLY CONVERTED INTO/FROM BINARY FORM.  A NON-
C         ZERO RESULT RETURNED FROM THIS TEST ENDS THE PROGRAM
C
        IF(IEL2(1).GT.NINE.OR.IEL2(2).GT.NINE.OR.IEL2(3).GT.NINE)GOTO16
        CALL ATOI(IEL1,3,0,IEL,NTEST)
        IF(NTEST.NE.0)GOTO9999
        TILT=IEL/10.0
C
C         THIS ENSURES THAT TILT=IEL1
C
     16   CONTINUE
        INDEX=1
        IF(TILT-PTILT.GE.0.4)GOTO78
        IF (TILT-PTILT.LT.-0.5)GO TO 99
C
C         PROCESSING OF THE FIRST RADIAL OF DATA BEGINS HERE.  TEST FOR
C         RANGE INTERVAL (IRI) AND LOAD THE ARRAYS ICLASS WITH 180 VALUES
C         OF REFLECTIVITY DATA FOR THE 1 KM INTERVAL AND 90 VALUES FOR
C         THE 2 KM INTERVAL.
C
C         THERE ARE 860 REFLECTIVITY VALUES STORED IN ONE RECORD.  THIS
C         REPRESENTS 2 RADIALS OF DATA IN THE 1 KM MODE AND 4 RADIALS
C         IN THE 2 KM MODE.  IN THE 1 KM MODE, IHWORD(1-430)=1ST RADIAL,
C         (431-860)=2ND RADIAL.  IN THE 2 KM MODE, IHWORD(1-215)=1ST,
C         (216-430)=2ND, (431-645)=3RD, AND (646-860)=4TH.
C
     86 CONTINUE
C
        IF(IRI.EQ.IONE)GO TO 5
C
        DO 600 I=1,180
    600 ICLASS(I+20)=IHWORD(I)
        GO TO 6
C
      5 DO 601 I=2,180,2
```

```
  601 ICLASS(I+20)=IHWORD(I/2)
C
C          THIS DO LOOP COMPUTES THE REFLECTIVITIES FOR 100 RANGES FROM
C          THE DIGITIZED DATA IN ICLASS.  THE RANGE IS I + KRANGE.  FOR
C          AN EXPLANATION OF THE EQUATION FOR ZW(II,I), SEE CHAPTER II.
C
    6 DO 10 I=IADDR,100,IADDR
      K=I+KRANGE
      ZW(II,I)=0.0
      ARNG=FLOAT( K )
      IF (ICLASS(K).LE.34)GOTO10
      ZW(II,I)=10.**(-0.1*CALIB(ICLASS(K))+2.*ALOG10(ARNG)+WAVEC)
      IF(TILT.LT.0.5)GOTO311
      GOTO10
  311 ZINTRP=ZW(II,I)
C
C          IF THE TILT ANGLE IS LESS THAN 0.5 DEGREE, THE ZW DATA ARE
C          ADDED INTO THE LOWER LAYER PVSZ ARRAY, OTHERWISE THEY ARE NOT.
C          ZINTRP IS THE INTERPOLATED VALUE OF THE REFLECTIVITY AND IT IS
C          ALWAYS DIVIDED BY THE APPROPRIATE DIVISOR BEFORE SUMMATION.
C
      IF(ZINTRP.LE.1.0)GOTO10
      PVIZI(II,I)=PVIZI(II,I)+              ZINTRP/IDIVI(I)
      PZ(II,I)=ZINTRP
   10 CONTINUE
      IF (TILT.LE.0.5) GOTO58
      CALL INTRP2(TILT,II )
C
C          THE INTRP2 SUBROUTINE USES THE TILT ANGLE AND THE CODED AZIMUTH
C          TO ACCOMPLISH THE LAGRANGIAN INTERPOLATION ALONG THE RADIAL OF
C          DATA FOR 100 KM OF RANGE.
C
   58 CONTINUE
.C
C          THE SECOND RADIAL OF DATA IS CONVERTED AND PROCESSED AS ABOVE.
C
      IF (KAZ.LT.LASTAZ) GO TO 68
      IF(IAZ2.LT.KAZ.AND.IAZ2.GT.LASTAZ)GO TO 77
      IF (IAZ2.LT.180) GOTO71
      GO TO 69
   68 IF(IAZ2.LT.KAZ.OR.IAZ2.GT.LASTAZ)GO TO 77
 ·69 II=IAZ2-KII
      GO TO 72
   71 II=IAZ2+KKII
   72 CONTINUE
      IF(INDEX.EQ.1)GOTO166
      IF(IEL2(1).GT.NINE.OR.IEL2(2).GT.NINE.OR.IEL2(3).GT.NINE)GOTO166
      CALL ATOI(IEL1,3,0,IEL,NTEST)
      IF(NTEST.NE.0)GOTO9999
      TILT=IEL/10.0
  166 CONTINUE
      INDEX=2
      IF(TILT-PTILT.GE.0.4)GOTO78
      IF (TILT-PTILT.LT.-0.5)GO TO 99
   87 CONTINUE
C ·
      IF(IRI.EQ.IONE)GO TO 705
C
      DO 700 I=1,180
  700 ICLASS(I+20)=IHWORD(I+430)
      GO TO 706
C
```

```
    705 DO 701 I=2,180,2
    701 ICLASS(I+20)=IHWORD(I/2+215)
    706 DO 11 I=IADDR,100,IADDR
        K=I+KRANGE
        ZW(II,I)=0.0
        ARNG=FLOAT(K)
        IF (ICLASS(K).LE.34)GOTO11
        ZW(II,I)=10.**(-0.1*CALIB(ICLASS(K))+2.*ALOG10(ARNG)+WAVEC)
        IF(TILT.LT.0.5)GOTO321
        GOTO11
    321 ZINTRP=ZW(II,I)
        IF(ZINTRP.LE.1.0)GOTO11
        PVIZ1(II,I)=PVIZ1(II,I)+ZINTRP/IDIV1(I)
        PZ(II,I)=ZINTRP
 11     CONTINUE
        IF(TILT.LE.0.5)GOTO77
        CALL INTRP2(TILT,II)
     77 CONTINUE
C
        IF(IRI.EQ.IZRO)GO TO 15
C
C           IF THE RANGE INTERVAL IS 2 KM, THE THIRD AND FOURTH RADIALS
C           ARE PROCESSED AS ABOVE.  IF IN 1 KM MODE, ANOTHER DATA
C           RECORD IS READ.
C
        IF(KAZ.LT.LASTAZ)GO TO 368
        IF(IAZ3.LT.KAZ.AND.IAZ3.GT.LASTAZ)GO TO 377
        IF(IAZ3.LT.180)GO TO 371
        GO TO 369
    368 IF(IAZ3.LT.KAZ.OR.IAZ3.GT.LASTAZ)GO TO 377
    369 II=IAZ3-KII
        GO TO 372
    371 II=IAZ3+KKII
    372 CONTINUE
        IF(INDEX.EQ.2)GO TO 366
        IF(IEL2(1).GT.NINE.OR.IEL2(2).GT.NINE.OR.IEL2(3).GT.NINE)GO TO 366
        CALL ATOI(IEL1,3,0,IEL,NTEST)
        IF(NTEST.NE.0)GO TO 9999
        TILT=IEL/10.0
    366 CONTINUE
        INDEX=3
        IF(TILT-PTILT.GE.0.4)GO TO 78
        IF(TILT-PTILT.LT.-0.5)GO TO 99
     88 CONTINUE
C
        DO 900 I=2,180,2
    800 ICLASS(I+20)=IHWORD(I/2+430)
        DO 410 I=2,100,2
        K=I+KRANGE
        ZW(II,I)=0.0
        ARNG=FLOAT(K)
        IF(ICLASS(K).LE.34)GO TO 410
        ZW(II,I)=10.**(-0.1*CALIB(ICLASS(K))+2.*ALOG10(ARNG)+WAVEC)
        IF(TILT.LT.0.5)GO TO 331
        GO TO 410
    331 ZINTRP=ZW(II,I)
        IF(ZINTRP.LE.1.0)GO TO 410
        PVIZ1(II,I)=PVIZ1(II,I)+ZINTRP/IDIV1(I)
        PZ(II,I)=ZINTRP
    410 CONTINUE
        IF(TILT.LE.0.5)GO TO 377
        CALL INTRP2(TILT,II)
```

```
    377 CONTINUE
C
C          PROCESSING OF THE FOURTH RADIAL BEGINS HERE
C
        IF(KAZ.LT.LASTAZ)GO TO 468
        IF(IAZ4.LT.KAZ.AND.IAZ4.GT.LASTAZ)GO TO 15
        IF(IAZ4.LT.180)GO TO 471
        GO TO 469
    468 IF(IAZ4.LT.KAZ.OR.IAZ4.GT.LASTAZ)GO TO 15
    469 II=IAZ4-KII
        GO TO 472
    471 II=IAZ4+KKII
    472 CONTINUE
        IF(INDEX.EQ.3)GO TO 466
        IF(IEL2(1).GT.NINE.OR.IEL2(2).GT.NINE.OR.IEL2(3).GT.NINE)GO TO 466
        CALL ATOI(IEL1,3,0,IEL,NTEST)
        IF(NTEST.NE.0)GO TO 9999
        TILT=IEL/10.0
    466 CONTINUE
        INDEX=4
        IF(TILT-PTILT.GE.0.4)GO TO 78
        IF(TILT-PTILT.LT.-0.5)GO TO 99
     89 CONTINUE
        DO 900 I=2,180,2
    900 ICLASS(I+20)=IHWORD(I/2+645)
        DO 411 I=2,100,2
        K=I+KRANGE
        ZW(II,I)=0.0
        ARNG=FLOAT(K)
        IF(ICLASS(K).LE.34)GO TO 411
        ZW(II,I)=10.**(-0.1*CALIB(ICLASS(K))+2.*ALOG10(ARNG)+WAVEC)
        IF(TILT.LT.0.5)GO TO 431
        GO TO 411
    431 ZINTRP=ZW(II,I)
        IF(ZINTRP.LE.1.0)GO TO 411
        PVIZI(II,I)=PVIZI(II,I)+ZINTRP/IDIVI(I)
        PZ(II,I)=ZINTRP
    411 CONTINUE
        IF(TILT.LE.0.5)GO TO 477
        CALL INTRP2(TILT,II)
    477 CONTINUE
C
        GO TO 15
C
C          THIS PROCEDURE CONTINUES UNTIL ALL OF THE DATA ARE READ FOR A
C          TILT SEQUENCE.
C
C
     78 CONTINUE
        ICOUNT=ICOUNT+1
        IF(ICOUNT.GT.1) GOTO83
C
C          THE FOLLOWING CODE DEVELOPS AND PLOTS THE ZERO DEGREE
C          REFLECTIVITY MAP. USING SUBROUTINE PLOTZ.
C
        DO 81 II=1,100,IADD
        DO 81 I=IADDR,100,IADDR
        ZP(II,I+KRANGE)=0.0
     81 ZP(II,I+KRANGE)=ZW(II,I)
        CALL QD2(ILEFT,JDOWN,KII,KKII)
        MM=1
        LVL=0
```

```
C
C          THE Z(X,Y) ARRAY IS CONVERTED TO DBZ AND PLOTTED.
C
      DO 82 I=1,51
      DO 82 J=1,51
      IF (Z(I,J).LE.1.0)Z(I,J)=1.0
      Z(I,J)=10.*ALOG10(Z(I,J))
   82 CONTINUE
      CALL PLOTZ(IDATE,NENDT,LVL,ILEFT,JDOWN,MM)
C
C          THE ARRAY Z IS WRITTEN TO TAPE FILE IRIT TO BE USED LATER WITH
C          A CONREC SUBROUTINE WHICH CONTOURS THE DATA AND DRAWS MAPS ON
C          THE CALCOMP PLOTTER.
C
      WRITE(IRIT,6006)Z
 6006 FORMAT(200F5.1,89F5.1)
   83 CONTINUE
      DO 84 I=1,100
   84 HT1(I)=HT2(I)
      PTILT=TILT
C
      GO TO(86,87,88,89),INDEX
C
C          GOES BACK TO WHERE IT LEFT OFF PROCESSING THE RADIALS
C
C          WHEN TILT BECOMES MORE THAN .5 DEG LESS THAN PTILT, THE
C          PROGRAM ASSUMES THAT THE SCAN SEQUENCE IS OVER AND TERMINATES
C          PROCESSING.  IT THEN BEGINS TO GENERATE THE OUTPUT MAPS.
C
   99 CONTINUE
C
C          THE LOWER LAYER PVSZ MAP (0-15 KFT) IS GENERATED FIRST
C          AND WRITTEN ON THE OUTPUT TAPE (IRIT)
C
      MM=2
      LVL=MM*5000
      DO 777 II=1,100,IADD
      DO 777 I=IADDR,100,IADDR
      ZP(II , I + KRANGE) =0.0
C
C          THE DUMMY ARRAY ZP IS LOADED WITH THE APPROPRIATE PVSZ ARRAY
C          AND SENT TO SUBROUTINE OD2.
C
      ZP(II , I + KRANGE) = 3 * PVIZ1(II,I)
  777 CONTINUE
      CALL OD2(ILEFT,JDOWN,KII,KKII)
      DO 150 I=1,51
      DO 150 J=1,51
      IF(Z(I,J).LE.1.0)Z(I,J)=1.0
      Z(I,J)=10*ALOG10(Z(I,J))
  150 CONTINUE
      CALL PLOTZ(IDATE,NENDT,LVL,ILEFT,JDOWN,MM)
      WRITE(IRIT,6006)Z
C
C          NEXT IS THE MIDDLE LAYER PVSZ MAP (15-35 KFT)
C
      MM=3
      LVL=MM*5000
      DO 778 II=1,100,IADD
      DO 778 I=IADDR,100,IADDR
      ZP(II , I + KRANGE) =0.0
      ZP(II , I + KRANGE) = 4 * PVIZ2(II,I)
```

```
778     CONTINUE
        CALL QD2(ILEFT,JDOWN,KII,KKII)
        DO 160 I=1,51
        DO 160 J=1,51
        IF(Z(I,J).LE.1.0)Z(I,J)=1.0
        Z(I,J)=10*ALOG10(Z(I,J))
160     CONTINUE
        CALL PLOTZ(IDATE,NENDT,LVL,ILEFT,JDOWN,MM)
        WRITE(IRIT,6006)Z
C
C           NOW THE UPPER LAYER PVSZ MAP (35-50 KFT) IS GENERATED
C
        MM=4
        LVL=MM*5000
        DO 779 II=1,100,IADD
        DO 779 I=IADDR,100,IADDR
        ZP(II , I + KRANGE) =0.0
        ZP(II , I + KRANGE) = 3 * PVIZ3(II,I)
779     CONTINUE
        CALL QD2(ILEFT,JDOWN,KII,KKII)
        DO 170 I=1,51
        DO 170 J=1,51
        IF(Z(I,J).LE.1.0)Z(I,J)=1.0
        Z(I,J)=10*ALOG10(Z(I,J))
170     CONTINUE
        CALL PLOTZ(IDATE,NENDT,LVL,ILEFT,JDOWN,MM)
        WRITE(IRIT,6006)Z
C
C           VIL IS CALCULATED IN A SIMILAR MANNER.  VIL IS MEASURED
C           IN KG/M**2
C
        MM=5
        LVL=MM*5000
        DO 780 II=1,100,IADD
        DO 780 I=IADDR,100,IADDR
        ZP(II,I+KRANGE)=0.0
  780   ZP(II,I+KRANGE)=VIZ(II,I)
        CALL QD2(ILEFT,JDOWN,KII,KKII)
        DO 180 I=1,51
        DO 180 J=1,51
        Z(I,J)=Z(I,J)/1000.0
  180   CONTINUE
        CALL PLOTZ(IDATE,NENDT,LVL,ILEFT,JDOWN,MM)
        WRITE(IRIT,6006)Z
        ENDFILE IRIT
C
C           THIS PUTS AN END-OF-FILE MARK ON THE TAPE, SO THESE 5 MAPS
C           COMPRISE ONE FILE
C
        WRITE(6,2000)IRIT
 2000   FORMAT('0','END OF FILE WRITTEN ON TAPE ',I2)
        IF (IDS.EQ.IONE) WRITE(6,7217)
 7217   FORMAT('0',' DEGREE SELECT = 2')
        IF(IRI.EQ.IONE) WRITE(6,7317)
 7317   FORMAT('0',' RANGE SELECT = 2 KM.')
C
C           THIS INDICATES WHETHER EITHER 2 DEG OR 2 KM MODE DATA WAS
C           PROCESSED.  DEFAULT VALUES ARE 1 DEG AND 1 KM.
C
        DO 781 II=1,100
        DO 781 I=1,100
        PVIZ1(II,I)=0.0
```

```
          PVIZ2(II,I)=0.0
          PVIZ3(II,I)=0.0
   781 VIZ(II,I)=0.0
          DO 782 I=1,100
          HT2(I)=0.0
   782 HT1(I)=0.0
C
C         REINITIALIZES THE ARRAY VALUES TO ZERO.
C         THE PROGRAM IS NOW READY TO READ ANOTHER INITIAL DATA CARD
C         AND BEGIN PROCESSING ANOTHER SCAN SEQUENCE.
C
          GO TO 1
999    WRITE(6,300)
300    FORMAT('0','$$$$$$$$      READ ERROR ENCOUNTERED    $$$$$$$$$$$$$$$')
          GO TO 99999
9999   WRITE(6,301)
301    FORMAT('0','$$$$$$$ ATOI NTEST ERROR    $$$$$$$$$$$$$$$$$$$$$$$$$')
99999 CONTINUE
          STOP
          END
C
C
C
C
          BLOCK DATA
          COMMON/BLOCKA/ZW(100,100),PVIZ1(100,100),PVIZ2(100,100),PVIZ3(100,
         1100),VIZ(100,100),KRANGE,A(4,4),IDIV1(150),IDIV2(150),IDIV3(150),
         2ZP(100,200),PZ(100,100),Z(51,51),CORECT(150),ICOUNT,HT1(100),
         3HT2(100),IADD,IADDR
          DATA A(1,2),A(2,3),A(3,4)/3*-1.0/,A(1,3),A(2,4)/2*-2.0/,A(1,4)/-3.
         70/,A(2,1),A(3,2),A(4,3)/3* 1.0/,A(3,1),A(4,2)/2*2.0/,A(4,1)/3.0/
          DATA VIZ,PVIZ1,PVIZ2,PVIZ3/40000*0.0/,IDIV1,IDIV2,IDIV3/450*0/
          DATA ZP/20000*0.0/,Z/2601*0.0/,CORECT/150*0.0/,PZ/10000*0.0/,
          END
C
C
C
C
          SUBROUTINE DIVIDE(NTLT)
          COMMON/BLOCKA/ZW(100,100),PVIZ1(100,100),PVIZ2(100,100),PVIZ3(100,
         1100),VIZ(100,100),KRANGE,A(4,4),IDIV1(150),IDIV2(150),IDIV3(150),
         2ZP(100,200),PZ(100,100),Z(51,51),CORECT(150),ICOUNT,HT1(100),
         3HT2(100),IADD,IADDR
C
C         THIS SUBROUTINE DETERMINES THE NUMBER OF ELEVATION ANGLES OF
C         DATA TO BE ADDED INTO EACH PVSZ LAYER FOR EACH RANGE GATE,
C         AND CALLS THEM IDIV1(I), IDIV2(I), AND IDIV3(I).
C
C
C         HT11 IS THE HEIGHT OF THE 15 KFT LEVEL IN KM
C         HT22 IS THE HEIGHT OF THE 35 KFT LEVEL IN KM
C         HT33 IS THE HEIGHT OF THE 50 KFT LEVEL IN KM
C         ELEV1 IS THE TILT ANGLE THAT PASSES THROUGH THE 15 KFT LEVEL
C         AT THE GIVEN RANGE
C         ELEV2 IS THE TILT ANGLE THAT PASSES THROUGH THE 35 KFT LEVEL
C         .T THE GIVEN RANGE.
C         ELEV3 IS THE TILT ANGLE THAT PASSES THROUGH THE 50 KFT LEVEL
C         AT THE GIVEN RANGE.
C
          SUBTLT=FLOAT(NTLT)
          DO 1 I=1,150
          R= FLOAT( I + KRANGE )
```

```
          RSQ = R**2
          CORECT(I)=(0.375 * RSQ)/ 6371.315
C
C             6371.315 IS THE RADIUS OF THE EARTH IN KM.  IF SOME OTHER UNIT
C          OF DISTANCE IS USED IN THE DIGITAZATION PROCESS, THEN THE
C          RADIUS OF THE EARTH IN THOSE UNITS MUST BE USED INSTEAD OF THIS
C          NUMBER.
C
          HT11=4.572-CORECT(I)
          HT22=10.668-CORECT(I)
          HT33=15.240-CORECT(I)
          ELEV1=ATAN2(HT11,R)*57.29578
          ELEV2=ATAN2(HT22,R)*57.29578
          ELEV3=ATAN2(HT33,R)*57.29578
C
C             IF THE ELEVATION ANGLE COMPUTED IS GREATER THAN THE LAST TILT
C          ANGLE INCREMENTED BY 1 DEGREE, THEN THE DIVISOR MUST BE
C          CALCULATED DIFFERENTLY.
C
          IF(ELEV1.GT.SUBTLT)GOTO10
          IDIV1(I) = IFIX(ELEV1)
11        CONTINUE
          IF(ELEV2.GT.SUBTLT)GOTO20
          IDIV2(I) = IFIX(ELEV2) - IDIV1(I)
12        CONTINUE
          IF(ELEV3.GT.SUBTLT)GOTO30
          IDIV3(I) = IFIX(ELEV3) - (IDIV1(I) + IDIV2(I))
          GOTO1
10        IDIV1(I) = IFIX((ELEV1 - SUBTLT)/2.0) + NTLT
          GOTO11
20        IDIV2(I) = IFIX((ELEV2 - SUBTLT)/2.0) + NTLT - IDIV1(I)
          GOTO12
30        IDIV3(I) = IFIX((ELEV3-SUBTLT)/2.0)+NTLT  -(IDIV1(I)+IDIV2(I))
C
          IF(IDIV1(I).EQ.0)IDIV1(I)=1
C
1         CONTINUE
          RETURN
          END
C
C
C
C
          SUBROUTINE INTRP2( TILT,II)
          DIMENSION RM(4)
          COMMON/BLOCKA/ZW(100,100),PVIZ1(100,100),PVIZ2(100,100),PVIZ3(100,
         1100),VIZ(100,100),KRANGE,A(4,4),IDIV1(150),IDIV2(150),IDIV3(150),
         2ZP(100,200),PZ(100,100),Z(51,51),CORECT(150),ICOUNT,HT1(100),
         3HT2(100),IADD,IADDR
C
C             THIS SUBROUTINE USES THE CODED AZIMUTH (II) AND THE ELEVATION
C          ANGLE TO PERFORM THE LAGRANGIAN INTERPOLATION ALONG THE RADIAL.
C
C
C
C
C          DEFINITIONS
C
C             PHI- THE TILT ANGLE IN RADIANS
C          R - RANGE OF THE SUMMATION COLUMN AT THE ZERO DEGREE TILT ANGLE
C          H - HEIGHT OF THE DATA POINT IN KM.
C          HT2(I) - THE HEIGHT IN METERS
C          IHT - HEIGHT OF THE DATA POINT IN KFT
```

```
C          RPRM - RADIAL DISTANCE TO THE INTERPOLATION DATA POINT
C
       IF(IADDR.EQ.1)GO TO 77
C
C          INITIALIZE OFF-DIAGONAL ELEMENTS OF A FOR 2 KM MODE.
C
       A(1,2)=-2.0
       A(1,3)=-4.0
       A(1,4)=-6.0
       A(2,1)=1.0
       A(2,3)=-1.0
       A(2,4)=-2.0
       A(3,1)=2.0
       A(3,2)=1.0
       A(3,4)=-1.0
       A(4,1)=3.0
       A(4,2)=2.0
       A(4,3)=1.0
   77  PHI=TILT*0.0174532
       DO 1 I=1,100,IADDR
C
C          THE INDICES FOR THE FOUR DATA POINTS USED IN THE LAGRANGIAN
C          INTERPOLATION ARE I, I+1, I+2, AND I-1 FOR THE 1 KM MODE AND
C          I, I+2, I+4, AND I-2 FOR THE 2 KM MODE.
C
       IP1=I+IADDR
       IP2=I+2*IADDR
       IM1=I-IADDR
       IF(IM1.LE.0.OR.IP2.GE.100)GOTO1
       ZINTRP=0.0
       R= FLOAT(I+KRANGE)
       H=   R*TAN( PHI )+CORECT(I)
       HT2(I)=H*1000.0
       IF(ICOUNT.LT.1)HT1(I)=HT2(I)
       DH=HT2(I)-HT1(I)
       IF(ZW(II,I).EQ.0.0.AND.ZW(II,IP1).EQ.0.0)GOTO1
       IHT=IFIX(H*3.28084+1.0)
       RPRM=SQRT(R**2+H**2)
       DELR=RPRM-R
C
       IF(IADDR.EQ.2)GO TO 20
C
       IF(DELR.LT.1.0)XCNT=0.0
C
C          IN THE 1 KM MODE, IF DELR IS GREATER THAN 1 BUT LESS THAN 2,
C          THEN THE INTERPOLATION POINT LIES BETWEEN I+1 AND I+2
C
       IF(DELR.GE.1.0.AND.DELR.LT.2.0)XCNT=1.0
       IF(DELR.GE.2.0.AND.DELR.LT.3.0)XCNT=2.0
       IF(DELR.GE.3.0.AND.DELR.LT.4.0)XCNT=3.0
       IF(DELR.GE.4.0.AND.DELR.LT.5.0)XCNT=4.0
       GO TO 22
C
C          IN THE 2 KM MODE, THE INTERVALS ARE DIFFERENT.
C
   20  IF(DELR.LT.2.0)XCNT=0.0
       IF(DELR.GE.2.0.AND.DELR.LT.4.0)XCNT=2.0
       IF(DELR.GE.4.0.AND.DELR.LT.6.0)XCNT=4.0
       IF(DELR.GE.6.0.AND.DELR.LT.8.0)XCNT=6.0
       IF(DELR.GE.8.0.AND.DELR.LT.10.0)XCNT=8.0
C
C          THE DATA POINT INDEX COUNTERS ARE INCREMENTED BY XCNT, WHICH
```

```
C           DEPENDS ON THE VALUE OF DELR.
C
   22  IP1=IP1+XCNT
       IP2=IP2+XCNT
       IM1=IM1+XCNT
       IF(IM1.LE.0.OR.IP2.GE.100)GOTO1
C
C          IF THE VALUE OF THE REFLECTIVITY ON EITHER SIDE OF THE INTER-
C          POLATION POINT ARE EQUAL, THEN NO INTERPOLATION IS NECESSARY.
C
       IF(ZW(II,IM1+IADDR).EQ.ZW(II,IP1))GO TO 16
       DELR=DELR-XCNT
       IF(DELR.LE.0.01)GOTO17
C
C          THE DIAGONAL ELEMENTS OF THE MATRIX USED FOR THE LAGRANGIAN
C          INTERPOLATION ARE COMPUTED.  THE OFF-DIAGONAL ELEMENTS ARE
C          ALWAYS THE SAME FOR A PARTICULAR RANGE INTERVAL, AND ARE
C          ALWAYS SET AT THE BEGINNING OF THE PROGRAM.
C
       ADDR=FLOAT(IADDR)
       A(1,1)=1.0*ADDR+DELR
       A(2,2)=DELR
       A(3,3)=-1.0*ADDR+DELR
       A(4,4)=-2.0*ADDR+DELR
       DO 3 K=1,4
       PROD=1.0
       DO 4 J=1,4
   4   PROD=PROD*A(K,J)
   3   RM(K)=PROD
       SUM=0.0
       K1=0
       DO 5 K=IM1,IP2,IADDR
       K1=K1+1
       ZPRM=ZW(II,K)/RM(K1)
       SUM=SUM+ZPRM
   5   CONTINUE
       DIAG=1.0
       DO 6 K=1,4
       DIAG=DIAG*A(K,K)
   6   CONTINUE
       ZINTRP=DIAG*SUM
       GOTO10
   16  ZINTRP=ZW(II,IP1)
       GOTO10
   17  ZINTRP=ZW(II,IM1+IADDR)
   10  CONTINUE
       IF(ZINTRP.LE.1.0)ZINTRP=1.0
C
C          WHEN ICOUNT IS 1, WE ARE IN THE BASE OR ZERO LEVEL AND CANNOT
C          INTEGRATE.
C
       IF(ICOUNT.LT.1)GOTO100
C
C          THE INTEGRATION OF LIQUID WATER CONTENT IS ACCOMPLISHED.
C
       VIZ(II,I)=VIZ(II,I)+(3.44E-3*(PZ(II,I)**.571+ZINTRP**.571)/2.)*DH
  100  CONTINUE
       PZ(II,I)=ZINTRP
       IF(ZINTRP.LE.1.0)GOTO1
C
C          IHT IS TESTED TO DETERMINE INTO WHICH LAYER THE  INTERPOLATED
C          REFLECTIVITY (ZINTRP) GOES.
```

```
C                                      /
        IF(IHT.GT.15.AND.IHT.LE.35)GOTO55
        IF(IHT.GT.35)GOTO56
        PVIZ1(II,I)=PVIZ1(II,I)+ZINTRP/FLOAT(IDIV1(I) )
        GOTO1
C
55      CONTINUE
        IF(IDIV2(I ).EQ.0) GOTO1
        PVIZ2(II,I)=PVIZ2(II,I)+ZINTRP/FLOAT(IDIV2(I))
        GOTO1
C
56      CONTINUE
        IF(IHT.GT.50)GOTO1
        IF(IDIV3(I ).LE.0)GOTO1
        PVIZ3(II,I)=PVIZ3(II,I)+ZINTRP/FLOAT(IDIV3(I))
1       CONTINUE
        RETURN
        END
C
C
C
C
        SUBROUTINE QD2 (ILEFT,JDOWN,KII,KKII)
        COMMON/BLOCKA/ZW(100,100),PVIZ1(100,100),PVIZ2(100,100),PVIZ3(100,
       1100),VIZ(100,100),KRANGE,A(4,4),IDIV1(150),IDIV2(150),IDIV3(150),
       2ZP(100,200),PZ(100,100),Z(51,51),CORECT(150),ICOUNT,HTI(100),
       3HT2(100),IADD,IADDR
        INTEGER AZONE,AZTWO,AZTHRE,AZMTH
C
C       THIS SUBROUTINE STEPS THROUGH THE RECTANGULAR GRID COORDINATES
C       AND COMPUTES A VALUE FOR EACH USING AN INTERPOLATION SCHEME WHICH
C       SELECTS DATA FROM THE 9 NEAREST CYLINDRICAL DATA POINTS CONTAINED
C       IN THE ZP ARRAY.  THE OUTPUT ARRAY, Z, IS RETURNED TO THE MAIN
C       PROGRAM FOR PLOTTING OR FURTHER USE.  SEE VOGEL'S (1973) THESIS
C       FOR EXPLANATION OF THE INTERPOLATION SCHEME.
C
C
C
C       DEFINITIONS
C
C           FLOATI - DISTANCE WEST (+) OR EAST (-) OF TAMU IN KM TO THE X
C                 GRID COORDINATE (I)
C           FLOATJ - DISTANCE NORTH (+) OR SOUTH (-) OF TAMU IN KM TO THE Y
C                 GRID COORDINATE (J)
C           R - THE DIRECT DISTANCE FROM TAMU TO THE GRID POINT IN KM
C           THETA - ANGLE, IN DEGREES FROM TRUE NORTH, OF THE GRID COORDINATE
C           AZMTH - THE NEAREST DATA AZIMUTH TO THETA
C           AZONE - THE NEAREST AZIMUTH TO THETA IN CODED FORM
C           REALI - THE NEAREST AZIMUTH IN DEGREES
C           X - PERCENTAGE OF DISTANCE FROM NEAREST ANGLE TO ANGLE OF
C                 THE GRID COORDINATE
C           IRI - THE NEAREST RANGE GATE TO THE GRID COORDINATE
C           REALJ - THE RANGE OF THE RANGE GATE IN KM
C           Y - PERCENTAGE OF DISTANCE FROM NEAREST RANGE GATE TO GRID POINT
C           AAA THROUGH III - THE 9 DATA POINTS TO BE USED IN THE QUADRATIC
C                 INTERPOLATION
C           B THROUGH F AND FONE - INTERPOLATED VALUES OF REFLECTIVITY
C
        DO 260 I=1,51
        FLOATI=FLOAT(2*I-ILEFT)
        DO 260 J=1,51
C
```

```
        Z  (I,J)=0.0
        FLOATJ=FLOAT(2*J-JDOWN)
        R=SQRT(FLOATI**2+FLOATJ**2)
        IF(R.LT.2.0.OR.R.GT.200.0) GO TO 260
        THETA=(ATAN2(FLOATI,FLOATJ))*57.2958
        IF(THETA.LT.0.0) THETA=THETA+360
        AZMTH=IFIX(THETA+0.5)
C
C          DIFFERENT INCREMENTS MUST BE SPECIFIED FOR EITHER
C          THE 2 DEG OR 2 KM MODE.
C
        IF(IADD.EQ.2)AZMTH=IFIX(THETA)/2*2+1
C
C          THIS INSURES THAT AZMTH IS ODD IN THE 2 DEGREE MODE
C
        IF(KII.GT.180.AND.AZMTH.LT.180)GO TO 213
        AZONE=AZMTH-KII
        GOTO214
C
  213   AZONE=AZMTH+KKII
  214   AZTWO=AZONE+IADD
        AZTHRE=AZONE-IADD
        REALI=FLOAT(AZMTH)
        X=THETA-REALI
        IR1=IFIX(R+0.5)
C
        IF(IADDR.EQ.2)IR1=(IFIX(R+.999)+1)/2*2
C
C          THIS INSURES THAT IR1 IS EVEN IN THE 2 KM MODE
C
        IR2=IR1+IADDR
        IR3=IR1-IADDR
        REALJ=FLOAT(IR1)
        Y=R-REALJ
C
        AAA=ZP(AZONE,IR1)
        BBB=ZP(AZONE,IR2)
        CCC=ZP(AZONE,IR3)
        DDD=ZP(AZTWO,IR1)
        EEE=ZP(AZTWO,IR2)
        FFF=ZP(AZTWO,IR3)
        GGG=ZP(AZTHRE,IR1)
        HHH=ZP(AZTHRE,IR2)
        III=ZP(AZTHRE,IR3)
C
        IF(AAA.NE.0.0.OR.BBB.NE.0.0.OR.CCC.NE.0.0.OR.DDD.NE.0.0.OR.EEE.NE.
       C0.0.OR.FFF.NE.0.0.OR.GGG.NE.0.0.OR.HHH.NE.0.0.OR.III.NE.0.0) GO
       CTO 236
        GO TO 260
C
  236   B=(DDD-GGG)/2.0
        C=(BBB-CCC)/2.0
        D=DDD-AAA-B
        E=CCC-AAA+C
        IF(X.GE.0.0) GO TO 248
        IF(Y.GE.0.0) GO TO 245
        F=III-AAA+B+C-D-E
        FONE=III
        GO TO 254
C
  245   F=AAA-B+C+D+E-HHH
        FONE=HHH
```

```
        GO TO 254
C
  248   IF(Y.GE.0.0) GO TO 252
        F=AAA+B-C+D+E-FFF
        FONE=FFF
        GO TO 254
C
  252   F=EEE-AAA-B-C-D-E
        FONE=EEE
  254   ZZ=AAA+(B*X)+(C*Y)+(D*X**2)+(E*Y**2)+(F*X*Y)
C
C          IF THE INTERPOLATED VALUE OF THE REFLECTIVITY IS NEGATIVE, THEN
C          DO A LINEAR INTERPOLATION USING THE 4 DATA POINTS SURROUNDING
C          THE GRID POINT.
C
        IF(ZZ.LT.0.0)GOTO500
        ZZ=AMAX1(ZZ,AMIN1(AAA,DDD,GGG,BBB,CCC,FONE))
        IF(ZZ.LT.0.0) GO TO 260
        Z  (I,J)=ZZ
        GOTO260
C
500     CONTINUE
        IR1 = IFIX( R )
C
        IF(IADDR.EQ.2)IR1=(IFIX(R+.999)+1)/2*2
C
        IR2=IR1+IADDR
        DR = R - FLOAT( IR1 )
        DELT = THETA - FLOAT( AZMTH )
        IF(DELT)100,101,102
  100   DT=(1.0+ABS(1.0+DELT))
        IF(KII.GT.180.AND.AZMTH.LT.180)GO TO 110
        AZTWO=AZMTH-KII
        GOTO120
C
  110   AZTWO=AZMTH+KKII
  120   AZONE=AZTWO-IADD
        GOTO 103
C
101     CONTINUE
        IF(KII.GT.180.AND.AZMTH.LT.180)GO TO 111
        AZONE=AZMTH-KII
        GOTO 121
C
  111   AZONE=AXMTH+KKII
121     AA = ZP(AZONE,IR2)
        BB=ZP(AZONE,IR1)
        GOTO104
C
  102   DT=DELT
        IF(AZMTH.LT.180) GOTO112
        AZONE=AZMTH-KII
        GOTO 122
C
  112   AZONE=AZMTH+KKII
  122   AZTWO=AZONE+IADD
103     AA = ZP(AZONE,IR2) + ( ZP(AZTWO,IR2) - ZP(AZONE,IR2))* DT
        BB = ZP(AZONE,IR1) + ( ZP(AZTWO,IR1) - ZP(AZONE,IR1))* DT
104     Z(I,J) = BB + ( AA - BB) * DR
C
  260   CONTINUE
        RETURN
```

```
      END
C
C
C
      SUBROUTINE PLOTZ (ND,NT,LVL,IL,JD,MM)
      DIMENSION BUF(126),DIG(10),NT(2)
      COMMON/BLOCKA/Zd(100,100),PVIZ1(100,100),PVIZ2(100,100),PVIZ3(100,
     1100),VIZ(100,100),KRANGE,A(4,4),IDIV1(150),IDIV2(150),IDIV3(150),
     2ZP(100,200),PZ(100,100),Z(51,51),CORECT(150),ICOUNT,HT1(100),
     3HT2(100),IADD,IADDR
      DATA BLNK/1H /,PLUS/1H+/
      DATA DIG/1H0,1H1,1H2,1H3,1H4,1H5,1H6,1H7,1H8,1H9/
C
C     THIS SUBROUTINE TAKES A 50 X 50 RECTANGULAR GRID ARRAY AND PLOTS
C     FIRST THE LEFT HALF AND THEN THE RIGHT HALF OF THE ARRAY.  THE
C     RESULTANT PLOT IS 25 INCHES SQUARE WHEN BOTH HALVES ARE PIECED
C     TOGETHER.  AT A 2 KM GRID INTERVAL, THE MAP COVERS A 100 KM SQUARE.
C     STARTING WITH THE UPPER LEFT HAND CORNER OF THE RECTANGULAR GRID,
C     DBZ VALUES FROM THE Z ARRAY ARE LOADED A LINE AT A TIME INTO THE
C     BUF ARRAY.  FIRST, THE 126 CHARACTERS IN BUF ARE SET EQUAL TO A
C     BLANK.  THEN EVERY 25 CHARACTERS ARE SET EQUAL TO A PLUS (+).  THESE
C     GRID MARKS REPRESENT A DISTANCE OF 10 KM.
C
C
C     DEFINITIONS
C
C     ARRAYS
C        BUF - STORAGE LOCATION OF DATA TO BE PRINTED ON EACH LINE.
C              126 CHARACTERS LONG
C        DIG - CONTAINS CHARACTER REPRESENTATION FOR INTEGER VALUES 0-9
C
C     OTHERS
C        BLNK - A HOLLERITH BLANK CHARACTER
C        PLUS - A HOLLERITH PLUS SIGN (+)
C        NN - COUNTER WHICH STEPS ACROSS THE PAGE IN INCREMENTS OF FIVE
C             PRINT LOCATIONS REPRESENTING 2 KM INTERVALS
C        NUM - INTEGER VALUE OF DBZ FOR GIVEN GRID POINT
C        ND1- CODED VALUE REPRESENTING 100'S DIGIT OF DBZ VALUE (SHOULD
C             BE ZERO)
C        ND2 - CODED VALUE REPRESENTING 10'S DIGIT OF DBZ VALUE
C        ND3 - CODED VALUE REPRESENTING UNITS DIGIT OF DBZ VALUE
C        IW - DISTANCE IN KM EAST OR WEST TO LOWER LEFT CORNER OF GRID
C        NS -DISTANCE IN KM NORTH OR SOUTH TO LOWER LEFT CORNER OF GRID
C        INN - COUNTER USED TO COMPUTE NN FOR RIGHT HALF OF MAP
C
      WRITE(6,400)
      DO 330 JJ=1,51
      J=52-JJ
C
      DO 310 I=1,126
      BUF(I)=BLNK
 310  CONTINUE
C
      IF(MOD((J-1),5).NE.0) GO TO 315
C
      DO 314 I=1,126,25
      BUF(I)=PLUS
 314  CONTINUE
C
C        DBZ DATA FROM THE Z ARRAY ARE ROUNDED TO THE NEAREST INTEGER
C        AND LOADED INTO THE PROPER LOCATION IN THE BUF ARRAY.  DECIMAL
```

```
C           NUMBERS ARE BROKEN INTO THE TENS AND UNITS DIGITS, WHICH ARE
C           LOADED AS CHARACTERS INTO THE BUF ARRAY AT LOCATIONS DETERMINED
C           BY THE COUNTER, NN.
C
315   DO 327 I=2,26
      NN=5*(I-1)+1
      NUM=IFIX(Z(I,J)+0.5)
      IF(NUM.LE.0) GO TO 327
      IF(NUM.LT.10) GO TO 325
      IF(NUM.LT.100) GO TO 323
      ND1=NUM/100+1
      BUF(NN-2)=DIG(ND1)
323   ND2=MOD(NUM,100)/10+1
      BUF(NN-1)=DIG(ND2)
325   ND3=MOD(NUM,10)+1
      BUF(NN)=DIG(ND3)
327   CONTINUE
C
C           AFTER THE ENTIRE LINE OF DATA IS LOADED (IT COVERS 50 KM EAST-
C           WEST AT A GIVEN DISTANCE NORTH), THE LINE IS PRINTED BY
C           PRINTING THE BUF ARRAY.
C
      WRITE(6,401) (BUF(III),III=1,126)
330   CONTINUE
C
C           THIS SECTION PRINTS THE CAPTIONS FOR THE MAPS.  CAPTIONS DEPEND
C           ON THE ILEFT AND JDOWN ENTERED.
C
      IWEST=IL-2
      IW=IABS(IWEST)
      JSOUTH=JD-2
      JS=IABS(JSOUTH)
      IF(IWEST.GE.0) GO TO 336
      IF(JSOUTH.GE.0) GO TO 340
      GO TO 341
C
336   IF(JSOUTH.GE.0) GO TO 338
      GO TO 339
338   WRITE(6,402) IW,JS
      GO TO 342
339   WRITE(6,403) IW,JS
      GO TO 342
340   WRITE(6,404) IW,JS
      GO TO 342
341   WRITE(6,405) IW,JS
342   GO TO (343,345,347,349,351),MM
343   WRITE(6,406) ND,NT,LVL
      GO TO 352
345   WRITE(6,407) ND,NT
      GO TO 352
347   WRITE(6,408) ND,NT
      GO TO 352
349   WRITE(6,409) ND,NT
      GO TO 352
351   WRITE(6,410) ND,NT
352   WRITE(6,400)
C
C           THE RIGHT HALF OF THE MAP IS LOADED AND PRINTED LIKE THE
C           LEFT HALF WAS.
C
      DO 377 JJ=1,51
      J=52-JJ
```

```
C
      DO 357 I=1,126
      BUF(I)=BLNK
357   CONTINUE
C
      IF(MOD((J-1),5),NE,0) GO TO 362
C
      DO 361 I=1,126,25
      BUF(I)=PLUS
361   CONTINUE
C
362   DO 375 I=27,51
      INN=I-25
      NN=5*(INN-1)+1
      NUM=IFIX(Z(I,J)+0,5)
      IF(NUM.LE.0) GO TO 375
      IF(NUM.LT.10) GO TO 373
      IF(NUM.LT.100) GO TO 371
      ND1=NUM/100+1
      BUF(NN-2)=DIG(ND1)
371   ND2=MOD(NUM,100)/10+1
      BUF(NN-1)=DIG(ND2)
373   ND3=MOD(NUM,10)+1
      BUF(NN)=DIG(ND3)
375   CONTINUE
C
      WRITE(6,401) (BUF(III),III=1,126)
377   CONTINUE
C
      WRITE(6,411)
      WRITE(6,412) ND,NT,LVL
C
400   FORMAT(1H1)
401   FORMAT(1H ,126A1,///)
402   FORMAT(' ','LE',///' ','THE LOWER LEFT HAND GRID MARK IS ',I3,
     C' KM WEST AND ',I3,' KM SOUTH OF CLL')
403   FORMAT(' ','LE',///' ','THE LOWER LEFT HAND GRID MARK IS ',I3,
     C' KM WEST AND ',I3,' KM NORTH OF CLL')
404   FORMAT(' ','LE',///' ','THE LOWER LEFT HAND GRID MARK IS ',I3,
     C' KM EAST AND ',I3,' KM SOUTH OF CLL')
405   FORMAT(' ','LE',///' ','THE LOWER LEFT HAND GRID MARK IS ',I3,
     C' KM EAST AND ',I3,' KM NORTH OF CLL')
406   FORMAT(' ','DATE',A3,' TIME',1I6,4X,'REFLECTIVITY VALUES, Z = 10**
     C(MAP VALUE/10), AT THE',I6,' FT LEVEL,',3X,'2KM X 2KM GRID
     CINTERVAL,')
407   FORMAT(' ','DATE',A3,' TIME',1I6,4X,'PARTIAL VIZ FROM SURFACE TO
     C15000 FT (IN DBZ),')
408   FORMAT(' ','DATE',A3,' TIME',1I6,4X,'PARTIAL VIZ FROM 15000 TO
     C35000 FT (IN DBZ),')
409   FORMAT(' ','DATE',A3,' TIME',1I6,4X,'PARTIAL VIZ FROM 35000 TO
     C50000 FT (IN DBZ),')
410   FORMAT(' ','DATE',A3,' TIME',1I6,4X,'TOTAL VIL FROM SURFACE TO
     C50000 FT (IN GM/M**2),')
411   FORMAT(1H ,124X,2HRE)
412   FORMAT(' ','DATE',A3,' TIME',1I6,4X,'LEVEL',I6,' FT,')
      RETURN
      END
C
C
C
C
      SUBROUTINE LOAD(CALIB)
```

```
C
C            THIS SUBROUTINE RECONSTRUCTS THE RADAR CALIBRATION CURVE AND
C            CONVERTS THE 256 DIGITAL INTEGERS TO EQUIVALENT DBM VALUES.
C            IT ALSO PRINTS OUT THE CALIB ARRAY.
C
       DIMENSION DIGITS(8),CALIB(255)
       READ(5,1100)DIGITS,DBM
1100   FORMAT(8F4.0,F6.2)
       IDIG = IFIX( DIGITS(1))
C
       DO 1 I = 1,IDIG
1      CALIB(I) = DBM
C
       DBM  = DBM + 10.0
C
       DO 2 J = 2,8
       JJ = J-1
       DBM  = DBM - 10.0
       DELD   = DIGITS(J) - DIGITS(JJ)
       DELCAL = 10.0/DELD
       IDELD = IFIX(DELD)
C
       DO 3 K = 1,IDELD
       KK = DIGITS(JJ) + K
3      CALIB(KK)  = CALIB(KK-1) - DELCAL
C
2      CONTINUE
C
       WRITE(6,2000) CALIB
 2000  FORMAT('0',20F6.1)
       RETURN
       END
C
C
C
C
C   ****** FOLLOWING THE DECK COMES MORE JCL AND THE DATA CARDS.
C
C
X/GO.SYSIN DD *
C
C          DON'T CHANGE THIS JCL CARD.
C
C          NEXT COME THE DATA CARDS.  FIRST IS THE RADAR CALIBRATION DATA
C          CARD.  THEN THE CARDS WITH THE INITIALIZING VALUES FOR THE SCAN
C          SEQUENCE.   ONE SUCH CARD IS REQUIRED FOR EACH SCAN SEQUENCE
C          THAT IS TO BE PROCESSED.  EXAMPLES FOLLOW.
C
  32   37   60   98 139 171 201 233 107.5
C
C          RADAR CALIBRATION DATA
C
00210208918100202002201008200230
162-38269351004020023210082002 38
C
C          SCAN SEQUENCE CARDS - 1 FOR EACH SCAN TO BE PROCESSED
C
C          THE FOLLOWING JCL CARDS DEFINE AND CONTROL THE INPUT AND
C          OUTPUT TAPES.
C
X/FT08F001 DD UNIT=TAPE9,VOL=SER=ZZ5618,DISP=(OLD,PASS),
X/ LABEL=(1,NL,,IN),DCB=(RECFM=FB,LRECL=884,BLKSIZE=884)
```

```
C
C          FT08 IS THE UNIT NUMBER (IRR). F001 INDICATES FOR WHICH RUN
C          THROUGH THE PROGRAM THIS INPUT IS TO BE USED. AND ZZ5618 IS
C          THE TAPE NUMBER.  THE SECOND CARD IS A CONTINUATION OF THE
C          FIRST AND MUST ALWAYS ACCOMPANY IT.  LABEL=(1..... INDICATES
C          WHICH FILE ON THE TAPE YOU WANT TO READ.  IN THIS CASE, IT IS
C          THE FIRST FILE.  FOR THE SECOND SCAN (BELOW) IT IS THE FIFTH
C          FILE.  NOTHING ELSE ON THESE CARDS CHANGES.
C
X/FT08F002 DD UNIT=TAPE9,VOL=SER=ZZ5618,DISP=(OLD,PASS),
X/ LABEL=(5,NL,,IN),DCB=(RECFM=FB,LRECL=884,BLKSIZE=884)
C
C          THE FOLLOWING PAIRS OF CARDS ARE FOR THE OUTPUT TAPE.
C
X/FT10F001 DD UNIT=TAPE9,VOL=SER=ZZ4971,LABEL=(15,NL,,OUT),
X/ DISP=(NEW,PASS),DCB=(RECFM=FB,LRECL=1445,BLKSIZE=13005)
C
C          ONCE AGAIN, FT10 IS THE UNIT NUMBER (IRIT), AND F001 IS THE
C          SAME AS ABOVE.  OUTPUT TAPE NUMBER IS ZZ4971.  LABEL=(15.....
C          MEANS THAT THE OUTPUT OF THE FIRST PROGRAM RUN (5 MAPS) WILL
C          BE FILE #15 ON THIS TAPE.  LIKEWISE. THE OUTPUT FROM THE
C          SECOND RUN WILL BE FILE #16.  NOTHING ELSE ON THESE CARDS
C          CHANGES.
C
X/FT10F002 DD UNIT=TAPE9,VOL=SER=ZZ4971,LABEL=(16,NL,,OUT),
X/ DISP=(NEW,PASS),DCB=(RECFM=FB,LRECL=1445,BLKSIZE=13005)
C
X*END
C          THIS IS ALWAYS THE LAST CARD IN THE DECK.
```

APPENDIX B

This appendix contains a commented copy of the computer program (RDRMAP) that produced the contoured reflectivity maps from the output arrays of the RADAR program.

```
C          'RDRMAP' - A CONREC PLOTTING AND CONTOURING PROGRAM
C
C          THIS PROGRAM TAKES THE 100 X 100 KM OUTPUT BOXES (51 X 51
C          ARRAYS) OF REFLECTIVITY AND VIL FROM THE 'RADAR' PROGRAM (APP.
C          A) AND PLOTS AN AREA OF INTEREST SPECIFIED BY THE PROGRAMMER
C          ON THE CALCOMP PLOTTER.  THE OUTPUT IS IN THE FORM OF A CON-
C          TOURED MAP OF REFLECTIVITY OR VIL.  THE VARIOUS PARAMETERS CAN
C          ALL BE SPECIFIED BY THE PROGRAMMER, AND THE PROGRAM IS SUFFIC-
C          IENTLY GENERAL THAT IT CAN BE USED FOR ANY GENERLAIZED PLOT
C          ROUTINE, NOT JUST THE 'RADAR' PROGRAM USED HERE.
C
C          SOURCES FOR THIS PROGRAM ARE:
C               (1)  REID - RM 617A OCM BLDG
C               (2)  NCAR LIBRARY ROUTINE TECHNICAL MANUAL
C               (3)  OS/360 LOCAL APPENDIX
C               (4)  CONREC APPENDIX
C
C
C          THE MECHANICS OF RUNNING THE PROGRAM ARE THE SAME AS FOR THE
C          'RADAR' PROGRAM WITH THE FOLLOWING ADDITIONAL REQUIREMENT.
C          NORMALLY YOU WILL ONLY PROVIDE THE INPUT TAPE AND THE DPC WILL
C          USE ONE OF THEIR TAPES FOR THE OUTPUT TAPE, WHICH IS CALLED
C          'CALCOMP'.  ACCORDINGLY, WHEN YOU FILL OUT THE JOB TICKET,
C          ENTER 'CALCOMP' AS THE OUTPUT TAPE.  YOU MUST ALSO FILL OUT
C          A 'CALCOMP JOB TICKET', WHICH IS AVAILABLE AT THE WINDOW OF
C          THE MACHINE ROOM WHERE YOU TURN THE TAPES IN.  THE SPACE MARKED
C          'TAPE VOLUME' ON THIS TICKET IS FOR THE OUTPUT TAPE AND SHOULD
C          BE MARKED 'CALCOMP', UNLESS YOU PROVIDE THEM WITH YOUR OWN
C          OUTPUT TAPE.  THE FINISHED PLOTS MAY BE PICKED UP IN THE I/O
C          ROOM, OR THEY WILL BE DELIVERED TO YOUR BOX ADDRESS WHEN THEY
C          ARE COMPLETED.
C
C
C   ************* JCL - JOB CONTROL LANGUAGE **************
C
C          WITH THIS JCL, THE PROGRAM RUNS IN 'FORTRAN IV G LEVEL 21'.
C          THE JCL WILL REQUIRE SOME MINOR CHANGES FOR EACH PROGRAM RUN.
C          NOTE THAT THE FIRST CHARACTER ON ALL JCL CARDS (COL. 1) SHOULD
C          BE A '/', REPRODUCED HERE AS AN 'X'.
C
C
X/RDRMAP    JOB (X999,006D,002,030,XX),'YOUR NAME
C
C          002 IS TIME IN MINUTES.  DON'T CHANGE.
C
X*PASSWORD       XXXX
X*SETUP
C
C          THIS TELLS THE MACHINE NOT TO RUN UNTIL THE TAPES
C          HAVE BEEN MOUNTED.
C
X*LEVEL          X
X*JOBPARM K=0,R=256,T=2,TAPE9=2
X/ EXEC FTNGPLOT,REGION=256K
X/FORT.SYSIN DD *
C
C          DON'T CHANGE THESE LAST THREE CARDS.
C
C
C
C   ************* THE MAIN PROGRAM DECK BEGINS HERE.
C
```

```
C      ****** NOTE *******
C          THE PARAMETERS SPECIFIED HERE WERE THE ONES USED TO PRODUCE THE
C          'NEAR RANGE' MAPS IN THIS PAPER, WHICH HAVE BEEN REDUCED TO
C          65% OF THE SIZE OF THE ORIGINALS.
C          A DETAILED EXPLANATION OF THE PARTS OF THIS PROGRAM CAN BE
C          FOUND IN CHAPTER III.
C
C
C
       DIMENSION ZARRAY(51,51),Z(26,26)
C
C          ZARRAY IS THE OUTPUT ARRAY FROM THE 'RADAR' PROGRAM, AND IS
C          100 X 100 KM ON A 2 KM GRID.  Z IS THE PORTION OF ZARRAY THAT
C          IS TO BE PLOTTED AND CONTOURED BY THIS PROGRAM.  ITS SIZE AND
C          POSITION WITHIN ZARRAY ARE DETERMINDD BY THE PROGRAMMER.
C          Z(26,26) SPECIFIES AN AREA 50 X 50 KM.
C
       COMMON/CONRE1/SIZEL,SIZEM,SIZEP,NLA,NLM,XLT,YBT,SIDE,NREP,NCRT,ILA
      *B,NULBLL,IOFFD,EXT,IOFFP,SPVAL,IOFFM,ISOLID
C
C          COMMON STATEMENT FOR CONREC.  DO NOT CHANGE.  FOR DETAILS ON
C          THE MEANING OF EACH ARGUMENT, SEE CONREC APPENDIX.
C
       SIZEL=1.97
C
C          SIZEL - SIZE OF LINE LABELS.  1.31=2MM.  DEFAULT OPTION (NO
C          CARD) IS 1.51
C
       NULBLL=1
C
C          NULBUL IS THE NUMBER OF UNLABELED LINES BETWEEN LABELED LINES.
C          DEFAULT=3, OR EVERY FOURTH LINE IS LABELED.
C
C
       INDEX=0
C
C          INDEX IS THE COUNT OF HOW MANY FILES (SCAN SEQUENCES) OF DATA
C          ARE READ FROM THE RADAR TAPE.  REMEMBER, THERE ARE FIVE MAPS
C          PER SCAN SEQUENCE.
C
       DO 99 II=1,3
C
C          THIS RUN PROCESSED THREE FILES (SCAN SEQUENCES) OF DATA.
C
       ICOUNT=0
C
C          ICOUNT IS THE MAP NUMBER.  THERE ARE FIVE MAPS PER FILE.
C
       INDEX=INDEX+1
C
       ICOR=0
       JCOR=25
C
C          ICOR AND JCOR ARE USED TO SHIFT THE STARTING POINT OF Z (LOWER
C          LEFT CORNER) TO A PARTICULAR POINT IS ZARRAY.  FOR EXAMPLE, IF
C          ICOR=0 AND JCOR=25, THEN Z(1,1)=ZARRAY(1,26).  SEE NOTE ABOVE.
C
    15 CONTINUE
       READ(8,6006,END=99)ZARRAY
  6006 FORMAT(200F5.1,89F5.1)
C
C          THIS IS THE SAME FORMAT USED ON TAPE IN THE RADAR PROGRAM.
```

```
C
      ICOUNT=ICOUNT+1
C
      DO 1 I=1,26
      DO 1 J=1,26
      IC=I+ICOR
      JC=J+JCOR
      Z(I,J)=ZARRAY(IC,JC)
    1 CONTINUE
C
C     THIS TRANFERS THE DATA TO BE CONTOURED INTO THE Z ARRAY.
C
      CALL SET(110,980,110,980,0.,25.,0.,25.,1)
C
C     THIS SUBROUTINE PHYSICALLY SETS UP THE GRAPH.  SEE CHAP. III.
C
      CALL PERIM(25,1,25,1)
C
C     THIS SUBROUTINE DRAWS THE BOX AROUND THE AREA AND PLACES TICK
C     MARKS AROUND THE PERIMETER OF THE BOX.  SEE CHAP. III.
C
      CALL PWRX(40,545,28H'PRU'KILOMETERS SOUTH OF CLL,28,1,,1,1)
      CALL PWRX(545,50,27H'PRU'KILOMETERS EAST OF CLL,27,1,,0,1)
C
C     THIS SUBROUTINE PRINTS THE LABELS ON THE MAP AND MUST BE CALLED
C     ONCE FOR EACH LABEL.  SEE CHAP. III.
C
      CALL PWRX(25.,90,7H'IRU'50,7,1,,0,1)
      CALL PWRX(20.,90,7H'IRU'40,7,1,,0,1)
      CALL PWRX(15.,90,7H'IRU'30,7,1,,0,1)
      CALL PWRX(10.,90,7H'IRU'20,7,1,,0,1)
      CALL PWRX( 5.,90,7H'IRU'10,7,1,,0,1)
      CALL PWRX(0.,90,6H'IRU'0,7,1,,0,1)
C
C     THIS PUTS THE NUMBERS ALONG THE X AXIS.
C
      CALL PWRX(100, 0.,7H'IRU'50,7,1,,0,3)
      CALL PWRX(100, 5.,7H'IRU'40,7,1,,0,3)
      CALL PWRX(100,10.,7H'IRU'30,7,1,,0,3)
      CALL PWRX(100,15.,7H'IRU'20,7,1,,0,3)
      CALL PWRX(100,20.,7H'IRU'10,7,1,,0,3)
      CALL PWRX(100,25.,6H'IRU'0,7,1,,0,3)
C
C     THIS PUTS THE NUMBERS ALONG THE Y AXIS.
C
C
      IF(ICOUNT.GT.4)GO TO 5
C
C     THIS SELECTS A DIFFERENT SET OF CONTOUR INTERVALS FOR THE VIL
C     MAP.
C
      CALL CONREC(Z(2,2),26,24,24,10.,60.,5.,1,-1,0)
C
C     THIS SUBROUTINE ACTUALLY DOES THE PLOTTING AND CONTOURING OF
C     THE DATA, AND IN THIS CASE, CONTOURS THE REFLECTIVITY MAPS
C     FROM 10 TO 60 IN 5 UNIT INCREMENTS.  SEE CHAP. III.
C
      GO TO 10
C
    5 CONTINUE
C
      CALL CONREC(Z(2,2),26,24,24,1.,20.,1.,1,-1,0)
```

```
C
C          THIS TIME THE VIL MAP IS DRAWN, CONTOURED FROM 1 TO 20 IN 1
C          UNIT INCREMENTS.
C
  10  CONTINUE
C
      CALL PLOT(12.,0.,-3)
C
C          THIS MOVES THE PEN TO A NEW LOCATION AND REINITIALIZES THE
C          COORDINATE SYSTEM IN PREPARATION FOR BEGINNING A NEW MAP.  SEE
C          CHAP. III.
C
      GO TO 15
C
  99  CONTINUE
C
      CALL PLOT(0.,0.,99)
C
C          THIS EMPTIES THE OUTPUT BUFFER AND IS NECESSARY TO END THE
C          PROGRAM.
C
      STOP
      END
C
C
C
C
C
C    *********** THE REST OF THE JCL FOLLOWS THE DECK.
C
C
X/LKED.DDNAME DD DISP=SHR,
X/ DSNAME=USER.OCN.GUINASSO.JOBLIB
X/LKED.SYSIN DD *
 INCLUDE DDNAME(CNRCSMTH.PWRX)
C
C          DON'T CHANGE THESE LAST FOUR CARDS.
C
C          NEXT COME THE INPUT CARDS - ONE SET OF THESE CARDS FOR EACH
C          FILE THAT IS TO BE PROCESSED.
C
X/GO.FT08F001 DD UNIT=TAPE9,VOL=SER=ZZ4971,
X/ LABEL=(03,NL,,IN),DISP=(OLD,PASS),
X/ DCB=(RECFM=FB,LRECL=1445,BLKSIZE=13005)
C
C          FT08 IS THE UNIT NUMBER THAT REFERS TO THE INPUT TAPE.
C          F001 IS THE FIRST FILE TO BE PROCESSED.
C          LABEL=(03,......) INDICATES THAT THIS FILE IS THE THIRD FILE ON
C          THE INPUT TAPE.
C          ZZ4971 IS THE ID NUMBER OF THE INPUT TAPE.
C
X/GO.FT08F002 DD UNIT=TAPE9,VOL=SER=ZZ4971,
X/ LABEL=(05,NL,,IN),DISP=(OLD,PASS),
X/ DCB=(RECFM=FB,LRECL=1445,BLKSIZE=13005)
C
C          THE SECOND FILE (SCAN SEQUENCE) TO BE PLOTTED IS THE FIFTH
C          FILE ON THE TAPE.
C
X/GO.FT08F003 DD UNIT=TAPE9,VOL=SER=ZZ4971,
X/ LABEL=(06,NL,,IN),DISP=(OLD,PASS),
X/ DCB=(RECFM=FB,LRECL=1445,BLKSIZE=13005)
C
```

```
X/GO.SYSIN DD *
X#END
C
C          THIS IS ALWAYS THE LAST CARD IN THE DECK
```

VITA

Michael A. Neyland was born in Frankfurt am Main, Germany, on 11 February 1949, to Lewis J. and Dorothy M. Neyland. Because his father was an Air Force officer, he attended school in Montana, Iceland, Maryland, Alabama, South Carolina, and Germany before graduating from Roy J. Wasson High School in Colorado Springs, Colorado in 1967.

Mike entered the United States Military Academy in 1967 and graduated with a Bachelor of Science degree in Engineering and a commission as a 2nd Lt. in the Air Force in June 1971. He immediately entered the Air Force Basic Meteorology program at the University of Utah, and graduated with a Bachelor of Science degree in Meteorology in June 1972. Subsequent tours of duty included weather forecasting at an Air Force base weather station, and three years of flying weather reconnaissance with the 54th Weather Reconnaissance Squadron, the Typhoon Chasers, on Guam.

In January 1977 Mike entered Texas A&M University to pursue a Master of Science degree in Meteorology under the auspices of AFIT. His permanent mailing address is in care of his parents at 2006 McArthur Avenue, Colorado Springs, Colorado, 80909.